AN ABSTRACT OF THE THESIS OF

Joseph A. DiPietro for the degree of Doctor of Philosophy in Geology presented on February 16, 1990.

Title: Stratigraphy, Structure, and Metamorphism Near Saidu Sharif, Lower Swat, Pakistan.

Redacted for privacy

Abstract approved: _____
Dr. Robert D. Lawrence

The stratigraphy exposed on the Indian plate, south of the Main Mantle thrust (MMT) is Precambrian-Cambrian(?) Manglaur formation, Jobra formation (age unknown), and the Late Paleozoic-Early Mesozoic Alpurai group. Cambrian-Early Ordovician(?) Swat granitic gneisses intrude the Manglaur (garnetiferous schist) formation but are unconformably overlain by the Alpurai group which consists of the Marghazar (amphibolitic schist), Kashala (calc-schist), Saidu (graphitic phyllite) and Nikanai Ghar (marble) formations. Paleogene(?) tourmaline granite gneiss intrudes the unconformity. The Jobra (calc-silicate) formation occurs as lenses unconformably(?) above the Swat gneiss and unconformably(?) below Marghazar formation. Lower Swat existed as a highland, upthrown by normal faulting, during Marghazar deposition. Presumably this is associated with breakup of Gondwana. By Kashala time the area was receiving carbonate shelf deposition. The Saidu formation may represent a starved basin, or a transition to deeper oceanic depths.

The rocks are exposed in a dome that resulted from

the superposition of four fold phases. All folds developed during Eocene-Oligocene metamorphism when the Indian plate collided with the Kohistan arc along the MMT. The earliest superposed small-scale folds represent a progressive F_1/F_2 deformation that is associated with a composite (S_1/S_2) regional foliation but with only a single set of NNW-SSE trending, west-vergent large-scale folds (termed F_2). F_1/F_2 occurred in the Eocene during WSW-directed overthrusting of the MMT suture complex. Geothermometry and geobarometry suggest peak metamorphic conditions of 540 to 630°C and 8.1 to 9.2 kbar. These conditions occurred during a phase of static recrystallization that followed F_2. P-T paths calculated from garnet zoning profiles suggest that temperatures were at least 15° lower and that pressures were 1 to 3 kbars higher during F_2. Development of N-S trending, upright, F_3 folds are associated with strike-slip faulting in the MMT north of Lower Swat. F3 was followed, in the Oligocene, by a final phase of south-directed thrusting, retrograde metamorphism, and development of E-W trending, upright to south-vergent F4 folds. F4 is the earliest indication of N-S compression on the Indian plate.

Stratigraphy, Structure, and Metamorphism Near Saidu Sharif, Lower Swat, Pakistan

by

Joseph A. DiPietro

A THESIS

submitted to

Oregon State University

in partial fulfillment of
the requirements for the
degree of

Doctor of Philosophy

Completed February 16, 1990

Commencement June, 1990

APPROVED:

Redacted for privacy

Associate Professor of Geology in charge of major

Redacted for privacy

Professor and Chairman of Geosciences

Redacted for privacy

Dean of the Graduate School

Date thesis is presented February 16,1990

Typed by Joseph A. DiPietro

ACKNOWLEDGMENTS

This thesis would not have been possible without the advice, encouragement, logistical and financial support of Bob Lawrence. Bob visited me several times in the field and read several early drafts. His ideas, comments, criticisms, and the many hours of informative discussion on all aspects, from the smallest microstructure to the regional tectonics, has resulted in a much stronger thesis. I have also benefited from early critical reviews and discussions of the thesis by John Dilles. I sincerely appreciate the time and effort that Bob and John expended on my behalf.

Later reviews and comments by Bob Yeats and Jack Rice reveled some weaknesses which, fortunately, I was able to address prior to final submittal of the thesis. Discussions with Jack, on some of the metamorphic aspects, were particularly helpful. The structure paper (chapter 3) was also reviewed by C. Page Chamberlain and David Prior.

Kevin Pogue mapped critical relationships near Baroch and in the Peshawar Basin south of Lower Swat. Without any preconceived notion on our part, and without difficulty, we were able to correlate the metamorphic stratigraphy in Lower Swat with the fossiliferous stratigraphy in the Peshawar Basin. Needless to say, without Kevin's help, and the many discussions I have had with him, the regional significance of the Lower Swat stratigraphy would be far less clear.

Mirza Shahid Baig mapped the Besham area, about 45 km northeast of Lower Swat. It is amazing how, in such a short distance, the geology can change so drastically! As a result of visiting Shahid in the field, and discussions with him afterward, we were able to "see" how our areas were related, and how they fit into the

larger framework of the Himalaya. Certainly, my regional understanding of the Himalayan system benefited greatly from Shahid's and Kevin's work.

I would like to thank Imtiaz Ahmad and Mohammad Riaz for introducing me to the geology in Lower Swat and for acclimating me to the customs of Pakistan. I also benefited from discussions with Ahmad Hussain, Larry Snee, M. Qasim Jan, Bob Lillie, Arif A.K. Ghauri, and A.H. Kazmi. Roger Nielsen and Bill Gallahan offered much needed help and advice on working the microprobe.

The people of Swat are just fantastic! They are gracious and generous in every way. I will never forget my experiences in the mountains and remote villages of their enchanted land. I especially thank Ziarat Khattak and Zafar Ali for awesome field assistance.

I also want to thank the members, past and present, of the Lower Crust Band. Its really been a pleasure to jam with you guys.

Finally, I thank my family, and especially my mother, for supporting me in whatever it was I was doing.

Financial support was provided from grants NSF INT 86-09914 and NSF EAR 86-17543 to Bob Lawrence.

**"We all dearly love our own intellectual children,
especially if born of much labor and thought;
but I am sure that I am willing, like Jephtha of old,
to sacrifice, if need be, this my fairest daughter
on the sacred alter of truth."**

Joseph Le Conte

Theories of the Origin of Mountain Ranges
Journal of Geology, vol.1, no.6, p.563, 1893

TABLE OF CONTENTS

INTRODUCTION..... 1

STRATIGRAPHY OF INDIAN PLATE ROCKS SOUTH OF THE MAIN MANTLE THRUST, LOWER SWAT, PAKISTAN..... 4
ABSTRACT..... 4
INTRODUCTION..... 5
PREVIOUS WORK..... 6
GENERAL GEOLOGY..... 9
MANGLAUR FORMATION..... 12
UNIT M1..... 13
UNIT M2..... 13
UNIT M3..... 14
AGE AND CORRELATION..... 14
SWAT GRANITIC GNEISS..... 15
FLASER GRANITIC GNEISS..... 16
AUGEN GRANODIORITE GNEISS..... 17
AGE CONSTRAINTS..... 19
INTRUDED ZONE A..... 21
INTRUDED ZONE B..... 22
JOBRA FORMATION..... 23
ALPURAI GROUP..... 25
MARGHAZAR FORMATION..... 26
UNIT Am1..... 27
UNIT Am2..... 28
UNIT Am3..... 29
UNIT Am4..... 31
KASHALA FORMATION..... 32
NORTHERN AREA..... 32
SOUTHERN AREA..... 34
SAIDU FORMATION..... 35
NIKANAI GHAR FORMATION..... 36
AGE, FACIES CHANGES, AND DEPOSITIONAL ENVIRONMENT OF THE ALPURAI GROUP..... 39
TOURMALINE GRANITE GNEISS..... 43
MINOR INTRUSIVE ROCKS..... 45
BIOTITE GRANITE AND GRANITIC GNEISS... 45
METAGABBRO..... 47
PYROXENE GRANITE..... 48
CARBONATITE..... 48
LEUCOGNEISS OF QUESTIONABLE PROTOLITH. 49
XENOLITH OF QUESTIONABLE PROTOLITH.... 49
CONTACT RELATIONSHIPS..... 50
CONCLUSIONS..... 58

TABLE OF CONTENTS (CONTINUED)

STRUCTURE AND METAMORPHISM SOUTH OF THE MAIN MANTLE THRUST, LOWER SWAT, PAKISTAN..... 61
ABSTRACT..... 61
INTRODUCTION..... 62
GEOLOGIC SETTING..... 63
METAMORPHISM IN THE LOWER SWAT SEQUENCE.. 65
MESOSCOPIC STRUCTURES..... 67
FOLDS..... 67
FOLIATIONS..... 68
LINEATIONS..... 72
SEQUENCE OF CRYSTALLIZATION AND FOLIATION DEVELOPMENT..... 78
S_1 PHASE..... 79
INTER-KINEMATIC PHASE..... 79
REGIONAL S_2 FOLIATION DEVELOPMENT PHASE..... 78
POST-S_2 ANNEALING PHASE..... 82
F_3 PHASE..... 84
RETROGRADE PHASE..... 85
F_4 PHASE..... 85
DISCUSSION..... 96

METAMORPHIC PRESSURE - TEMPERATURE CONDITIONS OF INDIAN PLATE ROCKS SOUTH OF THE MAIN MANTLE THRUST, LOWER SWAT, PAKISTAN..... 107
ABSTRACT..... 107
INTRODUCTION..... 108
GEOLOGIC SETTING..... 108
DISTRIBUTION OF METAMORPHIC FACIES..... 113
TIMING OF METAMORPHIC CONDITIONS..... 115
ANALYTICAL METHODS..... 117
GEOTHERMOMETRY AND GEOBAROMETRY..... 119
GARNET ZONING PATTERNS AND P-T PATHS..... 130
MARGHAZAR GARNETS..... 132
DISCUSSION OF MARGHAZAR GARNETS..... 140
MANGLAUR GARNETS..... 142
DISCUSSION OF MANGLAUR GARNETS..... 149
DISCUSSION OF A POSSIBLE P-T-t PATH... 150
CONCLUSION..... 153

REFERENCES..... 155

APPENDIX I SUMMARY OF ROCK TYPES IN THE LOWER SWAT AREA..... 170
APPENDIX II MINERAL COMPOSITION DATA..... 174
APPENDIX III EQUATIONS OF STATE FOR PRESSURE-TEMPERATURE CALCULATIONS..... 180
APPENDIX IV XRF ANALYSIS OF A CARBONATITE..... 182

LIST OF FIGURES

Figure		Page
1.	Tectonic map of northern Pakistan.	2
2.	Tectonic map of northern Pakistan showing topographic features.	3
3	Comparative structural/stratigraphic columns from Lower Swat.	11
4.	Typical exposures of the Swat gneiss.	20
5.	Contact relationships at Lewanai Ghar.	54
6.	Contact relationships at hill 3338.	55
7.	T-X(CO_2) phase diagram.	57
8.	A recumbent, isoclinal F_1/F_2 fold in the Marghazar formation.	74
9.	View looking southeast at the overturned F_2 syncline near Ilam.	76
10.	Inferred mineral stability in relation to the deformational phases.	77
11.	Examples of S_1 foliation.	87
12.	Examples of inter-kinematic porphyroblast growth and shear associated with development of dominant S_2 foliation.	89
13.	Examples of post-S_2 recrystallization.	92
14.	Garnet in the hinge area of an F_3 crenulation fold.	95
15.	Schematic block diagram showing the inferred origin of the large-scale fold sequence.	105
16.	Schematic diagram showing the inferred sequence of faulting in the suture zone.	106
17.	Geologic map of the Lower Swat area showing locations of microprobe samples.	110

LIST OF FIGURES (CONTINUED)

Figure		Page
18.	Photomicrographs of garnet from the Marghazar formation.	137
19.	Compositional profiles across garnets 6-416C and 6-261B2 of the Marghazar formation.	138
20.	Calculated P-T trajectories of garnets 6-416C and 6-261B2 of the Marghazar formation.	139
21.	Photomicrographs of garnet from the Manglaur formation.	146
22.	Compositional profiles across garnets 6-140Aa, 6-140Ab, and 6-452B of the Manglaur formation.	148
23.	Inferred P-T path of the Marghazar formation based on the calculated P-T trajectories of garnets 6-416C and 6-261B2.	152

LIST OF TABLES

Table		Page
1.	Mineral associations in the 43 B/6 quadrangle.	111
2.	Estimated modal mineralogy of rock samples analyzed by microprobe.	112
3.	Composition data.	126
4.	Temperature - pressure estimates.	127
5.	Mineral abbreviations and activity/ composition relationships.	128
6.	Amphibole composition.	129

LIST OF PLATES

Plate		Page
1.	Geologic map of the Lower Swat area near Saidu showing locations of cross sections.	in pocket
2.	Geologic map of the 43 B/6 15' quadrangle.	in pocket
3.	Explanation to the geologic map of the 43 B/6 15' quadrangle.	in pocket
4.	Generalized stratigraphic columns from five areas in Lower Swat.	in pocket
5.	Lower hemisphere equal area projections of lineation data from the 43 B/6 15' quadrangle.	in pocket

STRATIGRAPHY, STRUCTURE AND METAMORPHISM NEAR SAIDU SHARIF, LOWER SWAT, PAKISTAN

INTRODUCTION

The state of Swat is located in the foothills of the Himalayan mountains where the Peshawar Basin, at an altitude of 457 meter (1500 feet) near Baroch, gives way to 5500 meter (18000 foot) mountains in Kohistan, north of Saidu Sharif (Saidu for short; Figures 1 and 2). The spectacular scenery is matched only by the geology. The southern part of Swat lies on the Indian plate where Precambrian to Mesozoic limestones, quartzites, and argillites record a history of shelf deposition interrupted by numerous erosional unconformities (Pogue and others, in prep.). This rock sequence can be followed northward into progressively higher grade rocks that culminate in a structural dome where rocks are at kyanite grade. The northern flank of this dome is terminated by a major suture-zone melange called the Main Mantle thrust. This melange separates the Indian plate rocks from amphibolites that are considered to be part of a Mesozoic island arc complex (Tahirkheli and others, 1979).

This thesis examines the stratigraphy, metamorphism, and structural development of the dome just south of the Main Mantle thrust near Saidu. It is written as three manuscripts. The first paper describes each rock unit and correlates the stratigraphy in the metasedimentary rocks with the fossiliferous strata to the south. The second paper relates fold and foliation development with the timing of metamorphic mineral growth and with movement in the overlying suture zone. The final paper documents the pressure-temperature conditions of metamorphism and presents a possible P-T path followed by the rocks during part of the metamorphism.

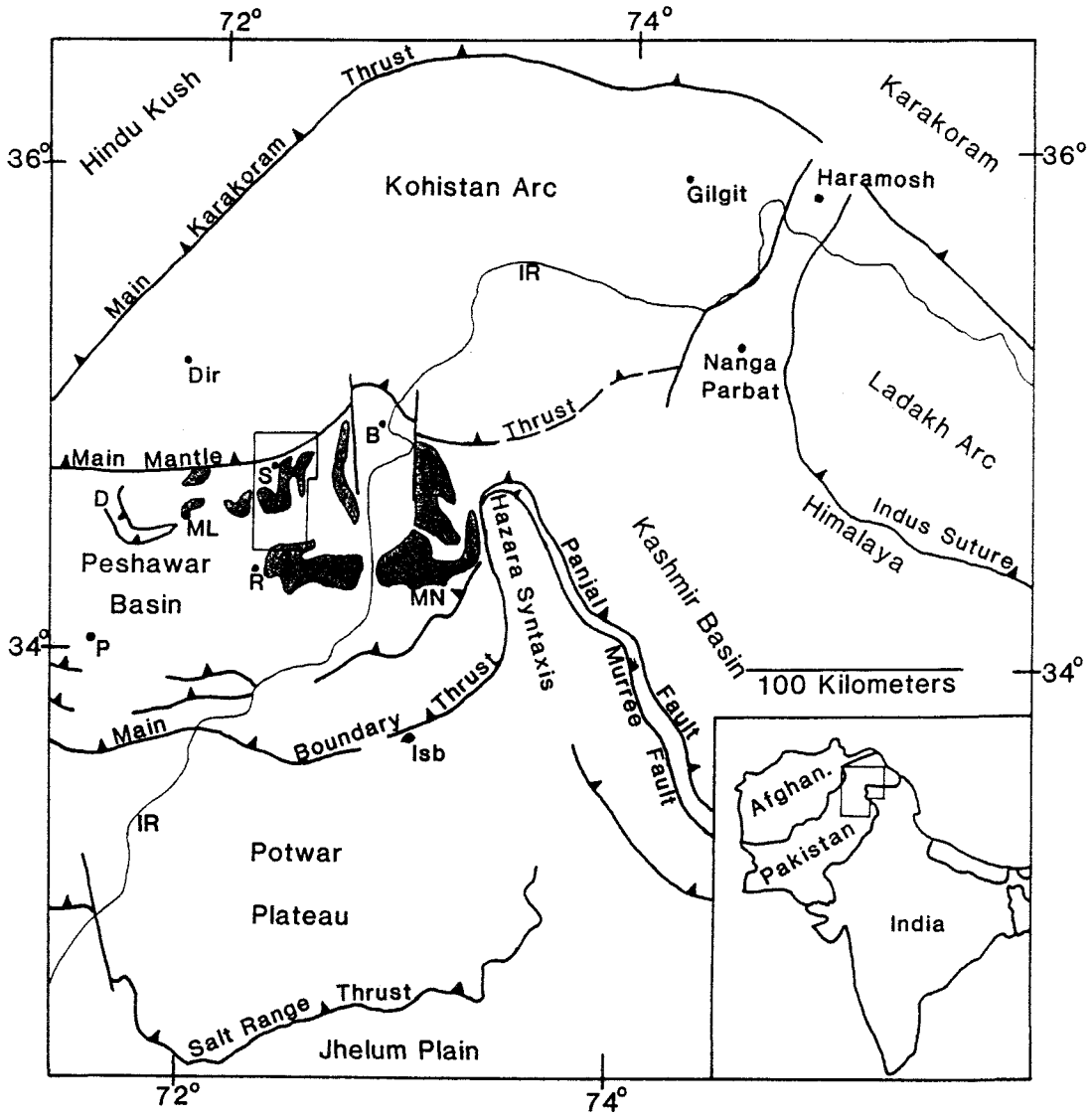

Figure 1. Tectonic map of northern Pakistan. Box surrounding Saidu shows the location of the geologic map in Plate 1. B-Besham; D-Dargai Klippe; IR-Indus River; Isb-Islamabad; ML-Malakand; MN-Mansehra; P-Peshawar; R-Rustam; S-Saidu. Major granitic intrusive bodies in Swat and Hazara are shaded.

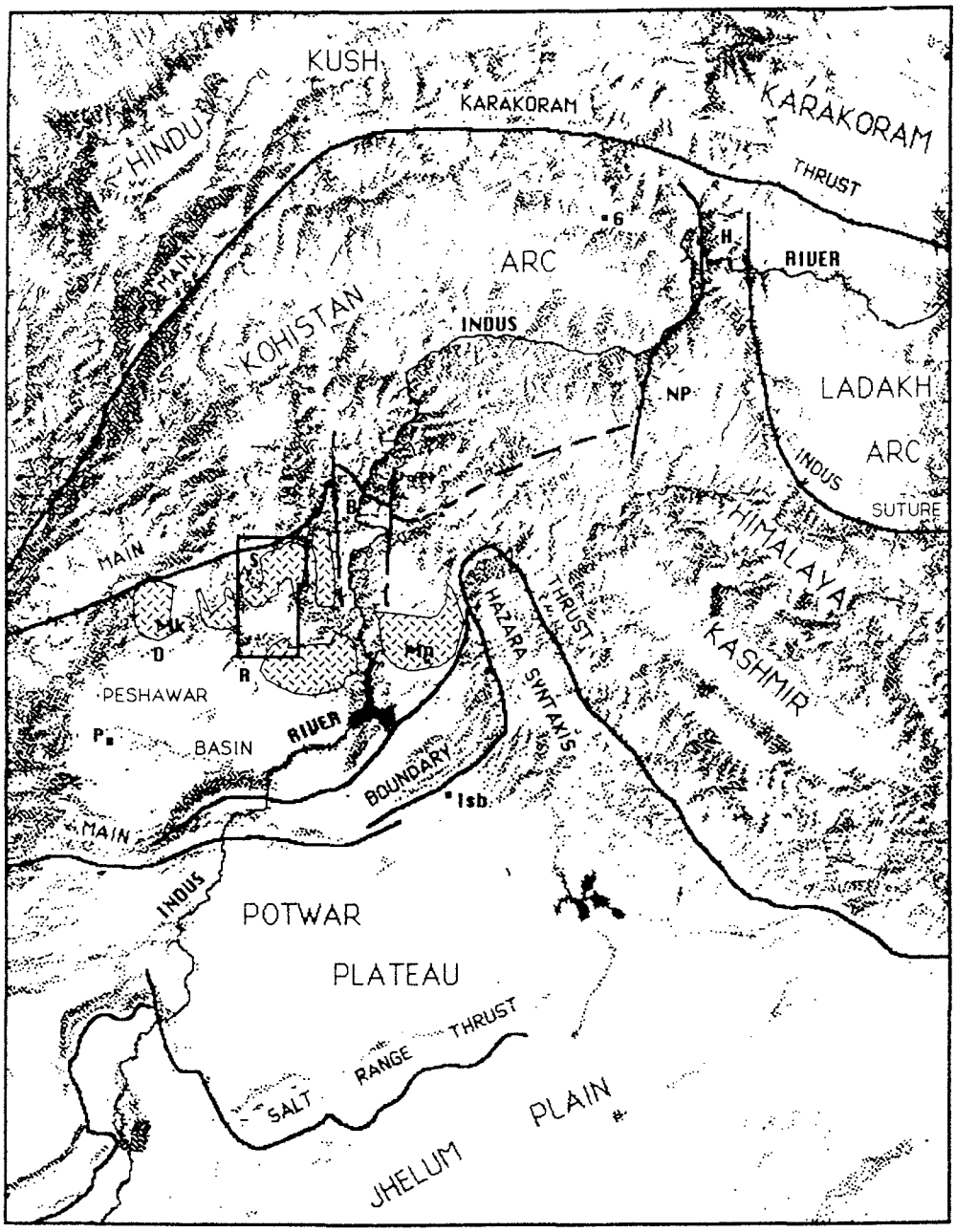

Figure 2. Tectonic map of northern Pakistan showing topographic features. B-Besham; D-Dargai Klippe; G-Gilgit; H-Haramosh; Isb-Islamabad; MK-Malakand; MN-Mansehra; NP-Nanga Parbat; P-Peshawar; R-Rustam; S-Saidu. Box surrounding Saidu shows location of geologic map in Plate 1. Major granitic intrusive bodies are shown with cross-hatches.

STRATIGRAPHY OF INDIAN PLATE ROCKS SOUTH OF THE MAIN MANTLE THRUST, LOWER SWAT, PAKISTAN

ABSTRACT

The metamorphic sequence in Lower Swat is described and placed into the geologic framework of Pakistan. The stratigraphic sequence is Manglaur formation, Jobra formation, Alpurai group. The Precambrian-Cambrian(?) Manglaur formation consists of garnetiferous schist, quartzite, and tremolite marble. It is correlated with the Tanawal formation of Pogue and others (in prep.). Cambrian-Early Ordovician(?) Swat augen-flaser granite and granodiorite gneisses intrude the Manglaur formation. These units are separated from the Alpurai group by an erosional unconformity. Paleogene(?) tourmaline granite gneiss intrudes the unconformity. The Alpurai group consists of four formations. The amphibolitic Marghazar formation occurs at the base and is overlain by calc-schists and marbles of the Kashala formation. Graphitic phyllites of the Saidu formation are at the top of the sequence in the north but, toward the south, the Saidu is replaced by marbles of the Nikanai Ghar formation. Fossil evidence indicates that the Marghazar formation is Mississippian or younger and that the overlying formations are Triassic or younger. The Jobra calc-silicate formation occurs as rare lenses unconformably(?) above the Swat gneiss and unconformably(?) below Marghazar formation. The age of this unit is unknown. The relationships suggest that Lower Swat existed as a highland with active normal faulting during, and perhaps prior to, deposition of the Marghazar formation. The Marghazar formation may be a rift facies associated with the breakup of Gondwana. I correlate it with the "agglomeratic slates" and Panjal

Traps of western India. The Kashala and Nikanai Ghar formations may represent a transition to a stable, shelf environment. These units may correlate, in part, with the Zanskar Supergroup of western India. The Saidu formation may represent a starved basin, or a deepening of the shelf to oceanic depths. It may correlate with the Lamayuru Formation of western India.

INTRODUCTION

Although much is known about the post-collisional tectonics of the Himalayan system in Pakistan (Yeats and Lawrence, 1984; Burbank and others, 1985, 1988; Lillie and others, 1987; Yeats and Hussain, 1987), few detailed studies are available that relate the pre-collisional development of the suture zone with associated deformation on the Indian plate. Lower Swat is an exceptional region in which to address this concern because critical structural relationships have not been significantly overprinted by the post-collisional deformation that has affected other parts of Pakistan. For example, high-grade metamorphic rocks directly below the suture zone in Lower Swat pass southward into low-grade fossiliferous strata. There is no documented disruption of the stratigraphy by post-metamorphic faults such as is present in the Hazara region of Pakistan (Calkins and others, 1975; Bossart and others, 1988; Treloar and others, 1989b, Figures 1 and 2). In order to properly understand the structural development of the Lower Swat region, it is fundamental to establish the stratigraphy of the metamorphic rocks and to clarify their relationship to the fossiliferous strata in the south.

Previous attempts at establishing a stratigraphy have met with some success, but have fallen short of

clearly defining the limits, contact relationships, age, and correlation of each rock unit with the stratigraphy in other parts of Pakistan. At present, there is much confusion regarding these relationships. For example, recent workers have assigned a Precambrian (Searle and others, 1987; Treloar and others, 1989c) or all inclusive pre-Permian age to the metamorphic sequence (Butler, 1986; Coward and others, 1987) but give no evidence for their conclusions.

In this paper, I revise and describe the stratigraphy in the metamorphic rocks in detail. Evidence for unconformities within the stratigraphic section is presented and major lithologic differences between rocks above and below the unconformities are outlined. Age constraints, depositional environment, and correlation with the fossiliferous strata in the south are also discussed. In addition, a history of multiple granitic intrusions is demonstrated.

The conclusions presented in this report are based primarily on detailed mapping of the 43 B/6 15 minute quadrangle ($34^{o}30'$to $34^{o}45'$ latitude; $72^{o}15'$ to $72^{o}30'$ longitude) and on reconnaissance traverse mapping of surrounding areas. The geology of the study area is shown in Plate 1. A detailed map of the 43 B/6 quadrangle is presented in Plates 2 and 3.

PREVIOUS WORK

The stratigraphy of Lower Swat was originally established by Martin and others (1962) and by King (1964). They described a sequence of quartz-schists, amphibolites, calc-schists, and phyllites, which they named the Lower Swat-Buner schistose group (Figure 3a). The base of this sequence is intruded by augen and tourmaline granite gneisses which they called the Swat granites and granitic gneisses. Martin and others

(1962) and King (1964) considered at least the upper part of the Lower Swat-Buner schistose group to be Upper Paleozoic or younger on the basis of poorly preserved fossils at Nikanai Ghar (King, 1961). They did not suggest an age for the granitic gneisses although King (1964) suspected that they intruded during Himalayan-age deformation. Stauffer (1967; 1968) re-examined the fossils and assigned a probable Silurian-Devonian age to the metasedimentary rocks and a probable Tertiary age to the granitic rocks. A second reconnaissance visit to this area resulted in the same general conclusion (Jan and Tahirkheli, 1969).

In the Hazara region of Pakistan, Le Fort and others (1980) obtained a whole rock Rb/Sr date of 516 $\pm$16 Ma for emplacement of the Mansehra granite (Figures 1 and 2). This granite was later considered to be lithologically similar to, and therefore contemporaneous with, the granitic gneisses in Lower Swat (Jan and others, 1981; Le Fort and others, 1983). In order to explain the apparent discrepancy of Upper Paleozoic metasedimentary rocks intruded by Lower Paleozoic granitic rocks, Lawrence and Ghauri (1984), and Kazmi and others (1984, 1986) proposed that the granitic rocks intrude only the lower part of the metasedimentary sequence and that an unconformity separates these rocks from the overlying metasedimentary rocks. Based on the presence of an unconformity, Kazmi and others (1984) discarded the designation Lower Swat-Buner schistose group and introduced the name Manglaur schist for rocks intruded by granitic gneisses, and the names Alpurai schist and Saidu schist for rocks that unconformably overlie Manglaur schist and granitic gneisses (Figure 3b). Palmer-Rosenberg (1985), Ahmad (1986) and Ahmad and others (1987) found that the tourmaline granite gneisses intruded the lower part of the Alpurai schist

and therefore questioned the existence of an unconformity. They also introduced the name Nikanai Ghar marble for a thick sequence of poorly foliated marble in the southern part of Lower Swat which they considered to be in fault contact with the Alpurai schists (Figure 3c).

In this report I consider the Alpurai schist to be a group that is subdivided into the Marghazar, Kashala, Saidu, and Nikanai Ghar formations. The Manglaur schist and a new unit, the Jobra calc-silicates are considered to be formations separate from the Alpurai group. The Manglaur formation is Precambrian to Cambrian(?) in age and is intruded by augen-flaser granitic gneisses of probable Cambrian-Early Ordovician age (Figure 3d). The three largest bodies of augen-flaser gneiss are the Ilam, Loe Sar, and Sangar gneisses (Plate 2). Collectively they are referred to as the Swat gneisses. The Manglaur formation and Swat gneisses are separated from the Alpurai group by an erosional unconformity. Conodonts collected from the Alpurai group are Upper Paleozoic and Triassic in age (Pogue and Hussain, 1988; Pogue and others, in prep.). The Jobra formation, of unknown age, occurs as small isolated lenses between the Ilam gneiss and Alpurai group. I suspect that the Jobra formation unconformably overlies the Ilam gneiss and unconformably underlies the Alpurai group. Tourmaline granite gneiss intrudes the lower part of the Alpurai group. It is considered to be Paleogene(?) in age and separate from the Swat gneisses. Small bodies of biotite granite, metagabbro, carbonatite, and pyroxene granite also intrude the sequence. My generalized stratigraphy is compared with earlier versions in Figure 3.

GENERAL GEOLOGY

The Lower Swat sequence was deformed and metamorphosed during the Eocene and Oligocene (Lawrence and others, 1985; 1989). The largest structure is a gneiss dome with the Swat granitic gneisses and the Manglaur formation in the core (Plate 1). The rocks are at kyanite grade in the core of the dome where four fold phases are present (DiPietro and Lawrence, 1988; in prep.; chap. 3 this thesis). Outcrop-scale superposed F_1 and F_2 folds represent a syn-metamorphic progressive deformation. Both are tight to isoclinal and nearly recumbent with NNW-SSE axial trends. They are associated with the dominant regional foliation (termed S_2) and with west-vergent, large-scale folds (termed F_2). An earlier S_1 foliation is preserved locally in the micaceous rocks, but large-scale folds associated with F_1 are not recognized. F_3 and F_4 folds are developed on both a small and a large-scale. F_3 folds trend generally north-south and are also syn-metamorphic. They are open and upright with axial surfaces that dip steeply to the east. F_4 folds are upright to south-vergent with east-west axial trends (Plate 1). They are associated with retrograde metamorphism.

Deformation and metamorphism decrease gradually toward the south where, at Baroch, the rocks are at chlorite grade. The Kashala formation in this area is intruded by biotite-bearing granites of the Ambela complex. South of Daggar, the contact with the Ambela intrusive complex is sharp and parallel with foliation. Rafiq (1987) considers this to be an intrusive contact complicated by later shearing.

To the north, the Lower Swat sequence is truncated by the Main Mantle thrust zone (MMT) which consists of serpentinite, talc-carbonate schist, greenschist, and blueschist blocks in a sheared, greenschist facies

matrix (Kazmi and others, 1984; Lawrence and others, 1989). This suture zone separates the Lower Swat sequence from the Kohistan island arc sequence and is considered to be the western continuation of the 2500 km long Indus-Tsangpo suture zone (Gansser, 1964, 1980; Tahirkheli, 1979a, 1979b; Yeats and Lawrence, 1984). In some areas the MMT is more than a kilometer wide. The Kishora thrust defines the southern limit of the MMT, whereas the Kohistan thrust defines its northern limit (Kazmi and others, 1984; 1986; Lawrence and others, 1989).

In this report, the term psammitic schist refers to rocks with a fine-grained sandy texture consisting mainly of quartz and feldspar with minor mica. The mineral assemblages indicated below represent the overall average of numerous thin sections and are listed starting with the most abundant mineral first. Minor minerals are those that are common but are not present everywhere. Much of the chlorite above the garnet isograd is retrograde. Common rock types in each unit are listed in Appendix I.

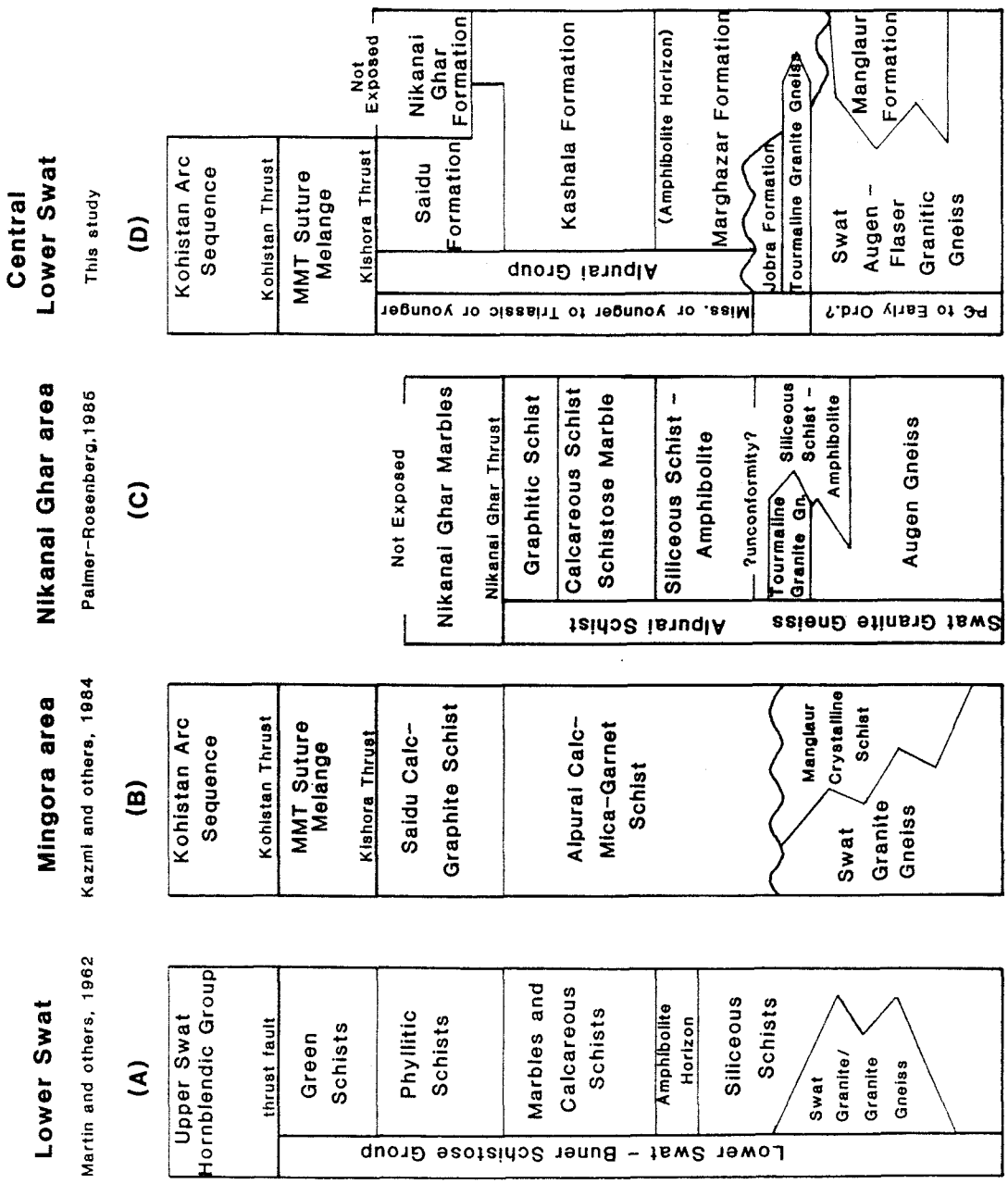

Figure 3. Comparative structural/stratigraphic columns from Lower Swat.

MANGLAUR FORMATION

The Manglaur formation is the oldest unit recognized. It is intruded by the Swat granitic gneiss and is unconformably overlain by the Marghazar formation of the Alpurai group. It takes its name from Manglaur village, 10 km east of Saidu (Kazmi and others, 1984). The proposed type locality is along the ridge, Baqar Mora, located immediately north of Pacha (Plate 2). The observed maximum exposed thickness, uncorrected for strain and folding is 1500 meters.

The Manglaur formation is restricted to the eastern part of the area below a thin layer of Ilam gneiss and partially above the Loe Sar gneiss (Plates 1 and 2). In the south, the overlying layer of Ilam gneiss locally pinches out so that the Manglaur formation is directly overlain by the Marghazar formation. All known occurrences of Manglaur formation are at garnet grade or higher. Descriptions by Martin and others (1962), however, suggest that the Manglaur formation may occur in lower grade rocks, along the northern margin of the Ambela complex, east of the study area.

The Manglaur formation is subdivided into three map units in the 43 B/6 quadrangle (Plate 2). Unit M1 is undifferentiated and consists predominantly of garnetiferous schists. Unit M2 is separated on the basis of abundant interlayers of quartzite, quartz mica schist and/or feldspathic quartzite which occur principally in the south, as lenses near the top of the Manglaur formation. Unit M3 is separated on the basis of abundant interlayers of tremolite marble, and occurs principally in association with unit M2. Minor interlayers of graphitic schist, biotite schist and amphibolite are present throughout the Manglaur formation. Rocks correlated with the Manglaur formation

are abundant in intruded zones A and B (Plates 1 and 2) and also occur as xenoliths in the granitic gneisses.

UNIT M1

Undifferentiated Manglaur formation consists principally of quartz-rich, garnetiferous schists composed of quartz, muscovite, biotite, oligoclase, and garnet. Typical exposures consist of micaceous garnet-bearing varieties that grade into, or are interlayered with, quartzo-feldspathic varieties in which garnet is less common. In many areas, the micaceous and quartzo-feldspathic rocks show distinctive layering at a scale of less than ten centimeters. Minor amounts of intrusive rock and rocks that characterize units M2 and M3 are included in this map unit.

UNIT M2

The principal rock types in this unit are foliated quartzite, garnetiferous quartz-mica schist, and feldspathic quartzite. The common mineral assemblage for the first two rocks is quartz-muscovite-garnet. Both plagioclase and biotite are absent. The feldspathic quartzites are characteristically dark colored and very fine-grained (<0.1 mm) with the assemblage quartz, sericite, biotite, oligoclase, and minor garnet. Locally they contain trace amounts of kyanite and fibrolite. Interlayers of pelitic schist are common.

In a peculiar outcrop at the south end of Baqar Mora the pelitic schists contain abundant lenses of quartzite that are two or three centimeters thick and up to six centimeters long. Most have the appearance of pebbles, however, a few are rectangular suggesting alternatively that they are actually pulled-apart remnants of thin quartzite layers.

UNIT M3

This unit is distinguished by the presence of tremolite marbles which occur principally as lenses or interlayers associated with unit M2. The marbles also occur locally in unit M1 where they are associated with pelitic schists or graphitic schists. The common assemblage is dolomite-tremolite-calcite with minor phlogopite or graphite. The assemblage quartz-tremolite-calcite is less common. A few interlayers of pure calcite marble also occur.

AGE AND CORRELATION

The Manglaur formation records a largely clastic deposit of quartz-rich sediments. Abundant foliated quartzite, quartz mica schist, and tremolite marble distinguish it from the Alpurai group.

There are no fossils in the Manglaur formation. Its age is, however, constrained by the age of the intruded Swat gneiss. Unfortunately, the Swat gneiss has not been radiometrically dated. Le Fort and others (1980; 1983), and Jan and others (1981) consider the Swat gneisses to be contemporaneous with Cambrian to Early Ordovician augen granite gneisses that are present throughout the Lesser Himalaya; including the Late Cambrian Mansehra granite in Hazara, Pakistan (Figure 1). If this correlation is correct, then the Manglaur formation can be no younger than Cambrian. Pogue and Hussain (1988) and K.R. Pogue (per. comm., 1989) have described lithologies similar to the Manglaur formation in the Precambrian to Cambrian(?) Tanawal formation east of Rustam (Figure 1). I, therefore, consider the Manglaur formation to be Precambrian to Cambrian in age and correlate it with the Tanawal formation of Pogue and Hussain (1988). Calkins and others (1975) indicate that the Tanawal formation in Hazara is intruded by the

Mansehra granite.

One problem with this correlation is that marble is more common in the Manglaur formation than in the Tanawal formation. The marble occurs as lenses near the top of the Manglaur formation. It is possible, therefore, that the Manglaur and Tanawal formations are stratigraphic equivalents but that the top of the Manglaur formation is younger than the top of the Tanawal formation.

SWAT GRANITIC GNEISS

The Swat augen-flaser granitic gneiss crops out as a series of elongate masses that extend across the study area. From west to east, the three largest are the Ilam (ISg1), Loe Sar (ISg2), and Sangar gneisses (ISg3) respectively (Plate 2). Three additional bodies are considered to be part of the same contemporaneous suite. These are the Choga and Mansehra granitic gneisses located east of Plate 1, and the Dopialo Sar granitic gneiss, located west of Plate 1 (Figure 1). Megacrystic granites also occur in the Ambela complex and some of these may be contemporaneous with the Swat gneisses. Small bodies of augen-flaser gneiss occur in the Manglaur formation.

Two main types of granitic gneiss are distinguished. The first is a flaser granite gneiss with a light-colored, coarse-grained groundmass (Figure 4a). The second is an augen granodiorite gneiss with a dark-colored, fine-grained groundmass (Figure 4b). Both contain equigranular leucogranitic gneisses with variable amounts of biotite, muscovite and rare magnetite. Xenoliths are common and resemble rocks in the Manglaur formation. Pegmatites and large quartz

veins are common only in the flaser gneisses.

The augen and the flaser gneisses are considered to be contemporaneous, although the flaser gneiss may represent a later intrusive phase. Contacts between the two are well exposed in the vicinity of Loe Sar and are typically gradational over several hundred meters. Sharp contacts occur locally.

Contacts between the Swat gneisses and the Manglaur formation are typically sharp and concordant with foliation although, in a few areas, the contact is interlayered or transects foliation at a low angle.

The contact between the Ilam gneiss and the Alpurai group is always sharp. This contact is an erosional unconformity which, in most areas, is concordant with foliation/bedding in the Alpurai group. In at least one area, discussed later, the contact is at a high angle to foliation.

FLASER GRANITIC GNEISS

The flaser granitic gneiss is, by far, the most abundant intrusive rock in the area. The Ilam and Sangar gneisses, as well as many of the smaller bodies, are composed primarily of flaser gneiss. In addition, the western and southern margins of the Loe Sar body are composed partly of flaser gneiss. The common assemblage is K-feldspar-quartz-plagioclase-muscovite-biotite. The latter two minerals occur in roughly equal amounts and together, make up about 10% of the rock. Epidote is the most common accessory phase although garnet and sphene also occur. Accessory tourmaline occurs in small clumps rather than disseminated throughout the rock. Butt and Shah (1985) reported blue beryl in veins associated with the Ilam gneiss. No blue beryl was found during this investigation and none was reported by previous workers (Martin and others, 1962; King, 1964; Jan and

Tahirkheli, 1969).

The flaser gneiss is characterized by abundant K-feldspar which occurs both as augen and as groundmass grains. In some areas, K-feldspar makes up more than 50% of the rock. The flaser texture is the result of nearly complete recrystallization of megacrysts into quartzo-feldspathic pods that are surrounded by an anastomosing, mica-rich, foliation (Figure 4a). Granite gneisses, compositionally identical to the flaser gneiss, but without the flaser texture occur in some areas. In other areas, the rocks are strongly lineated. The average grain size of the groundmass is between 0.75 and 1.0 mm.

A tectonic origin for the flaser foliation is clearly indicated where it crosses from flaser gneiss into equigranular, leucogranitic gneiss. The flaser foliation is pervasive throughout the Ilam and Sangar bodies. None of the Swat gneiss bodies become progressively more massive, augen-rich or undeformed toward their center. Augen-rich intervals occur randomly and are not uncommon near the margins of the gneiss. The largest augen in the flaser gneiss are 12 cm in their long dimension.

AUGEN GRANODIORITE GNEISS

Augen granodiorite gneiss is restricted to the Loe Sar area. Most of the Loe Sar body, part of the Ilam body southeast of Manglaur, and much of the intrusive rock in intruded zone B is composed of augen gneiss (Plates 1 and 2). The common assemblage is quartz-plagioclase-K-feldspar-biotite-muscovite. Biotite is commonly two or more times more abundant than muscovite, and these two minerals together make up as much as 20% of the rock. Garnet is the most common accessory phase. Epidote, tourmaline, sphene and rare kyanite (surrounded

by white mica) also occur.

Augen in the granodiorite gneiss are smaller and volumetrically less abundant relative to those in the flaser gneiss (Figure 4b). They occur dispersed in a very fine-grained, micaceous matrix in which the average grain size is less than 0.2 mm. The largest augen are less than 7 cm long and although fractured, they retain their original euhedral habit. Because the rock is so fine-grained, individual augen, less than 0.5 mm in diameter, can be recognized. Plagioclase augen are common in addition to K-feldspar. The overall texture is gneissic or mylonitic, rather than flaser, and is pervasive throughout the Loe Sar gneiss. The augen gneiss, in general, contains less K-feldspar and more biotite than the flaser gneiss.

Fine-grained gneisses, compositionally similar to the augen gneiss, but without augen, are common in the augen granodiorite gneiss. These layers contain appreciable amounts of garnet and rare kyanite. Some may be xenoliths, but more likely, most represent originally augen-poor aluminous granitic rock.

A biotite gneiss occurs as a thin mantle along the southwest margin of the Loe Sar gneiss (not shown in Plate 2). The rock is often mixed or interlayered with augen granodiorite gneiss and appears granitic (intrusive) in the field. Study of a single thin section revealed the assemblage plagioclase-quartz-biotite-sericite-garnet with kyanite present as relict grains preserved in sericite clots. The rock may represent a separate, late, phase of the Loe Sar intrusion, or may represent an area of local, "in situ," anatectic melt.

AGE CONSTRAINTS

No intrusive ages have been obtained for the Swat gneisses. The youngest possible age for emplacement is Mississippian, based on the unconformably overlying Mississippian or younger Alpurai group. Most workers consider the Swat gneisses to be contemporaneous with the Mansehra granites and gneisses of Hazara, Pakistan, which have a Late Cambrian whole rock Rb/Sr date of 516 ±16 Ma (Le Fort and others, 1980). Radiometric dates ranging from Cambrian to Lower Ordovician have been reported from other augen granitic gneisses in the Lesser Himalaya, (Le Fort and others, 1983; Le Fort, 1986). I, therefore, consider the Swat gneisses to be Cambrian to Early Ordovician in age. Older megacrystic granites (circa 1900 Ma) have also been reported (Valdiya, 1983). Exposures of the Mansehra gneiss at the latitude of Besham are texturally similar to the augen granodiorite gneiss.

Figure 4. Typical exposures of the Swat gneiss. a) Light-colored, coarse-grained flaser gneiss from the Ilam gneiss (St. 6-268). b) Dark-colored, fine-grained augen granodiorite gneiss from the Loe Sar gneiss (St. 6- 538). The pen in both photos is 12.5 cm long.

INTRUDED ZONE A

Intruded zone A consists principally of biotite-bearing quartzo-feldspathic schists and gneisses that contain either small augen of K-feldspar or small pods of recrystallized quartz and feldspar. The common assemblage is plagioclase-K-feldspar-quartz-biotite-muscovite with minor epidote. The augen and the recrystallized pods are typically less than one centimeter long. They occur either scattered in the rock or in layers in which they are variously abundant, sparse, or absent. Locally, the layers pass from augen-rich to augen-absent parallel to the strike of foliation. A few of the augen-rich layers west of D'kadda appear to be partially dismembered pegmatites.

The origin and correlation of this rock is not clear. It may be a metasedimentary rock that has been altered by metasomatism during intrusion of the Ilam gneiss. However, a granitic protolith is favored for several reasons; the rock unit lacks a clearly defined metasomatic reaction front; augen are absent in interlayered pelitic schists; the rock contains abundant K-feldspar which is not present in other rocks in the Manglaur formation; and its contact with the Ilam gneiss is locally gradational. The quartzo - feldspathic schists and gneisses may represent a local margin of granodioritic rock associated with the Ilam gneiss. Similar rocks, mostly without augen, are common as xenoliths (autoliths?) in the Ilam gneiss.

A lens of marble is present within intruded zone A near Sher Atrif (Plate 2). Included in this lens is a 7 meter thick layer of coarse-grained, unfoliated rock of nearly pure diopside (>95%). In thin section, the diopside is randomly oriented and fractured with ragged edges rimmed by tremolite. The fractures are filled

with tremolite and calcite. The diopside is believed to have formed by contact metasomation of a dolomite with silica-rich fluids expelled during intrusion of the Ilam gneiss. The fabric was altered, but not destroyed, by later, Himalayan-age, regional metamorphism. This conclusion lends support to an intrusive origin for the quartzo-feldspathic schists and gneisses, and shows that a thermal event, related to intrusion of the Ilam gneiss, preceded the regional metamorphic event.

Other rock types in intruded zone A include pelitic schists which are common in the central and northern parts of the belt, and tourmaline granite gneisses, which are abundant in the central part of the belt. Flaser gneisses, and biotite granites and granitic gneisses (described in a later section) occur throughout the belt. The pelitic schists are typically knotted with an abundance of large garnet porphyroblasts. In a few areas, near the contact with the Ilam gneiss, the schists contain large porphyroblasts of hornblende. These rocks are correlated with the Manglaur formation.

INTRUDED ZONE B

Intruded zone B consists of undifferentiated Manglaur formation that is invaded by, or interlayered with, leucogranites, leucogneisses, and augen granodiorite gneisses. Minor intrusive bodies, including amphibolite and carbonatite, also occur. The various intrusive rocks are present in layers ranging from less than one meter to more than 20 meters thick. Contacts with the metasedimentary rocks are sharp and generally parallel to foliation.

The leucogranites and leucogneisses are distinctive and, in general, are restricted to this map unit. The

composition and texture of these rocks are highly variable. Some contain the assemblage K-feldspar-quartz-plagioclase-biotite. Others lack both K-feldspar and biotite and/or contain appreciable muscovite, tourmaline and/or garnet. Most are coarse-grained. Some are massive, without a foliation, while others are strongly foliated. Along a roadcut south of Jambil, a dark grey, fine-grained rock, with the assemblage plagioclase-biotite-quartz-garnet-magnetite appears to grade directly into a light colored, coarse-grained, leucogneiss with the assemblage K-feldspar-quartz-plagioclase. All gradations between these two rocks occur.

Many of the intrusives, particularly the strongly gneissic ones, are probably contemporaneous with the Swat gneisses. However, unfoliated leucogranites locally cross-cut foliation in the schists. These are believed to have intruded during the Himalayan metamorphism.

JOBRA FORMATION

The Jobra formation is mapped separately from the Alpurai group and Manglaur formation because it is lithologically distinct and because its age and contact relationships with the other units is not certain. The Jobra formation crops out as small, isolated lenses that overlie the Ilam gneiss and underlie the Marghazar formation (Plate 2). The largest exposure and proposed type locality occurs in the village of Jobra, in the core of a major syncline south of Ilam. Smaller lenses also occur in this area and on hill 3338, which is located directly west of Pacha Fort (Plate 2). The Jobra formation is not in contact with the Manglaur

formation.

The principal rock in the Jobra formation is a fine-grained (<0.5 mm) wollastonite-bearing calc-silicate marble that occurs interlayered with quartzite, tremolite marble, pelitic schist and amphibolite. The assemblage of the wollastonite calc-silicate is calcite-microcline-hydrogrossular-grossular-wollastonite-salite-quartz with accessory sphene. The minerals are aligned parallel to a strong regional foliation and, in thin section, appear to be in textural equilibrium. The rock has a distinctive ribbed appearance on outcrop that is produced by the differential weathering of alternating centimeter thick layers of tremolite marble. The tremolite marble contains calcite, dolomite, tremolite, and chlorite and is similar to marble in the Manglaur formation, except for the presence of chlorite.

The lower contact with the Ilam gneiss is sharp with no interlayering. It is not clear if this is an intrusive or unconformable contact. Shams (1963) reported a similar calc-silicate assemblage in a xenolith within the Ilam gneiss near the village of Manglaur. If the Jobra formation correlates with this xenolith then the contact with the Ilam gneiss is intrusive. In this case, the Jobra formation may correlate with either the Early Cambrian Ambar dolomite of Pogue and Hussain (1988) and Pogue and others (in prep.), or with the Manglaur formation. Pogue and others (in prep.) indicate that the Ambar dolomite pinches out toward the north and, therefore, should not be present in Lower Swat. A correlation with the Manglaur formation is not favored because similar wollastonite-bearing calc-silicate rocks are absent in the Manglaur formation, and because the Jobra formation is nowhere in contact with the Manglaur formation.

If the Jobra formation unconformably overlies the Ilam gneiss, then it may correlate with either the Marghazar formation, or with part of the Early and Middle Paleozoic shelf sequence that is present south of the study area, in the Peshawar basin (Pogue and others, in prep.). The Jobra formation is not considered to be part of the Marghazar formation because calc-silicate rocks, tremolite marbles, and quartzites are absent in the Marghazar formation. In addition, the contact relationships between these two units (discussed in a later section) suggests, very strongly, that the Marghazar formation unconformably overlies the Jobra formation. My favored interpretation, therefore, is that the Jobra formation unconformably overlies the Ilam gneiss, and unconformably underlies the Marghazar formation such that the Jobra formation correlates with part of the Early and Middle Paleozoic shelf sequence in the Peshawar Basin. It may correlate with quartz-bearing limestones of the Devonian Nowshera Formation. In the Peshawar Basin, the Nowshera Formation unconformably underlies rocks that are stratigraphically equivalent to the Marghazar formation (e.g. the Jafar Kandao formation of Pogue and others, in prep.).

ALPURAI GROUP

The Alpurai group rests unconformably upon the Manglaur formation and Swat gneisses. It takes its name from Lower Alpurai village 32 km east of Saidu (Kazmi and others, 1984). The Alpurai group has a well defined, coherent stratigraphy that is subdivided into four formations. The general stratigraphic sequence is given in Figure 3d. The Marghazar formation occurs at the base and consists of pelitic, amphibolitic and

psammitic schists, phlogopite marbles, and amphibolites. It is overlain by the Kashala formation which consists of garnetiferous calc-schists, calc-phyllites, marbles and dolomitic marbles. The Kashala formation is overlain by black graphitic phyllites of the Saidu formation in the north, and by marbles and dolomitic marbles of the Nikanai Ghar formation in the south. Each formation is characterized by facies changes and thickness variations such that there is at least partial chronostratigraphic or lithologic equivalence between them. None of the above rock types are exclusive to a particular formation except for the psammitic and amphibolitic schists which are found only in the Marghazar formation. The names Marghazar and Kashala are new. Saidu calc-graphite schist (Kazmi and others, 1984) and Nikanai Ghar marble (Palmer-Rosenberg, 1985; Ahmad, 1986) were used previously for rocks that are considered herein to be part of the Alpurai group.

MARGHAZAR FORMATION

The Marghazar formation crops out in a belt that surrounds the Manglaur formation and Swat gneiss (Plate 1). South of the garnet isograd the Marghazar formation is mapped as the Jafar Kandao formation and Karapa greenschist by Pogue and others (in prep.) who have traced it further south into the Peshawar Basin (K.R. Pogue, pers. comm., 1989). The Marghazar formation takes its name from Marghazar village, 6 km south of Saidu. The proposed type locality is along Saidu Khwar (creek) and the adjacent road north and south of Marghazar village. The lower part of the Marghazar formation is intruded by tourmaline granite gneiss. The maximum observed thickness, including effects of

metamorphic flattening and internal folding is 1000 meters in the vicinity of Pacha where the Marghazar formation unconformably overlies the Precambrian Manglaur formation, and >1000 meters near Baroch, where the stratigraphically equivalent Jafar Kandao formation unconformably overlies the Devonian Nowshera Formation (Pogue and Hussain, 1988). Throughout most of its extent the Marghazar formation overlies granitic gneiss and is never more than about 500 meters thick. It thins to less than 50 meters in the area northwest of Dosara. The Jafar Kandao formation has yielded Late Devonian-Early Mississippian, Early Mississippian (Osagian), and Middle Pennsylvanian (Atokan) conodonts, indicating that the Marghazar formation is Mississippian or younger (K.R. Pogue, pers. comm., 1989; Pogue and others, in prep.). In a later section, I argue that most, or all, of the Marghazar formation is Pennsylvanian or younger. The Marghazar formation is subdivided into four map units in the 43 B/6 quadrangle (Plate 2). Each unit is briefly discussed below.

UNIT Aml

Unit Aml occurs either as a thin discontinuous horizon, or as isolated lenses, at or near the base of the Marghazar formation. The principal rock type is a dark grey to brown weathered phlogopite marble composed of calcite (70-90%), quartz, plagioclase, clinozoisite, phlogopite, muscovite, ilmenite, and minor sphene. At the outcrop, this rock resembles the calc-schists in the Kashala formation but it differs by containing phlogopite which is rare in the Kashala formation. White calcite marbles, some with accessory tremolite, phlogopite, dolomite and/or chlorite, also occur in this unit as do thin interlayers of pelitic, psammitic, and amphibolitic schist.

The phlogopite marbles occur principally in the northern part of the B/6 quadrangle where locally, they make up more than half of the Marghazar formation. Near Sipar, marbles and calc-schists, identical to those in the Kashala formation (eg. without phlogopite), occur throughout the Marghazar formation. Here the two formations are separated on the basis of interlayered psammitic schists and amphibolites in the Marghazar formation which are absent in the Kashala formation. When present, the phlogopite marbles form an important marker horizon that can be used to delineate the unconformity at the base of the Marghazar formation.

UNIT Am2

Unit Am2 represents the undifferentiated part of the Marghazar formation. The principal rock types are garnetiferous muscovite schist, epidote-biotite schist, and amphibolitic schist. Psammitic schist, feldspathic quartzite, calcite marble, amphibolite and rare graphitic schist also occur. Argillite, limestone, sandy limestone, quartzite and conglomerate occur near Baroch in the correlative Jafar Kandao formation.

The common mineral assemblage in the muscovite schist is quartz-muscovite-oligoclase-biotite-garnet with minor epidote, chlorite, ilmenite, rutile, and graphite. Locally, it grades into a calcareous schist. This is the only rock in the Alpurai group that is easily confused with schists in the Manglaur formation. Typically, the Marghazar schists contain less garnet and more mica, epidote, and calcite, relative to the schists in the Manglaur formation.

The biotite schists are distinctive in that they consist of up to 80% biotite and locally contain large cream colored porphyroblasts of epidote group minerals. The common assemblage is biotite-quartz-epidote-

plagioclase with minor calcite. The epidote in this rock, and throughout the Alpurai group, is Fe-poor epidote/clinozoisite with either normal or anomalous blue, middle-first-order interference colors. The optic sign can be negative or positive for different grains within a single thin section. In some instances, epidote is zoned from anomalous blue in the core to first order grey at the rim. Inclusions within garnet are typically anomalous blue.

The amphibolitic schists form a major part of unit Am2. The common assemblage is hornblende-quartz, however, these rocks are highly variable and may contain abundant biotite, epidote, garnet, plagioclase, muscovite, ilmenite, rutile, and/or calcite. They grade directly into amphibolites, biotite schists, and biotite-bearing psammitic schists. The relationships suggest a volcaniclastic protolith.

UNIT Am3

This unit consists principally of biotite-bearing psammitic schists interlayered with amphibolites. Minor interlayers of pelitic schist, amphibolitic schist, and calcite marble also occur. The psammitic schists form strong resistant outcrops which often have a gneissic texture that distinguishes them from other rocks in the Marghazar formation. The common assemblage is plagioclase-quartz-biotite, however, they are variable and locally contain significant amounts of muscovite, garnet, hornblende, k-feldspar, calcite, chlorite, and/or graphite.

Unit Am3 is mapped in three areas in the B/6 quadrangle (Plate 2). In the area northeast of Pacha it occurs at the base of the Marghazar formation in contact with augen gneiss. From here, it thins southward and transgresses up section until it is directly below the

amphibolite horizon (unit Am4) where it pinches out. Small pebbles of granitic material (intergrown plagioclase, highly perthitic microcline, and quartz), some up to 1/2 centimeter long, occur in the northern part of this lens. In the area just south of Marghazar, the psammitic schists dominate the entire section from the Ilam gneiss to the contact with the amphibolite horizon (unit Am4). In the third area, east of Amlukdarra, the psammitic schists are restricted to the upper part of the Marghazar formation just below the amphibolite horizon. A thin layer of biotite schist is common at the contact with the amphibolite horizon. The transition from muscovite schist (unit Am2) to psammitic schist (unit Am3) appears gradational in all three areas.

The origin of the K-feldspar in the groundmass of some of the psammitic schists is significant in terms of the regional interpretation of the Marghazar formation. Three possibilities exist: 1) the protolith was a granite; 2) the protolith was an arkose; 3) the K-feldspar is metamorphic in origin. In either of the first two possibilities the K-feldspar would be interpreted as part of the original protolith that recrystallized during subsequent metamorphism. The field relationships suggest that the psammitic schists are sedimentary in origin. The schists themselves are highly variable in composition and locally contain small pebbles. They occur in a well layered sequence that includes marbles, muscovite schists, and amphibolites. They show no cross cutting relationships and locally, they grade into biotite schists or amphibolitic schists. Similar psammitic schists occur as minor interlayers in units Am1 and Am2. The first possibility is therefore eliminated. Although the metamorphic grade is high, there is no conclusive evidence that the

K-feldspar formed during regional metamorphism. Muscovite is present in some of the rocks, but aluminosilicate minerals are absent. The preferred interpretation, therefore, is that the psammitic schists represent a metamorphosed arkose, with K-feldspar-bearing clasts, preserved from the original protolith. The logical source for the K-feldspar is the Swat gneiss directly below the Marghazar formation. This conclusion supports the interpretation of an unconformity between the Marghazar formation and the Swat gneisses.

UNIT Am4

This unit consists of a persistent amphibolite horizon that was first recognized by Martin and others (1962) and King (1964) (Figure 3a). It is 20 to 50 meters thick and is present at the top of the Marghazar formation throughout the study area. Except for rare interlayers of feldspathic quartzite, no other rock types are present. In the area northwest of Dosara, the Marghazar formation is less than 50 meters thick and, except for a very thin sequence of pelitic schist, consists entirely of the amphibolite horizon.

The amphibolites in unit Am4, and throughout the Marghazar formation, are typically dark greenish grey, fine-grained (<0.5 mm), and well foliated. Medium or coarse-grained varieties are rare. The common assemblage is hornblende-plagioclase-quartz with minor garnet, epidote, biotite, calcite, ilmenite, and rutile. Hornblende typically makes up between 80 and 95 percent of the rock. The hornblende defines a foliation plane, but does not form a lineation. Just south of Daggar, the amphibolite horizon is lower grade and consists of hornblende/actinolite, albite, epidote, quartz, chlorite, and sphene with minor biotite, calcite and ilmenite. Further south near Baroch, the assemblage

is chlorite-quartz-ilmenite-albite-sphene with minor white mica. Pogue and others (in prep.) refer to the rock in this area as the Karapa greenschist. Here, the Karapa greenschist directly overlies the Jafar Kandao formation.

KASHALA FORMATION

The Kashala formation underlies a large area of Lower Swat on both the north and south flanks of the Nikanai Ghar formation. It takes its name from Kashala mountain about 13 km SSW of Saidu. The proposed type locality is along roadcuts on Dop Sar, just south of Saidu (Plate 2). The Kashala formation consists almost entirely of calcareous rocks. Pelitic schists and argillites occur but amphibolites, psammitic schists, and quartzites are absent. The observed thickness north of the Nikanai Ghar formation is between 300 and 700 meters. It thickens toward the south to more than 1200 meters near Baroch. The middle part of the Kashala formation, near Baroch, has yielded Upper Triassic (Carnian) conodonts suggesting a Triassic age for the Kashala formation and a Triassic or younger age for the Saidu, and Nikanai Ghar formations (K.R. Pogue, pers. comm., 1989; Plate 1). The lower contact with the amphibolite horizon of the Marghazar formation is sharp with minor interlayering within 1/2 meter of the contact. The rocks north and south of the Nikanai Ghar formation differ in some respects and will be described separately.

NORTHERN AREA

The following discussion applies to the area north of the Nikanai Ghar formation. In this area, the Kashala formation consists principally of three rock types: garnetiferous calc-schist, schistose marble; and

dark-grey foliated marble. These rocks occur interlayered on all scales from centimeter to tens of meters thick. Contacts between them are sharp, however, they grade into each other along strike such that the schistose marbles represent a rock type intermediate between the other two.

The calc-schist is fine-grained (<1.0 mm) and consists of muscovite, quartz, calcite, ilmenite, and garnet with common epidote, plagioclase, and rutile, and minor graphite, and chlorite. Rare pelitic layers lack calcite entirely. As calcite becomes more abundant, and garnet, muscovite and epidote become less abundant, the calc-schist grades into a schistose marble and finally into a well-foliated, dark-grey, medium-grained, marble with more than 95% calcite and only minor quartz and muscovite. Radiating prisms of amphibole occur, but biotite is absent, and dolomite is extremely rare. Kyanite (Martin and others, 1962; King, 1964; Tahirkheli and others, 1979), andalusite (King, 1964; Kazmer, 1986), staurolite (King, 1964), and cordierite (Palmer-Rosenberg, 1985), have been reported in these rocks but none were found within the confines of Plate 1. Chloritoid was found at one location shown in Plate 1. Quartz veins with coarse-grained kyanite occur in the Kashala formation further west, near Thana, and further east of Dosara.

There are minor changes in the rocks as the garnet isograd is approached. Garnet, in the calc-schists, becomes noticeably less abundant about three kilometers north of the garnet isograd. Southward, the rocks are finer-grained calc-phyllites with calcite, quartz, muscovite, ilmenite, rutile, and minor chlorite or epidote.

These rocks make up more than 90% of the northern Kashala formation. The only other common rocks are

coarsely crystalline marble that occurs in thin discontinuous lenses throughout the Kashala formation, and graphitic phyllite and schist which are restricted to the vicinity of Sipar and Bagra. The crystalline marbles and graphitic phyllites resemble rocks in the Nikanai Ghar and Saidu formations respectively.

The general stratigraphic succession of rocks in this part of the Kashala formation changes from north to south. In the north, most of the Kashala formation consists of garnetiferous calc-schist and schistose marble with minor foliated marble principally near the base. In the south, most of the Kashala formation consists of foliated marble and schistose marble. Calc-schist is less common and occurs principally near the base. West of Jowar, where the Kashala formation underlies the southern belt of Saidu formation, the schistose marble dominates the entire section.

SOUTHERN AREA

The following discussion applies to the area south of the Nikanai Ghar formation. The rocks previously described are present in this area but the dark-grey, foliated, calcite marble, dominates the entire stratigraphic succession. In addition, a fine-grained (<0.1 mm), poorly foliated, dolomitic marble is common from Daggar southward. This rock occurs as layers that pass directly into calcite marble, and is identical to the dolomitic marble in the Nikanai Ghar formation.

In summary, the rocks north and south of the Nikanai Ghar formation, although similar in many ways, show some marked contrasts. On the north side, the rocks consist almost entirely of calc-schist and marble, with marble becoming more abundant toward the south. Marble dominates the entire succession on the south side but the rocks are more variable with the addition of

dolomitic marble.

SAIDU FORMATION

The Saidu formation occurs in a northern belt that crops out along the south side of the Main Mantle thrust zone and in a southern belt that crops out near Jowar (Plate 1). The western continuation of the southern belt has not been mapped. One possibility is that it connects with the northern belt on the west side of the Dopialo Sar granitic gneiss, which is located immediately to the west of the study area (Figure 1). Another possibility is that it is a lens that pinches out toward the west. The type location of the Saidu formation is along road cuts east of Mingora, one kilometer north of Saidu (Martin and others, 1962; Kazmi and others, 1984). The present thickness of the Saidu formation varies from zero where it pinches out against the Nikanai Ghar formation to a maximum of about 1000 m west of the study area.

The Saidu formation consists almost entirely of fine-grained (<0.2 mm), grey to black, phyllite and phyllitic schist. Silty, laminated intervals occur locally but psammitic and amphibolitic intervals are absent. The common assemblage is muscovite-quartz-graphite-rutile-ilmenite with minor epidote, chlorite, and plagioclase. Garnet is present locally, but is uncommon, and does not characterize the rock. Interlayers of brown weathered schistose marble and dark grey, foliated marble (similar to those in the Kashala formation) represent the only other common rock types. These interlayers vary from a few centimeters to several tens of meters thick.

The lower contact is abrupt with typical Saidu phyllites in sharp contact with schistose marbles or garnetiferous calc-schists of the Kashala formation.

Near Sipar, the contact is less abrupt; graphite-bearing schists are present on both sides of the contact. Here the contact is placed where garnetiferous schists are no longer abundant. Stratigraphic equivalence between the lower part of the Saidu formation and the upper part of the Kashala formation is suspected because both underlie the Nikanai Ghar formation in the vicinity of Jowar and the Kashala formation becomes thicker toward the east where the Saidu formation pinches out (Plate 2).

The upper contact of the Saidu formation, in the northern belt, is with the Kishora thrust of the MMT zone. In the area just west of Saidu village, the Saidu phyllites are in sharp contact with distinctly green phyllites that contain lenses of talc carbonate and greenschist. These latter two rock types have been correlated with the Main Mantle thrust melange (Kazmi and others, 1984; 1986; Lawrence and others, 1989). The Kishora thrust, therefore, is placed at the first appearance of abundant green phyllite. Black phyllite and schistose marble occur within the green phyllite near the contact. Also, lenses of talc schist occur locally in the Saidu formation. These relationships indicate that the rocks are imbricated and that imbrication extends into the Saidu formation. The rocks in this area are very fine-grained and rarely show distinctive mylonitic fabrics.

NIKANAI GHAR FORMATION

The Nikanai Ghar formation is a large lens shaped body that occurs in the south-central part of Lower Swat (Plate 2). It consists of a well layered sequence of marbles and dolomitic marbles in which schistose, phyllitic or psammitic rocks are rare and amphibolites are absent. It takes its name from Nikanai Ghar, located about 25 km south of Saidu. The proposed type

locality is along stream valleys on the south side of Jafar Sar (Plate 2). The maximum exposed thickness of the Nikanai Ghar formation is about 1200 meters in the southern part of the area. The top of the formation is eroded.

The Nikanai Ghar formation consists principally of three rock types, all of which occur in lesser quantity in the Kashala formation. These are dark grey, foliated, calcite marble commonly with 1/2 cm bands of dolomitic marble; variegated, coarsely crystalline marble; and fine-grained (<0.1 mm) dolomitic marble. The dolomitic marble consists of up to 90% dolomite and typically occurs in lenses that pass directly into calcite marble. Relatively uncommon rock types include carbonate breccia; schistose marble (similar to Kashala formation); calcareous phyllite; graphitic phyllite (similar to Saidu formation); and feldspathic quartzite. The various rock types are interlayered at a scale of centimeters to tens of meters thick.

The contact between the Nikanai Ghar and Kashala formations is gradational. Thick sequences of dark grey marble occur in the Kashala formation near the contact along with minor intervals of schistose marble, garnetiferous calc-schist, and/or calc-phyllite. The contact is placed above the last appearance of schistose rock. This coincides roughly with the first appearance of crystalline marble in the Nikanai Ghar formation. Dark grey marbles are abundant on both sides of the contact.

Much of the thinning in the lens shaped Nikanai Ghar formation is apparently accommodated by facies changes with the Kashala formation along the southeastern contact between Daggar and Bagra. The contact on the northwest side remains at roughly the same stratigraphic position. On the southeastern side,

there is a gradual increase of interlayered calc-schist, coupled with a decrease of crystalline marble at progressively higher stratigraphic intervals from south to north toward Bagra. At its northeastern termination, near Bagra, crystalline marble is interlayered with schistose marble and garnetiferous calc-schist. Beyond this point, the Nikanai Ghar formation is not recognizable as a distinct lithologic unit. These relationships suggest at least partial stratigraphic equivalence between the top of the Kashala formation and the Nikanai Ghar formation.

At its southwestern end, northwest of Baroch, the Nikanai Ghar formation extends for less than five kilometers west of the study area where it terminates. Here the Nikanai Ghar formation completely overlies the Kashala formation. The termination, in this area, is due to erosion rather than to a facies change (K.R. Pogue, pers. comm., 1989).

The Nikanai Ghar formation is at the same stratigraphic position as the Saidu formation. Both overlie the Kashala formation in different parts of the map area. Near Jowar, where the Nikanai Ghar and Saidu formations are in contact, the Nikanai Ghar formation overlies the Saidu formation with a sharp contact. Palmer-Rosenberg (1985) mapped this contact as a south dipping, late to post-metamorphic fault. He based this conclusion on stratigraphic and structural discontinuities and on lithologic contrasts between the various units he was mapping as well as on a sheared and brecciated contact. He considered the fault to be a southward directed thrust with the Nikanai Ghar formation on the upper plate. This, in effect, makes the Nikanai Ghar formation a klippe or gravity slide block that was transported from north to south.

My own investigation suggests that this is a depositional contact. The contact is well exposed in several areas and no evidence of shearing or brecciation was noted. The continuation of this contact toward the east, between the Kashala and Nikanai Ghar formations, is highly gradational. Therefore, if shearing is present, it is minor in extent and does not appear to significantly disrupt the stratigraphy.

AGE, FACIES CHANGES, AND DEPOSITIONAL ENVIRONMENT OF THE ALPURAI GROUP

The Alpurai group is a well stratified unit with four distinctive formations. It is distinguished from the Manglaur formation by its overall stratigraphic continuity, by the abundance of calcareous, amphibolitic, and epidote-rich rock, and by the general lack of quartzite, quartz-mica schist, and tremolite marble.

The stratigraphy and facies characteristics of each formation in the Alpurai group are different in different parts of the study area. The general sequence in the northern part of the B/6 quadrangle is Marghazar marbles, schists, and amphibolites overlain by Kashala calc-schists, overlain by Saidu black phyllites (Plate 4b). In the southwestern part of the B/6 quadrangle, a similar sequence is overlain by the Nikanai Ghar marbles (Plate 4a). Further east, in the south-central area, the Saidu phyllites are absent and the stratigraphic sequence is Marghazar schists and amphibolites, overlain by Kashala schistose marbles, overlain by Nikanai Ghar marbles (Plate 4c). Still further east, near Bagra, the Nikanai Ghar marbles thin and appear to be both overlain and underlain by Kashala schistose marbles before pinching out entirely (Plate 4e). Reconnaissance in this area suggests that the Kashala formation is

overlain by Saidu black phyllites as shown in Plate 4e. In all of these areas, the Alpurai group unconformably overlies the Ilam gneiss or the Manglaur formation.

Alpurai group becomes thicker south of the 43 B/6 quadrangle near Baroch. Here, the stratigraphic sequence consists of Jafar Kandao (Marghazar) argillites, calc-phyllites, marbles, and conglomerates with the Karapa greenschist at the top. This sequence is overlain by Kashala marbles and calc-phyllites, which are overlain by Nikanai Ghar marbles (Plate 4d). Here, the Swat gneisses are absent and the Jafar Kandao formation unconformably overlies a thick sequence of Devonian and older quartzites, limestones, and argillites that span the Early and Middle Paleozoic (Pogue and Hussain, 1988; Pogue and others, in prep.). Part of this sequence has no obvious counterpart to the Lower Swat section and is younger than the supposed Cambrian to Early Ordovician Swat gneiss. This suggests that the Swat gneiss existed as a highland fault block near the outer edge of the continental shelf while shelf deposition was occurring further south (eg. shoreward, present position) during, and perhaps prior to, the time the Marghazar formation was deposited. The abrupt thickness changes in the Marghazar formation, from less than 50 meters to more than 1000 meters, near Bagra, also suggests syn-depositional faulting. In this area, the Marghazar formation is thickest where it overlies the Manglaur Formation and thins markedly where it overlies the Swat gneiss (Plate 1). The presence of granitic pebbles in unit Am3 of the Marghazar formation indicate a granitic source area. The relationships suggest that the Manglaur formation was uplifted and preferentially eroded producing a small depositional basin that was flanked by the eroding Swat gneisses and filled by the Marghazar formation as depicted in Plate

4e. The Marghazar formation, therefore, is interpreted to have been deposited on an irregular, erosional surface during active faulting.

The correlation between the Marghazar formation and the Jafar Kandao formation is based on similar lithologies in both units and on the presence of the amphibolite/greenschist horizon at the top of both units. Conodont-bearing samples of Late Devonian-Early Mississippian, and Early Mississippian (Osagean) age were recently collected from the Jafar Kandao formation south of Baroch (analyzed by B. Wardlaw; K.R. Pogue, pers. comm., 1989). A third sample from just below the Karapa greenschist, near Baroch, yielded a Middle-Pennsylvanian (Atokan) age (Plate 1). Conglomerates in the Jafar Kandao formation stratigraphically above the Early Mississippian conodont localities indicate that erosional unconformities are present in the sequence (K.R. Pogue, per. comm., 1989). Conglomerates are absent, but the variable lithologies suggest that erosional unconformities or disconformities may also be present in the Marghazar formation. On the other hand, amphibolites are present throughout the Marghazar formation, whereas greenschists are restricted to the top of the Jafar Kandao formation stratigraphically above the Middle Pennsylvanian fossil locality. In addition, the Jafar Kandao formation is, on average, more than twice as thick as the Marghazar formation. These relationships suggest that the Marghazar formation may correlate with only the top part of the Jafar Kandao formation and be entirely Pennsylvanian or younger.

The fossil ages in the south, and the stratigraphic correlations, indicate a post-Middle Pennsylvanian age for the amphibolite horizon at the top of the Marghazar formation. The widespread occurrence of this horizon, the association of the amphibolites with metagabbro

(discussed later), and the gradational contacts between the amphibolites, amphibolitic schists, biotite schists and psammitic schists, support the conclusion of Ahmad (1986) that the amphibolite horizon is a basaltic flow. The associated amphibolites, schists, and marbles may represent flows, tuffs, arkoses, or clastic limestones. Thus, the Marghazar formation may be a rift-related deposit and correlate with the Pennsylvanian to Lower Triassic "Agglomeratic slates" and Panjal Traps of western India (Wadia, 1934; Gansser, 1964; Fuchs and Gupta, 1971; Honegger and others, 1982). There are few feeder dikes in the study area. A possible source for the Marghazar amphibolites is east of the study area where A. Hussain (pers. comm., 1988) and Rafiq (1987) have reported abundant amphibolite and dolerite dikes.

The amphibolite horizon marks the end of volcanic and volcaniclastic deposition in Lower Swat. Subsequent deposition of the largely calcareous Triassic and/or younger Kashala and Nikanai Ghar formations suggests subsidence to continental shelf conditions. These rocks may correlate, in part, with the Upper Permian to Eocene Zanskar Supergroup of western India (Searle, 1983). The graphitic phyllites in the Triassic or younger Saidu formation may represent a transition to deeper water oceanic conditions, or possibly represent a starved basin. It may correlate with the Triassic to Cretaceous(?) Lamayuru formation of western India (Frank and others, 1977; Gansser, 1980, 1981). The Alpurai group, therefore, may record the entire history, from Late Paleozoic shallow water rifting associated with the breakup of Gondwana; to oceanic sedimentation associated with development of the Tethys ocean basin.

TOURMALINE GRANITE GNEISS

The tourmaline granite gneiss intrudes principally along the unconformity between the Ilam gneiss and Marghazar formation. Small lenses also occur within the Swat gneisses but are less common in the metasedimentary rocks. A mappable lens of tourmaline granite gneiss occurs in the Marghazar amphibolite horizon (unit Am4) on the ridge one kilometer southwest of Amlukdarra (Plate 2). This locality represents the stratigraphically highest occurrence known of tourmaline gneiss in the Alpurai group.

The texture and composition of the tourmaline gneiss are fairly consistent. It is typically leucocratic, equigranular, and well-foliated, with local lineated zones. The common assemblage is quartz-plagioclase-K-feldspar-muscovite with minor black tourmaline. Biotite typically is absent. The average grain size is between 0.5 and 1.5 mm. The rock grades locally into a finer-grained leucogneiss with the assemblage K-feldspar-quartz-plagioclase-biotite-muscovite. Tourmaline is typically absent in this rock. Rare interlayers of tonalitic gneisses occur, as well as interlayers of tourmaline aplite and tourmaline-bearing pegmatite. Augen are absent except for rare, widely scattered K-feldspar megacrysts less than two centimeters long. Discontinuous pegmatite stringers are present in many areas, and locally, these resemble the flaser texture of the Ilam gneiss.

Field relationships indicate that the tourmaline granite gneiss intrudes the Marghazar formation (Palmer-Rosenberg, 1985). Along much of its extent the contact is concordant with foliation and interlayering is absent. However, in a few areas, most notably at Amlukdarra (Plate 2), the contact is strongly

interlayered. Amlukdarra is also notable for the abundance of tourmaline. Quartz-garnet-tourmaline dikes and veins several meters thick, and with up to 50 percent tourmaline, occur in both the tourmaline granite gneiss and the Marghazar formation in this area.

Contacts between the tourmaline gneiss and the Swat gneisses are well exposed. In general, the contacts are sharp and concordant with the regional foliation although interlayering is common. In several areas, the flaser texture in the Ilam gneiss is poorly developed and the contact appears gradational. The rocks, however, can be distinguished based on the overall finer grain size, lighter color, presence of tourmaline, and absence of biotite, in the tourmaline granite gneiss.

The tourmaline granite gneiss was previously considered to be a late stage variant of the Swat gneisses (Martin et al.,1962; King, 1964; Palmer-Rosenberg, 1985; Shams, 1983). However, a younger age is demonstrated by the observation that metagabbros, amphibolites, and biotite granites intrude the Swat gneiss but are intruded by the tourmaline gneiss.

The age of the tourmaline gneiss is poorly constrained. In a few places, principally in the vicinity of Jogiano Sar, undeformed tourmaline pegmatites crosscut and post-date the foliation in the Swat gneiss. These post-deformational intrusions may be a late phase of the tourmaline granite gneiss. If so, then the tourmaline gneiss intruded during the Himalayan deformation and therefore is Paleogene in age. Fernandez (1983) previously considered moderately deformed tourmaline aplite and pegmatite veins in the Mansehra granite to be of Himalayan age. Also, Misch (1949) reported undeformed tourmaline granites in the Nanga Parbat massif of northern Pakistan.

One of the most interesting aspects of the tourmaline granite gneiss is that it intrudes as a sill principally along the unconformity between the Ilam gneiss and the Marghazar formation. As noted earlier, the Swat gneisses may have existed as a highland fault block near the outer edge of the continental shelf during part of the Paleozoic shelf deposition further south. It may have been along a major normal fault associated with this horst block that the tourmaline granite later intruded. The intrusion was deflected into a sill at the Ilam gneiss-Marghazar formation contact.

MINOR INTRUSIVE ROCKS

Several other intrusive rock types of minor extent occur in the 43 B/6 quadrangle. These include biotite granites and granitic gneisses, metagabbros, pyroxene granites, and carbonatites. In addition, two rocks of questionable protolith discussed here.

BIOTITE GRANITE AND GRANITIC GNEISS

These are the most extensive of the minor intrusive rock types. They occur as isolated lenses along a discontinuous belt that roughly coincides with intruded zone A. Three different groups of biotite granites and granitic gneisses are distinguished on the basis of mineralogy and texture. All three intrude the Ilam gneiss but are intruded by tourmaline granite gneiss. None intrude the Alpurai group.

The first group (BG1) are granites that occur at five isolated localities, none of which are easily accessible. The two most accessible are the northernmost locality at Salam Khan (located about

halfway between Saidu and Kokarai), and the southernmost locality located about two kilometers west of Pacha Fort. These rocks are grouped as a single unit based on similar mineralogy and texture, however it is not known if they are contemporaneous.

The rocks are equigranular with an average grain size of about 1 mm. Small (<1 cm) megacrysts of K-feldspar occur sporadically. Generally they are weakly foliated or without foliation. The common assemblage is plagioclase-quartz-K-feldspar-biotite, but actual mineral proportions are quite variable. In several thin sections quartz makes up less than 20% of the rock, and in one of these, K-feldspar is the most abundant phase. Biotite typically makes up between 10 and 15% of the rock. Muscovite (sericite) is restricted to alteration inclusions in plagioclase. Minor hornblende was noted in the field but none was seen in thin section. Rutile occurs as inclusions in quartz in one thin section. Igneous textures are locally preserved in which K-feldspar megacrysts are euhedral, unfractured, and contain inclusions of euhedral biotite and plagioclase. The plagioclase in the groundmass is also euhedral and contains abundant growth twins. Both biotite and plagioclase are randomly oriented with only slight recrystallization along grain boundaries. Quartz, in general, is recrystallized. The preservation of these textures suggests that the rocks may have intruded late during, or after, the deformational phase and, therefore, may be Cenozoic in age.

The second type of biotite-bearing granitic gneiss (BG2) occurs at one locality approximately 1.5 km west of D'kadda. This rock is equigranular with average grain size of about 2 mm. It has a strong gneissic texture and contains abundant small, vein-like, pegmatitic stringers. The common assemblage is

K-feldspar-quartz-plagioclase-muscovite-biotite with minor epidote. Biotite represents less than 10% of the rock. The age of this body is unknown.

The third biotite-bearing granitic gneiss (BG3) crops out at one locality at Salam Khan. It is very fine-grained with a strong gneissic to schistose fabric. Average grain size is less than 0.2 mm. The rock is leucocratic with a common assemblage of K-feldspar-quartz-plagioclase-muscovite-biotite-epidote. Its age and relation to the other biotite granitic gneisses is unknown.

METAGABBRO

Metagabbros are distinguished from other amphibolitic rocks by the presence of relict pyroxene and the lack of an obvious foliation. The common assemblage is plagioclase-(augite)-hornblende with minor biotite, quartz, garnet and ilmenite. The augite is preserved only as altered relict grains rimmed by hornblende. Plagioclase is strongly altered to epidote.

The metagabbros occur at two localities. The first is 1 km south of Jogiano Sar where metagabbros and associated amphibolites intrude the Ilam gneiss. The second locality is near Karakar Kandao where the metagabbro intrudes a xenolith near the margin of the Ilam gneiss. Here, the metagabbro becomes finer-grained and grades into foliated amphibolites. Veins of tourmaline granite gneiss intrude the amphibolite. The metagabbros are interpreted as dikes genetically associated with the amphibolites of the Marghazar formation.

PYROXENE GRANITE

These rocks are distinguished from other granitic rocks by the presence of aegirine-augite. They occur at two localities and at both places are only 1 or 2 meters thick. The first locality is in a stream bed between the villages of Ilam and Char. Here the rock consists of plagioclase-quartz-K-feldspar-biotite-aegirine/augite-ferrohastingsite-magnetite. The second locality is between Amlukdarra and Karakar Kandao where several layers of pyroxene granite intrude the Marghazar formation. The rocks here consist of K-feldspar-quartz-plagioclase-aegirine/augite-magnetite-biotite. Both rocks have a gneissic texture that is oriented parallel to the regional foliation. However, in both cases the pyroxenes and amphibole are not altered by the regional metamorphism. These relationships suggest that the rocks may have intruded during, or after, the Himalayan deformation and are Cenozoic in age.

CARBONATITE

Carbonatites in this area were first reported by Butt and Shah (1985). They identified an earthy (mottled) brown carbonatite and a sugary white carbonatite. Both are coarse-grained (2-5 mm) and appear massive (without foliation) at the outcrop. They occur principally as minor sills and dikes a meter or so wide that intrude the Manglaur formation in the area surrounding Jambil. Only the largest exposure, located along a roadcut 1 km south of Jambil, is shown in Plate 2.

The brown carbonatite consists of as much as 75% calcite with lesser amounts of sodic-plagioclase, K-feldspar, and biotite. Augite and magnetite are common accessories. Blue amphibole (riebikite) occurs in veinlets. The white carbonatite consists of more

than 80% calcite with minor augite. Zeolite and epidote group minerals fill many small cavities in the rock.

The mineralogy and lack of foliation in these rocks suggests that they intruded during, or after, the Himalayan deformation. LeBas and others (1987) have identified a belt of Tertiary carbonatites near the MMT zone in western Pakistan. The Lower Swat carbonatites may be contemporaneous with the carbonatites described by LeBas and others (1987).

LEUCOGNEISS OF QUESTIONABLE PROTOLITH

Two large bodies of leucogneiss occur in the Ilam gneiss between the villages of Char and Ilam (Plate 2). They are fine-grained and tend to be feldspar-rich with lesser amounts of quartz and muscovite. Their age and relationship to the flaser gneiss is unknown.

XENOLITH OF QUESTIONABLE PROTOLITH

The last, and perhaps most exotic, of the minor rock types occurs as a xenolith(?) in the Ilam gneiss. It is located at the eastern edge of Plate 2 about 2 km north of where the Ilam gneiss terminates. It is mapped as part of the Manglaur formation (unit Ml(?)). Tourmaline granite gneiss intrudes along its contact. The rock is fine-grained and consists of K-feldspar, hornblende, quartz, epidote, plagioclase, pyroxene(?), and garnet, with accessory calcite, Fe-oxide, and tourmaline. Hornblende occurs as relatively undeformed porphroblasts with a sieve texture that includes all the mineralogy except garnet. Hornblende-rich and hornblende-poor layers alternate on a scale of less than 1 cm producing a strong banded texture. The pyroxene(?) is fractured and extensively altered to an opaque, amorphous mass. This rock could be a skarn, or endoskarn, that was later regionally metamorphosed.

CONTACT RELATIONSHIPS

Contact relations between the various units just described have been puzzling for some time. Previous workers who recognized one metasedimentary unit, the Lower Swat-Buner schistose group, and one granitic unit, the Swat granitic gneisses, interpreted their contacts either as intrusive (Martin and others, 1962; King, 1964; Jan and Tahirkheli, 1969; Shams, 1983) or as a thrust fault (Humayun, 1985). Kazmi and others (1984) subdivided the metasedimentary rocks and introduced the concept of an unconformity below the Alpurai group. However, Palmer-Rosenberg (1985) showed that the lower part of the Alpurai group was intruded by tourmaline granite gneiss and therefore questioned the existence of an unconformity at this contact.

The current work is able to reconcile all of the field data. I have already presented evidence for the following sequence of events: 1) deposition of Manglaur formation; 2) intrusion of the Swat granitic gneisses; 3) uplift and erosion with probable normal faulting; 4) deposition of the Alpurai group unconformably upon the first two units; and 5) intrusion of the tourmaline granite gneiss. The tourmaline granite gneiss intrudes along the unconformity so that contact relations in many areas are obscured.

The principal evidence presented by Kazmi and others (1984) for an unconformity are the dissimilar lithologies of the Manglaur and the Alpurai rocks, and the widespread stratigraphic situation in which the same units in the Alpurai group overlie the Swat gneisses in the same order with an abrupt contact. If the age designations for the Manglaur formation and Swat gneisses are accepted, the newly discovered fossils in the Alpurai group and the correlative Jafar Kandao

formation also support an unconformity (Pogue and Hussain, 1988; Pogue and others, in prep.). Further evidence is the recognition of pebbles of granitic composition in the Marghazar formation and the complete lack of examples where Swat gneiss is interlayered with the Marghazar formation.

The unconformity below the Marghazar formation is exceptionally well exposed on Lewanai Ghar, which is located approximately 5 km northeast of Pacha (shown as elevation 4932 on Plate 2). The Ilam gneiss abruptly terminates in a well exposed area along the northwest flank of this mountain. Typical Marghazar formation rocks are present at the termination including a separate mappable horizon of psammitic schist (unit Am3).

Figure 5 is a detailed map showing the contact relationships at Lewanai Ghar. Note that both lithologic layering and foliation in the Marghazar formation strike directly into the Ilam gneiss. Where the Ilam gneiss is absent, the Marghazar formation strikes directly into the Manglaur formation. The Marghazar-Manglaur contact is delineated on the basis of distinctive marker horizons in each unit. The principal marker in the Manglaur formation is a quartz-mica schist. The marker in the Marghazar formation is a white, massive, phlogopite-marble that occurs near the base of the Marghazar formation (Figure 5). This marble is not the typical brownish marble but, nevertheless, is common in other areas near the base of the Marghazar formation. Even though the Marghazar formation strikes directly into the Swat gneiss, there is a complete lack of dikes, sills, or lenses of Swat gneiss in the Marghazar formation. By contrast, the Manglaur formation contains large lenses of Swat gneiss as well as layers of leucogranitic gneiss. This relationship

suggests that the Swat gneisses do not intrude the Marghazar formation.

The contact relationships of the Jobra formation are not as well constrained as those of the Manglaur formation. I have already indicated that the Jobra formation overlies the Ilam gneiss with a sharp contact that may be an unconformity. The contact with the Marghazar formation is not as obvious due to tight folding and the abundance of amphibolites and pelitic schists in both units. The distinction between the two formations is based on the presence of interlayered quartzites, tremolite marbles and wollastonite-bearing marbles, along with the absence of phlogopite marbles in the Jobra formation.

The contact between the two formations is best exposed on hill 3338, located in the southeast part of the 43 B/6 quadrangle, one km east of Pacha Fort (Plate 2). The hill is pictured in Figure 6a. Phlogopite marbles of the Marghazar formation (unit Aml), occur in a syncline at the top of the hill in contact with calc-silicate and tremolite marbles of the Jobra formation (Figures 6b, 6c, 6d). Tourmaline granite gneiss intrudes the Jobra formation. Interlayered calc-silicates and tremolite marbles, by virtue of their mineralogy, white color, and "ribbed" outcrop appearance, are easily distinguished from the brownish phlogopite marbles of the Marghazar formation. These provide the marker horizons used to delineate the contact. Note on the geological map (Figure 6c) that the calc-silicate marker horizon in the Jobra formation is truncated rather than folded around the central lens of tourmaline granite gneiss. Phlogopite marbles appear along strike within two meters of the last appearance of the calc-silicate horizon. It is unlikely that this change is due to an east-west trending fault because

other units do not show offset (note the straight trend of the calc-silicate horizon on the east side of the hill in Figure 6a). There is also no evidence for a folded fault zone at this contact. I interpret the contact as an unconformity between the Jobra and Marghazar formations.

Another possibility is that the assemblages in the various marbles resulted entirely from variations in fluid composition during metamorphism (Hewitt, 1973; Rice and Ferry, 1982; Rumble and others, 1982). If so, then the marbles could be stratigraphically equivalent and should be mapped as one unit. The stability field of each marble is illustrated in Figure 7. The isobaric univariant assemblage wollastonite-calcite-quartz in the Jobra formation must lie on equilibrium 6 whereas, the isobaric divariant assemblage calcite-dolomite-tremolite is constrained to lie between equilibria 2 and 3. The isobaric divariant assemblage phlogopite-calcite-quartz in the Marghazar formation is constrained to lie between equilibria 1 and 5. The stability fields of the Jobra tremolite marbles and the Marghazar phlogopite marbles overlap. This suggests that their differences are due to the bulk chemistry of the rocks. This does not prove an unconformity but it supports the interpretation that the Jobra and Marghazar marbles are separate mappable units. A detailed study of fluid composition variations during metamorphism has not yet been attempted. The Jobra formation, therefore, is considered to be older than the Marghazar formation and younger than the Manglaur formation. One possibility is that the Jobra formation correlates with quartz-bearing limestones of the Devonian, Nowshera Formation, which unconformably underlies the Jafar Kandao formation in the Peshawar Basin, south of Baroch.

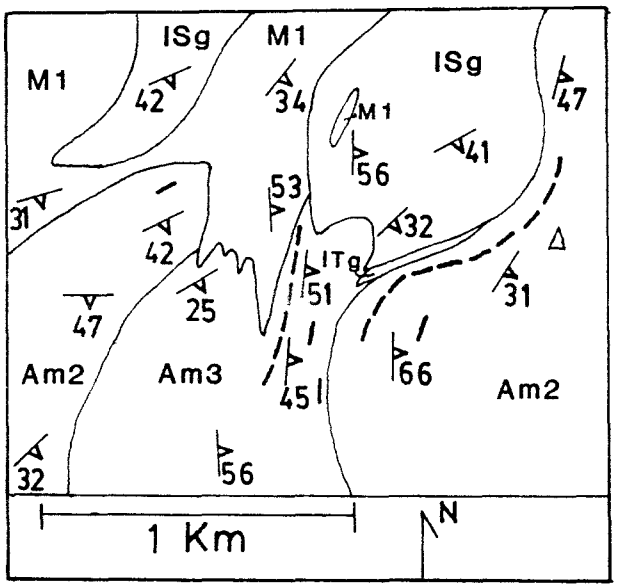

Figure 5. Contact relationships at Lewanai Ghar. M1-undifferentiated Manglaur formation; ISg-Swat gneiss; Am2-undifferentiated Marghazar formation; Am3-psammitic schist of the Marghazar formation; ITg-tourmaline gneiss; Δ -4932'. Dashed lines represent marble horizons in the Marghazar formation.

b)

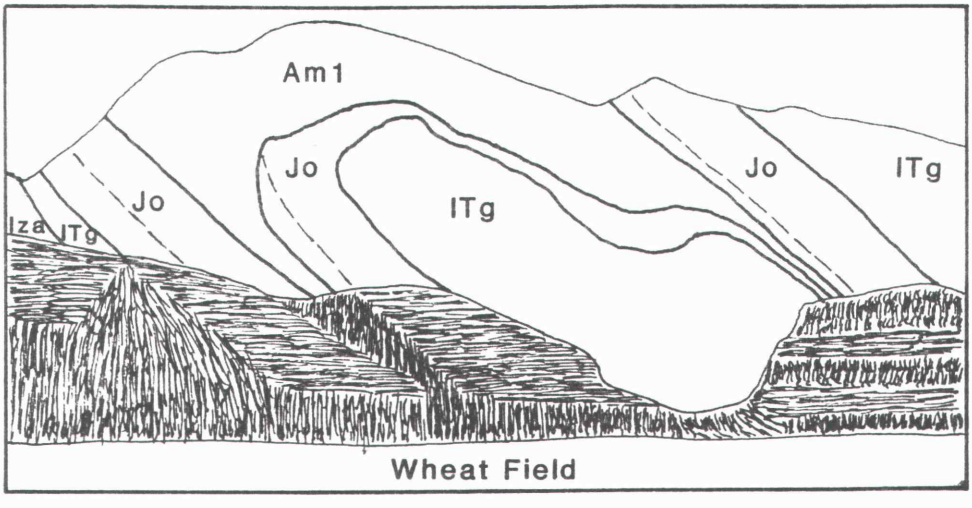

Figure 6. Contact relationships at hill 3338. a) Looking NNE at hill 3338. Horizontal field of view approximately 0.75 km. b) Sketch of the geology in the photograph. Figure 6 continued on next page.

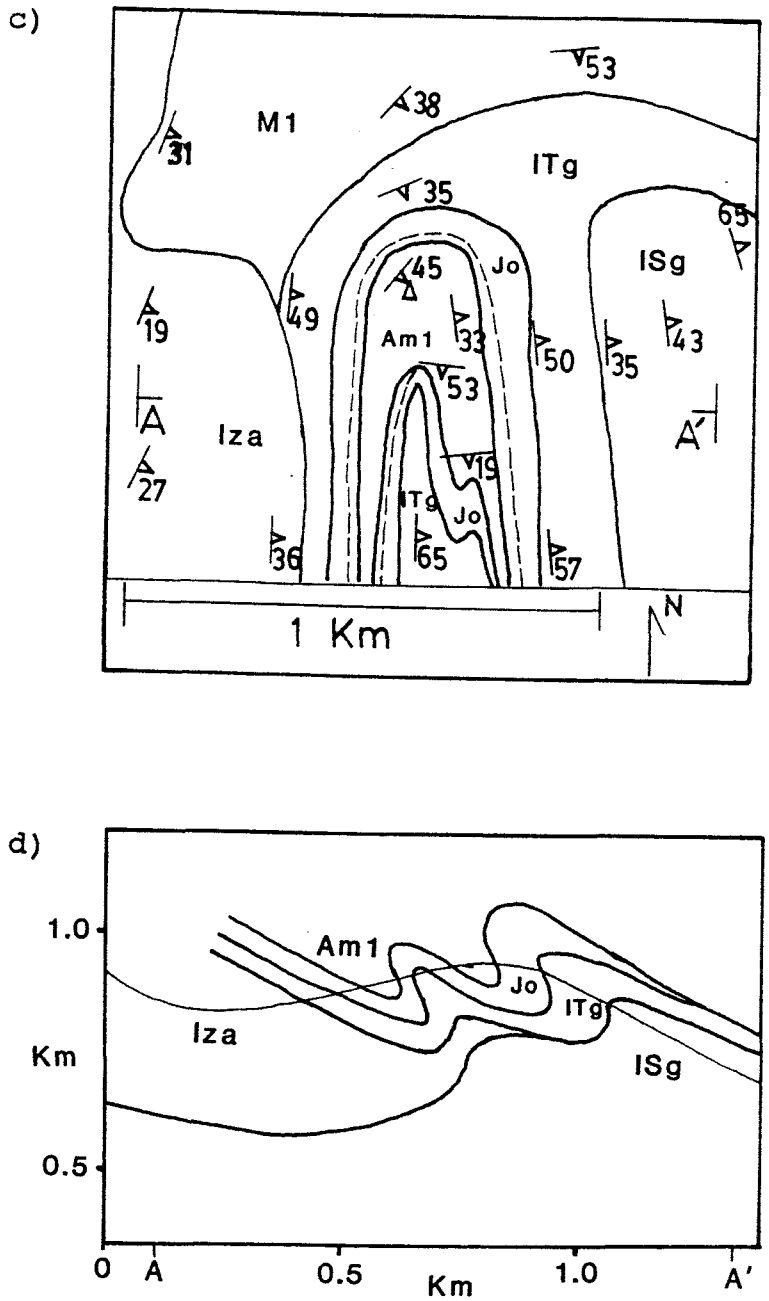

Figure 6, continued. c) Plan view showing the geology on hill 3338. d) Cross section A-A'. The location is shown in c. Ml-undifferentiated Manglaur formation; Jo-Jobra formation; Aml-marble unit of the Marghazar formation; ISg-Swat gneiss; Iza-Intruded zone A; ITg-tourmaline gneiss; Δ -3338'. The dashed line in b and c represents a calc-silicate marker horizon in the Jobra formation.

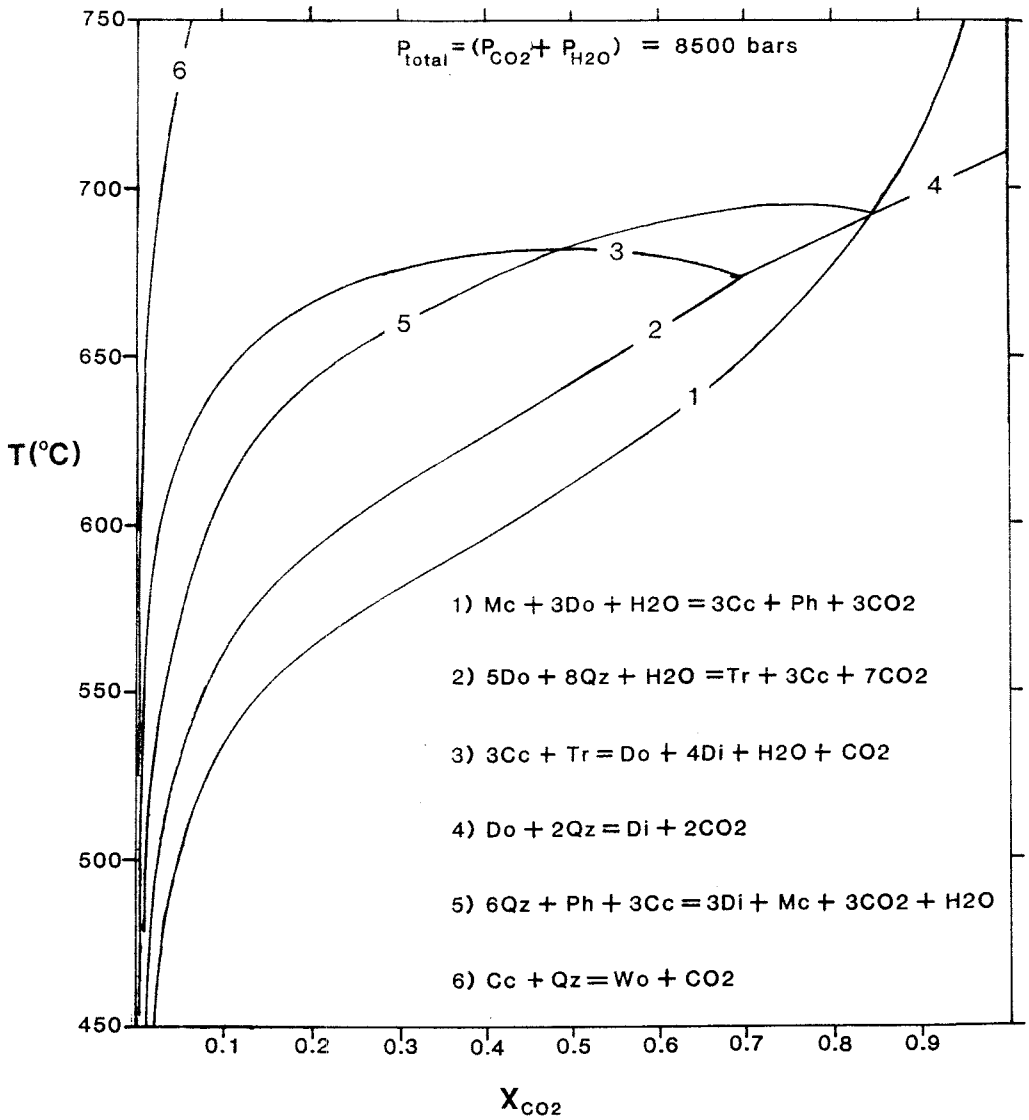

Figure 7. T-X(CO_2) phase diagram of selected equilibria at 8.5 Kbar among the pure, end-member phases calcite (Cc), diopside (Di), dolomite (Do), microcline (Mc), phlogopite (Ph), quartz (Qz), tremolite (Tr), wollastonite (Wo), in the system Al_2O_3, CaO, K_2O, MgO, SiO_2, CO_2, H_2O. The phase diagram was constructed using the computer program GEO-CALC (Brown and others, 1988). This program calculates the equilibrium position of a reaction using the thermodynamic database of Berman and others (1985) and Berman (1988). It incorporates the Kerrick and Jacobs (1981) equation of state for non-ideal mixing in H_2O-CO_2 fluids at elevated temperatures and pressures. A pressure of 8.5 Kbar was chosen on the basis of calculated P-T conditions in Lower Swat (chapter 4 of this thesis). Assemblages on the right are stable on the high temperature side of the equilibria.

CONCLUSIONS

The rocks that make up the Lower Swat region have been described, correlated and placed into the regional geologic framework of Pakistan. New formation names have been introduced and contact relationships have been clarified.

The Manglaur formation consists of quartz-rich schists with lenses of quartzite and tremolite marble. It is correlated with the Tanawal formation and assigned an age of Precambrian-Cambrian(?).

The Jobra formation contains distinctive calcite-quartz-wollastonite bearing rocks. It occurs as rare discontinuous lenses between the Ilam gneiss and Marghazar formation. Its age and contact relationships are not well constrained. I suspect that it unconformably overlies the Ilam gneiss and unconformably underlies the Marghazar formation.

The Alpurai group consists of a stratigraphic sequence that unconformably overlies the Manglaur formation and Ilam gneiss. It is divided into four distinctive formations. The largely amphibolitic Marghazar formation occurs at the base and is overlain by calc-schists and marbles of the Kashala formation. Graphitic phyllites of the Saidu formation occur at the top of the sequence in the north but, toward the south, the Saidu is replaced by poorly foliated marbles of the Nikanai Ghar formation. Each formation shows lithologic similarities with the overlying and/or underlying member formations. Correlation with fossiliferous strata in less deformed sections to the south indicate that the Marghazar formation is Mississippian or younger and that the overlying formations are Triassic or younger. I suggest that the Marghazar formation is Pennsylvanian or younger and that it correlates with the "Agglomeratic

slates" and Panjal Traps of the western Himalaya.

The Swat augen-flaser granitic gneiss intrudes the Manglaur formation. A light colored flaser granite gneiss and a dark colored augen granodiorite gneiss are distinguished. Both are thought to be contemporaneous with Cambrian to Early Ordovician augen granitic gneisses of the Lesser Himalaya. This is the interpreted age for the Swat gneiss, however, its age is constrained only by the unconformably overlying Late Paleozoic Marghazar formation.

The tourmaline granite gneiss intrudes the rock sequence principally along the unconformity between the Ilam gneiss and the Marghazar formation. The occurrence of undeformed tourmaline-bearing pegmatites, which crosscut regional foliation, suggests that the tourmaline granite gneiss is Paleogene in age.

Several minor intrusive rocks occur. These include biotite granites and granitic gneisses, metagabbros, pyroxene granites, and carbonatites.

The relationships suggest that Lower Swat existed as a highland at the outer edge of a continental shelf prior to and during deposition of the Marghazar formation. The area was receiving volcanic deposition and may have had active faults and topographic relief during Marghazar time. By Kashala time the area was receiving carbonate shelf deposition. The Saidu formation may represent a transition to oceanic conditions.

The regional deformation and metamorphism that strongly affected all but a few minor intrusive rocks is Eocene to Oligocene in age (Lawrence and others, 1985; 1989). Although contact metamorphic effects are locally preserved, there is no available evidence to suggest that the Manglaur formation was subjected to high-grade regional metamorphism and deformation prior to, or

during, intrusion of the Swat granitic gneisses. The Early Paleozoic intrusion appears to be anorogenic.

STRUCTURE AND METAMORPHISM SOUTH OF THE THE MAIN MANTLE THRUST, LOWER SWAT, PAKISTAN

ABSTRACT

In the Eocene-Oligocene, the Indian plate collided with the Kohistan arc along the Main Mantle thrust zone (MMT). The structure of the Lower Swat rock sequence, on the Indian plate directly south of the MMT, is a dome with a basement of granitic gneisses and quartz-rich schists unconformably overlain by amphibolitic and calcareous schists. The earliest superposed small-scale folds (F_1 and F_2) represent a progressive F_1/F_2 deformation that is associated with a single set of west-southwest vergent large-scale folds (termed F_2). These folds are inferred to have developed during oblique, west-southwest directed overthrusting of the MMT suture complex onto the Lower Swat sequence. Metamorphism began during F_1/F_2 as indicated by an S_1 foliation that developed during biotite-grade metamorphism. S_1 is preserved as a relict texture in porphyroblasts that grew during a subsequent inter-kinematic phase during garnet and higher grade metamorphism. The dominant, regional foliation (S_2) developed following the inter-kinematic phase. S_2 is associated with transposition of S_1 and rotation or dismemberment of porphyroblasts. Annealing recrystallization followed S_2 and continued during F_3 thereby destroying or masking possible pre-existing stretching fabrics. Superposed F_3 folds are upright and open with north-south axial trends. They may correlate with early doming of the Lower Swat sequence and with strike slip displacement in the northern part of the MMT, north of Lower Swat. F_3 was followed by retrograde metamorphism and development of east-west trending,

south vergent F_4 folds. F_4 may be associated with a final phase of southward directed thrusting and inactivity in the MMT. Correlation of published $^{40}Ar/^{39}Ar$ ages with the metamorphic fabrics suggest that F_1/F_2 and F_3 occurred in the Eocene, and that F_4 developed in the Oligocene. F_4 is the earliest indication of southward verging structures on this part of the Indian plate.

INTRODUCTION

In the Himalayan mountains, the northern terminus of the Indian plate is defined by the Indus-Tsangpo suture zone (Gansser, 1964, 1980). In the Lower Swat area of Pakistan, the western continuation of this suture is called the Main Mantle thrust or MMT (Tahirkheli 1979a, 1979b; Tahirkheli and others, 1979). Here, the MMT separates the Indian plate from the Kohistan andesitic arc (Figure 1). Convergence between the Indian plate and Kohistan began in the Mesozoic with initial collision by Eocene (Molnar & Tapponnier, 1975; Klootwijk, 1979; Patriet & Achache, 1984). The most recent activity in the MMT may have been in the Oligocene as suggested by different uplift rates in Kohistan relative to the Indian plate (Zeitler, 1985; Chamberlain and others, 1989). $^{40}Ar/^{39}Ar$ mineral ages of the metamorphosed Lower Swat sequence, on the Indian plate directly south of the suture zone, give hornblende cooling ages of about 38 Ma and muscovite cooling ages of about 30 Ma (Maluski & Matte, 1984; Lawrence and others, 1985; 1989). The metamorphism and related structural fabrics in these rocks, therefore, record an important part of the collision and the final emplacement of Kohistan against this segment of the

Indian plate.

With the exception of regional studies by Martin and others (1962), King (1964), and Jan and Tahirkheli (1969), a detailed investigation of deformation and metamorphism in the Lower Swat sequence has not been presented. More recent studies of this area have been undertaken in a cooperative program between Oregon State University, Peshawar University, the Geological Survey of Pakistan, and the Gemstone Corporation of Pakistan (Kazmi and others, 1984; 1986; Palmer-Rosenberg, 1985; Kazmer, 1986; Ahmad, 1986; Lawrence and others, 1989). This paper is part of this project and is based on the remapping at 1:50,000 of the 43 B/6 15 minute quadrangle (34°30' to 45' latitude; 72°30' to 45' longitude) and on reconnaissance traverse mapping of the surrounding area shown in Plate 1. The main focus is to report on the progressive development and significance of the metamorphic structures in the Lower Swat sequence directly south of the suture zone. My structural analysis suggests that the vergence in the Lower Swat sequence was toward the west or southwest during the Eocene, and that southward verging structures did not develop until the Oligocene, possibly after Kohistan was in its present position and the suture zone was inactive. The presence of westward verging structures adjacent to the nearly east-west striking MMT suggests oblique subduction and strike slip motion in the suture zone (DiPietro & Lawrence, 1988).

GEOLOGIC SETTING

Lower Swat is located in the hinterland of the Pakistani fold and thrust belt on the west side of the Nanga Parbat-Haramosh massif and Hazara-Kashmir syntaxial bend (Figure 1). Two distinct tectonic terrains are separated by the melange units of the Main

Mantle thrust zone (Plate 1; Appendix I).

North of the MMT the Kohistan area is interpreted as a Jurassic to Late Cretaceous island arc sequence metamorphosed to amphibolite facies in the Late Cretaceous (Tahirkheli 1979a, 1979b; Tahirkheli and others, 1979; Petterson & Windley, 1985; Coward and others, 1987; Treloar and others, 1989a).

South of the MMT, the Lower Swat sequence consists of Precambrian to Early Mesozoic, Indian plate, shelf deposits, intruded by granites of various ages, and metamorphosed to greenschist and amphibolite facies in the Eocene - Oligocene (Maluski & Matte, 1984; Lawrence and others, 1985, 1989; Treloar and others, 1989a; chapter 2, this thesis; Pogue and others, in prep.). The Swat granitic gneisses form the basement rock where they intrude the Manglaur formation. Both of these units are unconformably overlain by the Alpurai group which is subdivided into the Marghazar, Kashala, Saidu, and Nikanai Ghar formations (Appendix I). The Jobra formation occurs as discontinuous lenses unconformably(?) above the Swat gneisses and unconformably(?) below the Alpurai group (chapter 2, this thesis). Tourmaline granite gneisses intrude the sequence principally along the unconformity below the Alpurai group. Near Baroch, biotite granites of the Ambela complex intrude the Kashala formation. South of the study area, at the southern edge of the Peshawar Basin, low-grade to unmetamorphosed strata are imbricated along a series of thrust faults that includes the Main Boundary thrust (Yeats & Hussain, 1987). Cenozoic Siwalik and Murree molasse deposits occupy much of the area south of the Main Boundary thrust, including the Hazara syntaxis and Potwar Plateau (Kazmi & Rana, 1982). Further south, the currently active Salt Range thrust represents the southernmost foreland thrust fault

in this part of the Himalayan system (Yeats and others, 1984; Figure 1).

The Main Mantle thrust zone consists of three fault-bounded melange units; the Shangla melange, Charbagh melange, and Mingora melange. Each contains low-grade metavolcanic and ultramafic blocks in a sheared greenschist or lower grade matrix (Lawrence and others, 1983; Kazmi and others, 1984; 1986;). West of the study area, the Dargai klippe is an erosional outlier of suture zone rock that overlies the metamorphosed Indian plate rocks (Tahirkheli and others, 1979; Lawrence and others, 1989; Figure 1). The age of metamorphism of the MMT melange units is not clear. Northeast of Lower Swat, Maluski and Matte (1984) obtained a $^{40}Ar/^{39}Ar$ age of 83.5 $\pm$2 Ma on phengite in a blueschist block within the Shangla melange. This suggests that some of the blocks in the MMT were metamorphosed in the Late Cretaceous. However, on the basis of field relationships, I believe that the matrix, surrounding the blocks in, at least the southern part of the MMT zone (the Mingora melange, Appendix I, Plate 1), was metamorphosed in the Eocene-Oligocene with the Lower Swat sequence.

METAMORPHISM IN THE LOWER SWAT SEQUENCE

The Lower Swat sequence crops out in a dome that resulted from the superposition of east-west trending F_4 folds on generally north-south trending earlier folds (Plate 1b). The highest grade rocks are in the core of the dome where aluminosilicate minerals (principally kyanite) occur in trace amounts at isolated localities (Plate 1). Although there is no evidence for widespread "in situ" anatectic melting, thin layers of

leucogranitic rock within intruded zone B locally cross-cut the foliation in the schists. These rocks may represent syn-metamorphic melts derived from lower, unexposed parts of the metamorphic sequence.

Metamorphic grade decreases in all directions toward the peripheries of the dome. Rocks in the Alpurai group, surrounding the Swat granitic gneiss, are in the garnet zone. The assemblage garnet-chloritiod-chlorite was found in one rock in the Kashala formation near the western edge of the map area (Plate 1). A kyanite isograd could not be mapped because the Swat gneiss intervenes between kyanite zone rocks in the Manglaur formation and garnet zone rocks in the Alpurai group. Further south, a garnet "isograd" is mapped in the calcareous schists of the Kashala formation (Plate 1). This isograd is based on the first appearance of grossular-rich garnet. Reactions leading to the first appearance of garnet in these rocks are complex and require further study. The isograd assemblage is quartz-calcite-muscovite-clinozoisite-garnet-chlorite-ilmenite ($\pm$ graphite, $\pm$ rutile, $\pm$ plagioclase). Farther south, near Baroch, the rocks are at chlorite grade.

In the north, the rocks pass from kyanite zone in the core of the dome to chlorite zone in the suture zone. The disappearance of garnet, in this area, occurs at or very near the contact between the Kashala and Saidu formations and therefore, is controlled by changes in bulk chemical composition. All recognized fold deformations developed during or after Eocene-Oligocene metamorphism. Peak metamorphic conditions were attained during a phase of static recrystallization that occurred after the main (F_1 and F_2) phases of deformation.

MESOSCOPIC STRUCTURES

FOLDS

Four phases of superposed small-scale folds and three phases of superposed large-scale folds are recognized in the dome area. The earliest superposed small-scale folds (F_1 and F_2), are co-axial and co-planar with isoclinal, recumbent axial surfaces and fold axes that plunge gently toward the NNW and SSE (Plate 5b). Where they are superposed, F_1 folds deform bedding but not foliation whereas F_2 folds deform a bedding-parallel foliation. In some areas, F_2 folds are parasitic to larger F_1 folds (Figure 8). The similar geometry and orientation suggests that F_1 and F_2 developed at about the same time in different areas or rock types during progressive deformation. They cannot be separated into a relative time sequence except where they are superposed (Williams & Zwart, 1977). These two sets of folds are collectively termed F_1/F_2 in order to emphasize their progressive development.

The progressive small-scale F_1/F_2 deformation is associated with a single set of north-plunging, west-southwest vergent large-scale folds (Figure 9). These are the earliest large-scale folds recognized. I suggest that they are type 0 superposed folds (Ramsay, 1967) that developed progressively during the F_1 and F_2 deformations and did not become fully developed until the F_2 phase. I refer to them as F_2 in Plate 1 and in the text.

Large-scale F_2 folds are best developed along the west sides of the dome at the unconformity between the Swat gneiss and Marghazar formation (Plate 1a, 1b). They die out along strike in the northern and southern parts of the dome where the unconformity becomes upright. They also die out at stratigraphic levels above the

unconformity. For example, major F_2 folds only broadly fold the Kashala and Saidu formations, and the Kishora thrust may not be folded (Plate 1c).

The most common folds in the dome area are upright F_3 folds that deform F_1/F_2 folds and the regional foliation. Small-scale F_3 folds are closed to tight with variably dipping axial surfaces whereas large-scale F_3 folds are upright and open (Plate 1 & Figure 8b). Fold axes plunge gently, but variably toward the north or, less commonly, the south or southeast (Plate 5c). F_3 folds are roughly coaxial with F_1 and F_2 folds suggesting that F_3 is a continuation of the F_1/F_2 progressive deformation. F_1/F_2 and F_3 folds die out south of the garnet isograd.

F_4 folds are upright and variably tight to open, with axes that plunge gently toward the east (Plates 1 & 5d). Large-scale folds are deflected toward the northeast near the Ambela complex. North of the garnet isograd, F_4 folds gently deflect the northerly trending structures. South of the garnet isograd, they are the most obvious folds present and become south vergent. The superposition of the east-west trending F_4 folds on the generally north-south trending earlier folds has created the dome structure in this area.

FOLIATIONS

Throughout the area of the dome, except in the hinge areas of F_1/F_2 folds, the dominant, regional foliation is parallel to compositional layering. This foliation developed under prograde metamorphic conditions during the F_1/F_2 deformational phase and is designated as S_2. It is a penetrative foliation defined by the parallel arrangement of sheet silicates, amphiboles, and/or flattened and recrystallized feldspar megacrysts. Above the garnet isograd only relict

feldspar megacrysts in the Swat gneisses and rare pebbles in psammitic schists of the Marghazar formation have survived the recrystallization. Post-S_2 foliations associated with the F_3 and F_4 deformations are generally poorly developed and rarely replace S_2 as the dominant foliation.

In the granitic gneisses, psammitic schists, quartzites, and marbles, the regional S_2 foliation typically is the earliest and only microstructure present. The texture of the foliation, in thin section, is annealed due to strong post-S_2 recrystallization. In most of these rocks, matrix quartz, feldspar, and calcite grains are equidimensional and less than 1 mm in diameter. They show slight undulose extinction and/or deformation twins but grain boundaries are typically smoothly curved and triple junctions are common. The foliation is rarely microscopically crenulated or strongly deformed by later deformations.

Foliation development is more complex in the interlayered, less competent, pelitic schists and calc-schists. Not only is the regional S_2 foliation commonly deformed by F_3 and F_4 crenulation folds, but an earlier (S_1) foliation is preserved in some of the rocks above the garnet isograd. S_1 occurs only in micaceous rocks of the Marghazar formation, the Manglaur formation and, less commonly, in the Kashala and Saidu formations. It is best seen in thin section as inclusion trails within porphyroblasts and is not readily visible in the field or in hand specimen. For example, on the lower limb of the fold in Figure 8a, the dominant foliation in both rocks is parallel to compositional layering. In the psammitic schist, this is the only foliation present. In the biotite schist, an earlier foliation (S_1), is preserved in the microlithons of the dominant foliation. This type of relationship, where one rock contains one

foliation and the adjacent interlayered rock contains two, is fairly common in the Lower Swat area, where early fold hinges are absent or cannot be seen.

The S_1 foliation apparently developed locally in micaceous rocks during the early stages of F_1/F_2 deformation and was subsequently transposed during the later stages of this deformation (Bell, 1985; Treagus, 1988; Tobisch and Paterson, 1988). I interpret its origin as follows. In layers of strong competency contrast, the incompetent rocks are expected to undergo a greater degree of non-coaxial strain (or simple shear) such that during progressive deformation, the XY plane of the strain ellipsoid is rotated toward parallelism with compositional layering (Treagus, 1988). If the relict foliation becomes well developed during the early stages of progressive deformation due to recrystallization then, as a material plane, it may not be able to precisely track the XY plane of the strain ellipsoid during progressive rotational strain. Under prograde metamorphic conditions, the S_1 foliation could be folded, transposed, and destroyed, with a second (S_2) foliation developed that more closely reflects the subsequent orientation of the XY plane. During this stage, early formed, large-scale, upright folds (F_1?) could be overturned and tightened to form the observed F_2 structures.

By contrast, a foliation would have been only crudely or not at all developed in the more competent granitic gneisses and psammitic schists during the early low-grade stages of progressive deformation. The competent rocks, in addition, would be expected to undergo a more nearly coaxial strain (Lister & Williams, 1983; Treagus, 1988). Therefore, under prograde metamorphic conditions, the incipient foliation could be continuously rotated and recrystallized so that it

tracks the XY plane of the strain ellipsoid without transposition. The result is a single, dominant, foliation (termed S_2) that began to form during F_1 but was not fully developed until F_2. Thus, the regional foliation is interpreted as a composite (S_1/S_2) foliation with a protracted period of development that is dependent on rock type and spans the F_1 and F_2 deformational phases.

A protracted period of foliation development and the development of a composite foliation in the micaceous rocks during progressive deformation is not surprising considering the large competency contrast between these rocks and the granitic gneisses and psammitic schists. From the abrupt termination of F_3 crenulations at the contact with the psammitic schist in Figure 8c, one can see how a new fabric preferentially develops in the pelitic schists relative to the psammitic schists. The strong competency contrast is also reflected by the well developed cuspate-lobate forms of these folds (Ramsay, 1982). Thus, once a foliation is developed in a competent psammitic schist, it could be folded during the late stages of progressive F_1/F_2 deformation without being destroyed while a new, axial plane, foliation is developed in the interlayered pelitic schists as in Figure 8c.

These relationships indicate a complex history of fold generation, the interpretation of which, is scale dependent. At the regional scale, the observations are relatively simple. The first deformation resulted in large-scale folds (F_2) and a regional foliation (S_2) that was subsequently refolded by later deformations (F_3, F_4). At the scale of the outcrop, this first regional deformation produced multiple superposed small-scale folds (F_1, F_2), and a composite foliation (S_1, S_2) that was subsequently refolded by later deformations

(F_3, F_4).

LINEATIONS

Measured lineations in the 43 B/6 quadrangle include mesoscopic fold hinges, microscopic crenulation folds, and mineral lineations. When plotted together, they show wide scatter without a well defined maximum (Plate 5a). The scatter reflects lineation development and preservation during all the deformational phases. In order to reduce the amount of scatter, the fold and lineation data in Plate 5 are separated into two domains; one north of Jowar where north-south structures are prominent, and one south of Jowar where east-west structures are prominent.

The most common and widespread lineations are microscopic crenulation folds of the regional (S_2) foliation. In micaceous rocks it is common to find two crenulation orientations on the same foliation surface oriented parallel to the fold axes of larger-scale F_3 and F_4 folds. These crenulations are interpreted as products of the F_3 and F_4 deformations. F_3 crenulations plunge dominantly toward the N-NNW and S-SSE and are best developed north of Jowar (Plate 5e). F_4 crenulations plunge toward the east and are best developed south of Jowar, near the garnet isograd (Plate 5f). Associated S_3 and S_4 axial plane crenulation cleavages are very weakly developed (eg. stage 2 crenulation cleavage of Bell & Rubenach, 1983; Figure 8c). Other crenulations, not geometrically associated with F_3 or F_4 mesoscopic folds, may represent an intermediate weak deformation that occurred between the main F_3 and F_4 deformations.

Mineral lineations are weakly developed throughout the Lower Swat sequence. Where present, they are defined by preferred orientation of amphiboles, sheet silicates,

and feldspar augen and are oriented parallel to visible F_1/F_2 or F_3 fold axes. A strong mineral streaking (or stretching) lineation is not present on S_2 foliation surfaces.

Mineral lineations from metasedimentary rocks differ in orientation from lineations in the Swat granitic gneisses. Those in the metasedimentary rocks show a dominantly northerly and south-southeasterly trend that reflects the parallelism of these lineations with the F_1/F_2 and F_3 fold axes as noted in the field (Plate 5g). Mineral lineation data from the Swat gneisses show a variable but mainly northeasterly trend that is not obviously related to fold orientations (Plate 5h). This weak trend may more closely reflect a stretching direction in the Lower Swat sequence during post-S_2 annealing recrystallization, when peak metamorphic conditions prevailed. Lineation trends in the Swat gneiss are similar to mineral lineation trends, reported by King (1964), in the adjacent body of granitic gneiss just west of the study area (Figure 1). Previous workers (Maluski & Matte, 1984; Mattauer, 1986; Coward and others, 1986), have reported a widespread southward-directed stretching lineation as a key microstructure in this area. The data reported here and in King (1964) demonstrate that such a feature is not present.

Figure 8. A recumbent, isoclinal F_1/F_2 fold in the Marghazar formation. a) Overview of the fold. b) Closer view of the hinge area. The light colored rock is psammitic schist; the dark colored rock is biotite schist. The rock hammer in (a) is 38 cm long. The pen in (b) is 12.5 cm long. Figure 8 continued on next page.

Figure 8 continued. c) Close-up of hinge area. The location of (c) is shown in (a) and (b) with arrow and letter designation. In some parasitic folds, the dominant foliation in both the biotite schist and the psammitic schist is axial planar to the fold producing an apparent F_1 fold. In other parasitic folds (as in c) the dominant foliation in the psammitic schist is folded whereas the dominant foliation in the biotite schist is axial planar to the fold producing an apparent F_2 fold. This relationship suggests that F_1 and F_2 result from progressive deformation that, at the regional scale, cannot be separated into a relative time sequence. Note in (b) that the F_1/F_2 fold is refolded by an upright, asymmetric F_3 fold (arrow with no letter). In (c), the biotite schist is strongly crenulated by F_3 but the psammitic schist is not affected. This relationship shows how easily a new fabric develops in the micaceous schists relative to the more competent psammitic schists. The pen in (c) is 7.5 cm long.

Figure 9. View looking southeast at the overturned F_2 syncline near Ilam. Am = Marghazar formation; ISg = Swat granitic gneiss. The forested area in the foreground is underlain by Swat gneiss.

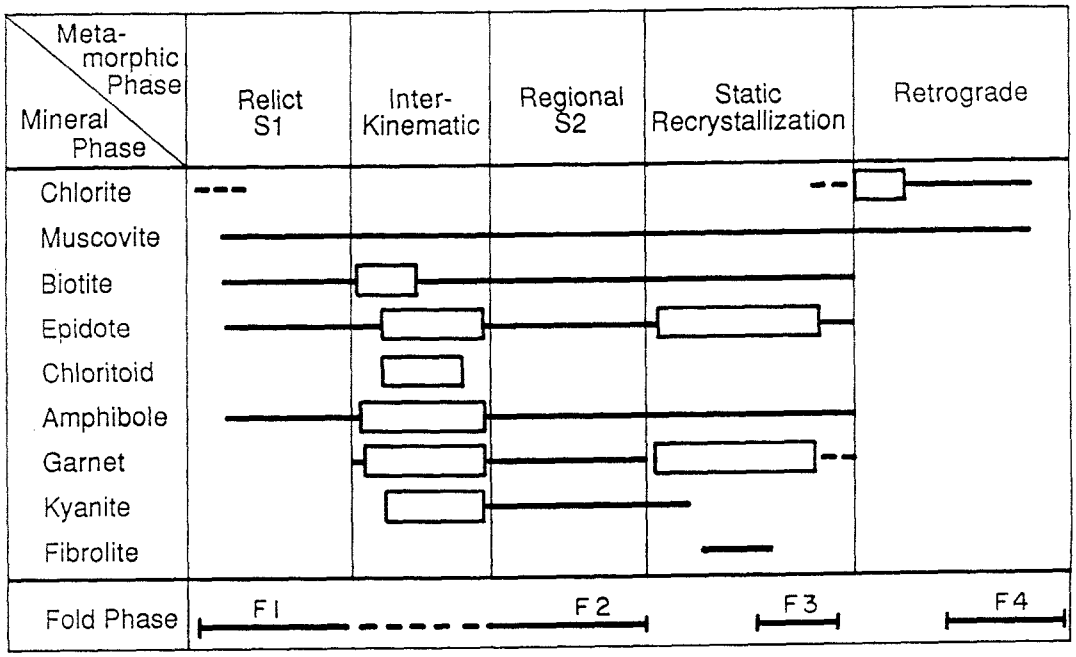

Figure 10. Inferred mineral stability in relation to the deformational phases for micaceous rocks of variable bulk composition above the garnet isograd. Lines represent mineral stability (dashed where inferred). Boxes represent significant porphyroblast growth. Garnet is inferred to be stable in the core of the gneiss dome during the latter part of F_3, but unstable near the garnet isograd. Chlorite porphyroblasts are restricted to the area near the garnet isograd.

SEQUENCE OF CRYSTALLIZATION AND FOLIATION DEVELOPMENT

Porphyroblast-matrix relationships and criteria for pre-, syn-, and post-kinematic mineral growth have been described by many authors. It has been found that many criteria are equivocal, particularly when applied to multiply deformed rocks (Vernon, 1978). For example, a porphyroblast that cuts across and truncates schistosity is generally considered to be post-kinematic with respect to the development of the schistosity. However, the same relationship is known to occur in relict sedimentary clasts that are unquestionably pre-kinematic (Ferguson and Harte, 1975). True age relationships are established only by combining several internally consistent criteria. The data presented here are based on criteria obtained from over 200 thin sections cut normal to foliation and both normal and parallel to the dominant lineation. Emphasis is placed on the sections that show particularly clear relationships.

Porphyroblast-matrix relationships in the Lower Swat sequence indicate a complex history of crystallization and recrystallization with multiple phases of deformation and porphyroblast growth during a single progressive metamorphism. The microstructures indicate the following sequence of events which are depicted schematically in Figure 10.

1) An early (S_1) phase of foliation development in some micaceous rocks under biotite-grade or lower metamorphic conditions with an incipient foliation developed in the gneissic rocks;
2) An inter-kinematic phase at garnet-grade or higher, in which porphyroblast growth was widespread;
3) A main (S_2) phase of foliation development with associated high-grade metamorphism, shearing in some rocks, and destruction of the early (S_1) foliation;

4) A post-S_2 annealing phase with widespread recrystallization and porphyroblast growth that destroyed some of the earlier fabrics;
5) An F_3 phase with the development of F_3 crenulation folds during continued recrystallization and porphyroblast growth;
6) A retrograde metamorphic phase in which garnet is altered to chlorite;
7) An F_4 phase with the development of F_4 crenulation folds during retrograde metamorphism. The F_4 deformation outlasted recrystallization.

S_1 PHASE

In thin section, the S_1 foliation is preserved in the micaceous rocks as inclusion trails within porphyroblasts, as well as, in pressure shadow areas created by the deflection of the dominant S_2 foliation around the porphyroblasts. Less commonly, the relict foliation is preserved as intrafolial microfolds in isolated microlithons within the dominant foliation. The limbs of these microfolds are either truncated or are continuous with the dominant foliation. Less than 20 thin sections, or roughly one quarter of the micaceous rocks examined, contain the S_1 foliation. Nearly all of these rocks contain porphyroblasts. Biotite is the highest grade index mineral that defines the S_1 foliation suggesting that the S_1 fabric developed at biotite grade or less (Figure 11).

INTER-KINEMATIC PHASE

The straight to slightly curved inclusion trails shown in Figure 11, suggest that the relict S_1 fabric was not crenulated or was weakly crenulated at the time that the biotite and plagioclase porphyroblasts grew. Other porphyroblasts with straight to crenulated S_1

inclusion trails are chloritoid, epidote, hornblende, and garnet. Widespread porphyroblast growth, between the late stages of S_1 foliation development and the early stages of S_2 foliation development, defines an inter-kinematic phase that separates the deformation associated with S_1 from the deformation associated with the dominant S_2 fabric in the micaceous rocks (Figure 10).

In psammitic schists that lack a relict S_1 foliation, some garnet porphyroblasts contain randomly oriented inclusions in their cores. This suggests that these garnets crystallized early during the development of the dominant foliation (Vernon, 1978). They may record porphyroblast growth during the inter-kinematic phase in rocks which had not yet developed a foliation.

Kyanite was found at 8 localities, in rocks that do not contain the S_1 foliation. However, I interpret initial crystallization of kyanite to be during the inter-kinematic phase. At four of the localities, kyanite occurs only in trace amounts as clumps that are surrounded by muscovite or garnet. At the other four localities, kyanite is more abundant and occurs disseminated throughout the rock as well as in clumps and microveins. Individual kyanite grains within the clumps and microveins are between 0.2 and 0.5 mm in length. They are randomly oriented and typically bent, broken, strongly undulose, and partly altered to sericite. Disseminated kyanite is finer-grained (<0.1 mm) and is undeformed and unaltered (Figure 12a). These relationships suggest that large grains of kyanite were present during the inter-kinematic phase of recystallization, prior to the full development of the regional foliation. These grains were deformed and recrystallized into multiple smaller crystals as foliation developed.

The inter-kinematic phase may represent a lull in deformational intensity immediately prior to the strong deformation associated with development of the regional foliation, or may simply represent a period of rapid porphyroblast growth during the early stages of progressive F_1/F_2 deformation under conditions of increasing metamorphic grade.

REGIONAL S_2 FOLIATION DEVELOPMENT PHASE

Evidence for a strong component of rotational shear strain during the main phase of foliation development is preserved, at the scale of the thin section, in micaceous rocks with inter-kinematic garnet porphyroblasts. These porphyroblasts contain inclusion trails that are not aligned from one garnet to the next within a single thin section. The mis-orientation suggests that the garnets were rotated after they formed. Other inter-kinematic garnet porphyroblasts appear to have been broken, crushed, and recrystallized during development of the regional foliation in a manner similar to that described for the kyanite clumps. Whether garnets were rolled or crushed appears to be partly a function of the competency contrast between the porphyroblast and matrix. Garnet porphyroblasts were rolled in rocks with a fine-grained micaceous or calcite-rich matrix, but were more typically crushed and recrystallized in rocks with a less micaceous, quartzo-feldspathic matrix.

An example of porphyroblasts that were later partly dismembered and rolled during development of the dominant S_2 foliation is shown in Figures 12b and 12c from a calc-schist of the Kashala formation. The straight inclusion trails in the cores and crenulated inclusion trails at the rims of the garnets in Figure 12b indicate that the garnet porphyroblasts grew during

the inter-kinematic phase. The orientation of crenulation folds within the garnet and chloritoid porphyroblasts varies by more than 60 degrees. This variation, coupled with the variable orientation of the straight inclusion trails in the cores of the garnets, suggests that the porphyroblasts were later rolled and broken during the main phase of S_2 foliation development, after they overgrew the crenulation folds.

Not all garnets show evidence of rolling. In many instances the internal foliation in the garnet is similarly oriented from one garnet to the next. In these cases it is probable that the developing S_2 foliation was rotated around a ridged, non-rotating porphyroblast as described by Ramsay (1962) and Bell (1985).

POST-S_2 ANNEALING PHASE

The post-S_2 phase of recrystallization and grain growth is particularly evident in the less micaceous rocks (granitic gneisses, psammitic schists, and marbles) which are characterized by coarse-grained (>0.5 mm), nearly granoblastic-polygonal textures. Idioblastic, "fish-net" or "web" garnets (Spry, 1969, p.187, 271) and micas oriented orthogonal to the foliation plane also suggest post-S_2 recrystallization (Figure 13a). Many of the fabrics that developed during the F_1/F_2 deformational phase have been destroyed in these rocks. For example, a strongly foliated garnet-muscovite-quartz schist from the Manglaur formation contains garnets that appear to be broken and flattened along the foliation plane to resemble a mylonite (Figure 13b). However, in thin section, the rock shows little textural evidence for shearing (Figure 13c). There are no obvious S-C fabrics, imbrications, or pull-apart features. The garnets are recrystallized and appear undeformed. Any kinematic indicator in this rock

would be difficult to interpret and would likely relate to a final movement direction associated with post-S_2 recrystallization. This complicates an attempt to relate the sense of shear to the kinematic history during the main F_1/F_2 phase of deformation.

The deformational history of the Swat granitic gneiss is also obscured by strong post-S_2 recrystallization. In the field, recrystallized augen in the flaser gneiss resemble semi-continuous pancakes in the plane of the foliation indicating a strong flattening component during deformation (Ramsay and Huber, 1983). Fernandez (1983) previously concluded that similar megacrystic granites and gneisses near Mansehra experienced a strong flattening deformation. Thin layers of mylonitic rock occur locally throughout the gneisses but are best developed (or best preserved) in the augen granodiorite gneisses near Loe Sar.

In thin section, recrystallized tails and pressure shadows are typically symmetric around preserved augen in the plane normal to foliation and parallel to lineation (Figure 13d). This also suggests a nearly coaxial flattening deformation (Choukroune and others, 1987). Non-coaxial strain, suggested by recrystallized tails and pressure shadows with asymmetric geometry (Simpson and Schmid, 1983; Lister and Snoke, 1984; Passchier and Simpson, 1986), are rare and generally restricted to the augen granodiorite gneisses. Abundant mica in these rocks may have pinned grain boundaries and prevented extensive post-S_2 grain growth thereby preserving some of the early developed asymmetric fabrics. If similar asymmetric fabrics were present in the coarse-grained flaser gneiss, they have largely been destroyed by post-S_2 recrystallization and grain growth. Thus, a coaxial flattening deformation associated with post-S_2 recrystallization in the granitic gneisses may

mask an earlier phase of shearing deformation that is only poorly preserved in the augen gneisses. The examples in Figures 11 and 12 indicate that regional S_2 foliation development and associated shearing occurred during garnet and higher grade metamorphic conditions that outlasted the F_2 deformation (Figure 10).

Kinematic indicators derived from S-C fabrics, and asymmetric fabrics are plotted in Plate 1b. Many of the indicators are from rocks that have undergone extensive post-S_2 grain growth and therefore should be viewed as suspect. In general S-C fabrics, like the lineations, do not show a regional movement pattern. A few suggest northward movement. It is probable that some of the kinematic indicators reflect uplift of the dome following the F_2 phase of deformation, but no firm conclusions are possible from this data.

F_3 PHASE

Garnet porphyroblasts in the Manglaur formation overgrow F_3 crenulation folds indicating that, in these rocks, garnet-grade metamorphism outlasted F_3. In the Alpurai group, above the garnet isograd, micas, epidotes, and amphiboles show sharp, high-angle grain boundaries in the hinge areas of F_3 crenulation folds and garnet is present within F_3 crenulations (Figure 14). This relationship suggests continued garnet-grade recrystallization during at least the early stages of F_3 deformation in these rocks. Nearer to the garnet isograd, garnet typically overgrows the dominant S_2 foliation but is absent in the hinge zones of F_3 crenulation folds. This suggests that garnet grew only during a short period of time that began during post-S_2 recrystallization and ended prior to, or during, the early stages of F_3 deformation. It is at this time that the garnet isograd was set.

RETROGRADE PHASE

In the core of the dome, garnets show only minor alteration to chlorite or biotite. Kyanite, however, is strongly altered to sericite and late-formed fibrolite is present at two localities (Plate 1a). The presence of post-F_3 garnet in the Manglaur formation suggests that retrograde metamorphism occurred after F_3 in these rocks.

Garnets at or near the garnet isograd are strongly altered to chlorite. Most of the alteration occurs where the garnets impinge against the S_2 foliation which is flattened around the porphyroblast. If some of this flattening is related to F_3 then retrograde metamorphism began prior to or during F_3 in these rocks. Also common in the vicinity of the garnet isograd are helicitic, post-S_2 porphyroblasts of chlorite that apparently represent post-S_2 mineral growth at temperatures below the stability of the garnet-zone assemblage.

F_4 PHASE

The F_4 deformational phase occurred near the end of retrograde metamorphism and outlasted recrystallization (Figure 10). F_4 crenulation folds deflect around pre-existing garnets which are preferentially replaced by chlorite on the limbs of the folds. The texture of muscovite in the hinge areas of F_4 crenulation folds is variable. Some grains are polygonized; others show strong undulose extinction. Complete recrystallization is rare. Post-metamorphic F_4 deformation is evident by slight undulose extinction the in groundmass grains.

Particularly strong deformation associated with the F_4 phase is noted locally in marbles that occur at the base of the Marghazar formation in contact with Swat and tourmaline granite gneisses. Some of these rocks show a sheared fabric in which a flattened and strongly twinned

matrix of calcite encloses pulled-apart and deformed grains of feldspar and phlogopite. This well preserved low temperature deformation may be related to shearing of the ductile marble against the granitic massif during uplift.

Figure 11. Examples of S_1 foliation. a) A pulled-apart and recrystallized biotite porphyroblast that is surrounded by the dominant (S_2) foliation (horizontal in the photograph). The relict-S_1 foliation is preserved in the pressure shadow area of the porphyroblast and consists of quartz, muscovite, biotite, plagioclase, graphite, and rutile. The same relationship occurs in a plagioclase porphyroblast just below the biotite which contains biotite-bearing S_1 inclusion trails. Marghazar formation, St. 6-582. Figure 11 continued on next page.

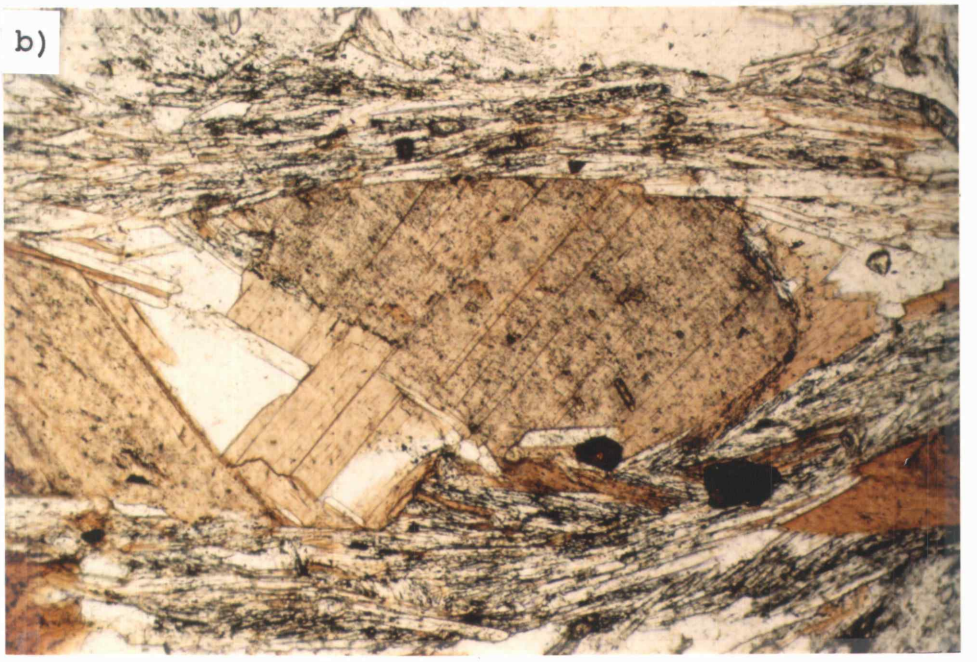

Figure 11 continued. b) Biotite porphyroblast with straight S_1 inclusion trails of graphite that truncate against the dominant S_2 foliation. The porphyroblast appears to be pulled apart and syn-S_2 biotite (without graphite inclusions) grows in optical continuity in the pressure shadow areas. A biotite beard occurs at the lower right of the porphyroblast. Same slide as (a), both 1.3 mm in long dimension.

Figure 12. Examples of inter-kinematic porphyroblast growth and shear associated with development of dominant S_2 foliation. a) Foliation is deflected around a clump of coarse-grained, strongly deformed kyanite (high relief mineral, Ky) suggesting that kyanite was present during the inter-kinematic stage, prior to the full development of the foliation. Fine-grained, recrystallized, kyanite is abundant in the matrix. A tail of fine-grained kyanite extends off the lower left of the clump and into the matrix. Loe Sar gneiss, St. 6-550, long dimension is 3.3 mm. Figure 12 continued on next page.

Figure 12 continued. b) Two inter-kinematic garnets (both partially broken and dismembered). Kashala formation; St. 6-187. Discussion continued on next page.

Figure 12 continued. Both garnets in (b) contain straight inclusion trails near their cores and crenulated inclusion trails at their rims. The trails in both garnets are oriented at an angle to the regional foliation and at an angle of nearly 90° to each other. The regional foliation is oriented generally horizontally in the photomicrograph but is strongly deflected around the porphyroblasts. The garnet in the lower left is in contact with chloritoid (arrow). Weakly crenulated relict-S_1 inclusion trails pass from garnet into chloritoid. Continuity is partly disrupted by pressure solution and deposition of opaque residue between the grains. The inclusion trails are abruptly truncated by the dominant S_2 foliation at the lower right of the chloritoid. Long dimension is 11 mm.
c) Left side of the lower left garnet shown in (b). The orientation is 30° counterclockwise from that shown in (b). The straight S_1 inclusion trail near the garnet core becomes weakly crenulated near the rim and then, still within the garnet, swings abruptly into parallelism with the dominant S_2 foliation which is marked by abundant graphite. The S_1 foliation in the garnet is continuous to semi-continuous with the dominant foliation outside the garnet. The arrow points to the edge of the garnet crystal. The garnet has an idioblastic rim that overgrows the graphite-rich S_2 foliation suggesting post-S_2 growth of garnet. Long dimension is 1.3 mm.

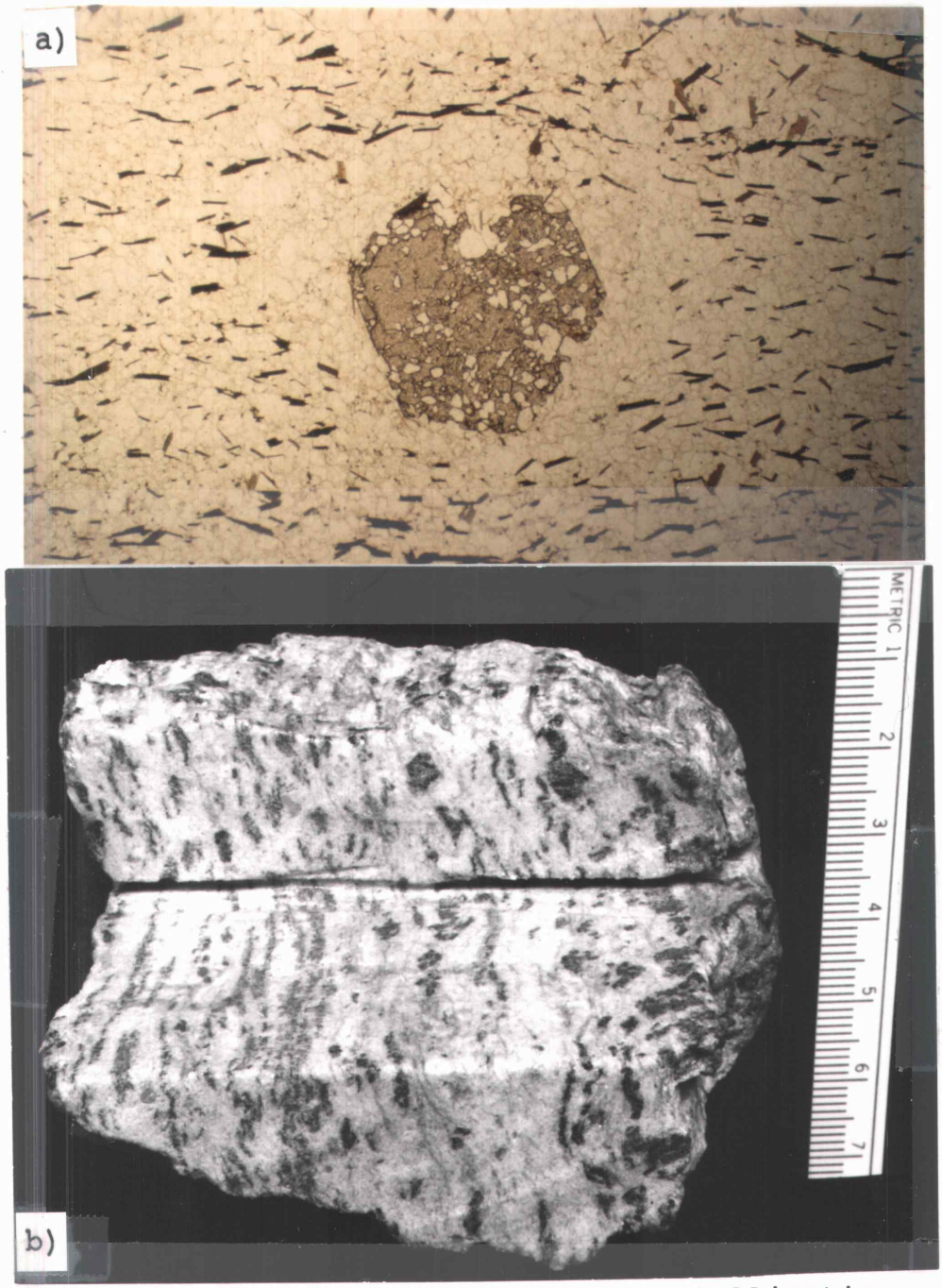

Figure 13. Examples of post-S_2 recrystallization. a) Sub-idioblastic "fish-net" garnet surrounded by a biotite deficient halo. Quartz inclusions increase in size from core to rim where they approach the size of the groundmass suggesting garnet growth during static recrystallization. Marghazar formation; St. 6-433; long dimension is 6.7 mm. b) Hand specimen of a garnet-muscovite-quartz schist from the Manglaur formation. The rock shows crushed and lineated garnet. Manglaur formation, St. 6-179. Figure 13 continued on next page.

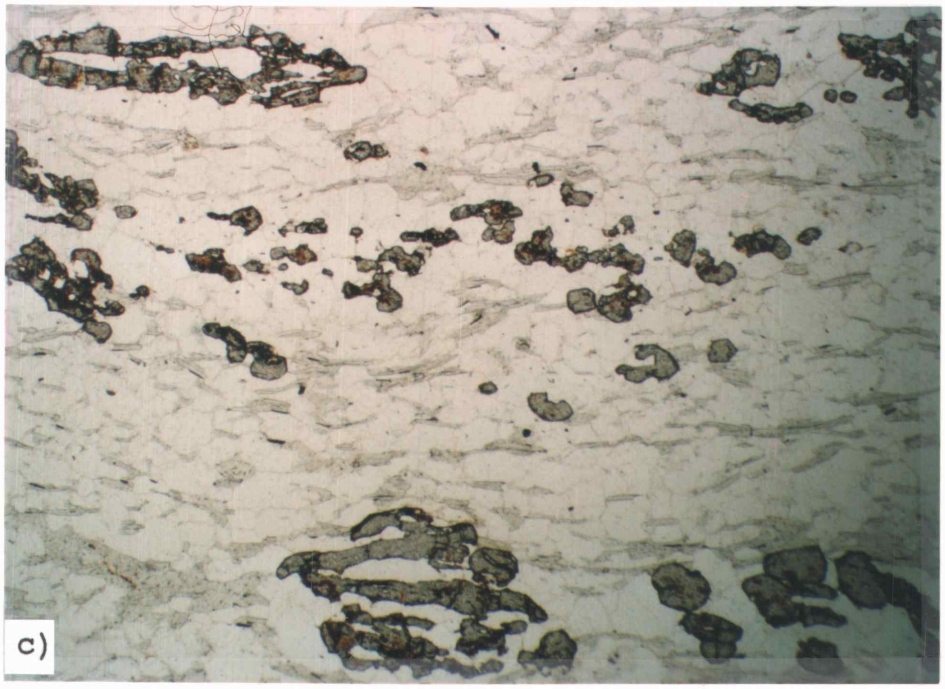

Figure 13 continued. c) Photomicrograph of rock in (b). The section is oriented normal to foliation and parallel to the long axis of the garnet lineation. The garnets occur either as skeletal porphyroblasts or as recrystallized groundmass grains that form trains in the foliation plane. Each train is made up of numerous, tiny, individual, sub-idioblastic, garnets that have grown laterally into each other along quartz boundaries to produce the skeletal structure. Quartz grains are equidimensional with slightly curved grain boundaries and local polygonal texture. Muscovite shows no internal deformation and cross micas are present. Long dimension is 6.7 mm. Figure 13 continued on next page.

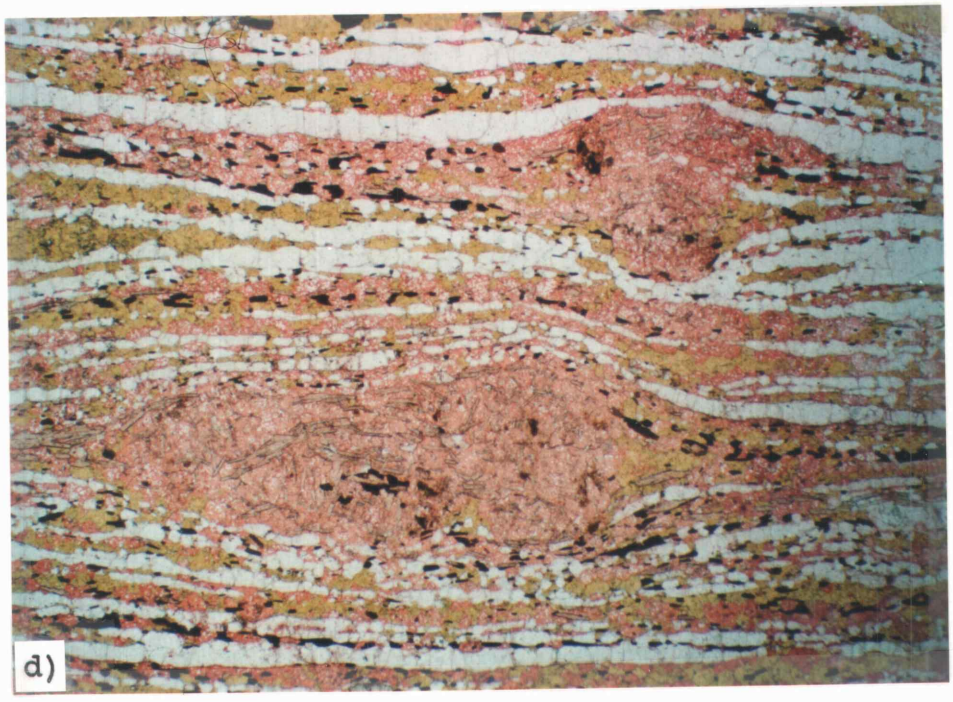

Figure 13 continued. d) Strongly differentiated ribbon texture of the Swat augen granodiorite gneiss. The section is oriented normal to foliation and parallel to lineation and is stained for K-feldspar and plagioclase. Recrystallized tails surrounding augen of K-feldspar and plagioclase are predominantly symmetric, suggesting a coaxial, flattening deformation. Note the generally equidimensional grain shapes and straight grain boundaries indicative of static recrystallization. Loe Sar gneiss; St.6-220; long dimension is 6.7 mm.

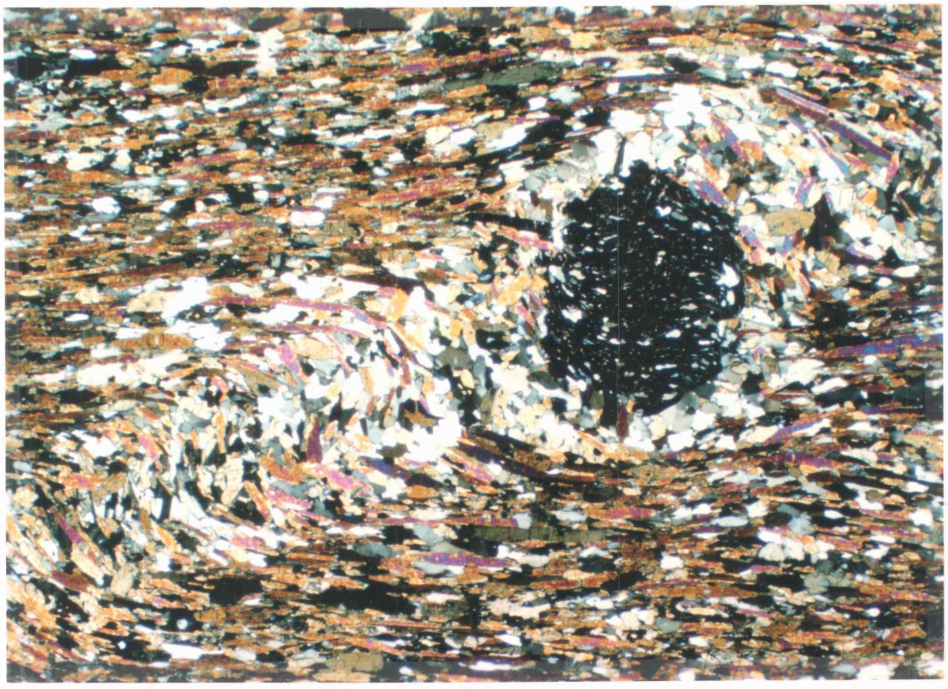

Figure 14. Garnet in the hinge area of an F_3 crenulation fold. Hornblende is recrystallized in the hinge area as shown by the sharp, high angle grain boundaries. Marghazar formation; St.6-50; long dimension is 6.7 mm; crossed nicols.

DISCUSSION

The relationship of folding to thrusting in the MMT gives an indication of when the suture zone was active. Although the regional S_2 foliation is continuous across the Kishora thrust and into the Mingora melange (Kazmer,1986), there is no clear evidence that the Kishora thrust is folded by F_1/F_2 folds. As noted previously, large-scale F_2 folds appear to die out below the thrust fault. Kazmer (1986) noted an early fold phase in the Lower Swat sequence that is not present in the Mingora melange. Lawrence and others (1989), however, have suggested that the Dargai klippe, located 50 km to the west of Plate 1 and presumably part of the Mingora melange, is deformed by first phase folds. These relationships are consistent with the interpretation that the Kishora thrust was active prior to and during F_1/F_2 fold development. The Kishora thrust is everywhere in contact with the Saidu formation. There are no known areas in Lower Swat where the thrust completely cuts out Saidu formation and comes in contact with Kashala formation. This suggests that the Kishora thrust overrode the Lower Swat area along a thrust flat at the top of the Alpurai group, presumably during the F_1/F_2 deformation.

The small-scale F_1 and F_2 folds represent a progressive F_1/F_2 deformation that is associated with a single set of west-southwest vergent large-scale folds (F_2). The large-scale F_2 folds may have developed in response to intense localized shear strain related to movement on the Kishora thrust. The folds nucleated at the interface between competent granitic gneisses and overlying incompetent schists of the Marghazar formation. Primary thickness variations in the Marghazar formation indicate that this interface was an irregular,

erosional surface (chapter 2, this thesis). As such, this interface was ideal for the nucleation of recumbent fold structures by shear folding (Hudleston, 1976, 1977; Cobbold and Quinquis, 1980). The mechanism envisioned is similar to model 3 of Brun and Merle (1988) with initial buckling instability (F_1?, relict-S_1?) followed by shear flow and amplification into recumbent folds (F_2, S_2), followed by development of upright buckle folds (F_3) during progressive deformation (Figure 15). The metamorphic structures indicate that the F_1/F_2 deformation occurred during prograde metamorphism. The main phase of shearing, or the one best preserved in the microstructures, occurred at garnet or higher grade, after the inter-kinematic phase of porphyroblast growth. The shearing phase is best preserved in the schists by rotated and/or crushed and recrystallized porphyroblasts. The granitic gneisses display fabrics more characteristic of a coaxial flattening deformation which is probably related to post-S_2 recrystallization. This recrystallization may mask an earlier phase of rotational shear deformation as zones of high shear strain are evident, particularly in the augen granodiorite gneiss. Large-scale F_2 folds die out at stratigraphically higher positions in the Alpurai group where shear is taken up by layer parallel flow and fault displacement in the overriding suture zone.

The Kishora thrust is folded by F_3. Martin and others (1962) and King (1964) mapped a large, north plunging syncline northeast of Dosara that folds the Kishora thrust. Reconnaissance in this area suggests that this is an F_3 syncline. Kazmer and others (1983) and Kazmer (1986) also mapped north plunging folds that deform the thrust. Movement on the Kishora thrust, therefore, must have ended prior to the F_3 phase.

Although F_3 deforms the Kishora thrust it is not certain that it deforms the Kohistan thrust (Plate 1). Kazmer and others (1983) and Kazmer (1986) concluded that the Kohistan thrust was emplaced after the Kishora thrust was folded by north plunging folds. This suggests that the northern part of the suture zone and the Kohistan thrust were still active during F_3.

The Kohistan thrust trends roughly WSW-ENE in Lower Swat. Therefore, it is difficult to determine if it is folded by the east-west trending F_4 folds. However, east-west trending folds are known in the Kohistan arc, north of the thrust (Coward and others, 1982). Some of these folds may be related to the F_4 folds in the Lower Swat sequence. If so, then this suggests that Kohistan was in its present position, and the suture zone was inactive, prior to the end of the F_4 phase.

Metamorphic overprinting of the early deformational history in Lower Swat complicates attempts to relate mineral lineation data and kinematic indicators to the direction of thrusting in the suture zone. The lack of a strong mineral stretching fabric associated with the F_1/F_2 deformation is due to recrystallization and grain growth during the post-F_2 annealing phase when peak metamorphic conditions prevailed. The weak northeasterly trend and gentle plunge of mineral lineations in the Swat gneiss may reflect the stretching direction in the Lower Swat sequence during this recrystallization.

Because of the metamorphic overprinting, I consider the vergence of the large-scale folds in the Lower Swat sequence to be the best preserved indicators of thrust direction. The fold relationships suggest that the suture zone was active during the F_1/F_2 and F_3 fold phases. The general north-south orientation and westward vergence of these folds, argues for east-west shortening. This would imply oblique convergence between

Kohistan and the Lower Swat sequence with a large component of strike slip motion in the generally east-west trending suture zone.

Alternatively, the large-scale F_2 and F_3 folds could be interpreted as sheath folds with axes oriented parallel to a southward thrust direction. Such an interpretation is not supported by field data because: (1) the sense of closure of the major F_2 anticline and syncline in Plate 1 is opposite to the sense of closure expected for a sheath fold anticline-syncline pair developed during southward directed movement (Cobbold and Quinquis, 1980; Hudleston, 1986). (2) The hinge line variation of small-scale F_1/F_2 and F_3 folds is much less than 90^{o}. This suggests that small-scale sheath fold geometry is not developed (Ramsay & Huber, 1987; Skjernaa, 1989). (3) The continuity of marker horizons in the field does not give large-scale sheath fold geometry. (4) The restricted occurrence of overturned large-scale F_2 folds at the western margin of the dome, coupled with the absence of overturned rock along the southern margin, suggests general westward vergence. (5) The nearly coaxial geometry of F_3 with F_1/F_2, and their development during the same metamorphic event, suggests that F_3 is a continuation of the F_1/F_2 progressive deformation (e.g., Brun & Merle, 1988). The large-scale, upright, F_3 folds imply generally east-west compression. (6) Mineral lineations and kinematic indicators do not support a strictly southward movement direction.

My interpretation, therefore, is that the suture zone melanges overrode the Lower Swat sequence on the Kishora thrust during the F_1/F_2 deformational phase with the transport direction probably toward the west or southwest (Figure 16). The Kishora thrust became inactive during F_3 and motion was transferred to predominantly strike slip faults in the northern part of

the suture zone. The change from westward to southward vergence in the Lower Swat sequence began with F_4. This change may reflect a transition from Kohistan mainly sliding along the northern edge of Lower Swat to it being thrust southward into its present position along the Kohistan thrust. Convergence was first taken up by the development of F_4 folds and later by the initiation of thrust faults in the Pakistani foreland. Activity in the MMT ended prior to the end of the F_4 phase.

Lawrence and others (1985) and L. Snee (in Palmer-Rosenberg, 1985) obtained $^{40}Ar/^{39}Ar$ ages of 39.9 $\pm$0.2, 39.8 $\pm$0.3 and 37.1 $\pm$0.7 Ma from hornblende in the Marghazar formation near Jowar, and ages of 30.6 $\pm$0.4 and 29.5 $\pm$0.3 Ma from muscovite in the Kashala formation from the same area. Maluski and Matte (1984) obtained a $^{40}Ar/^{39}Ar$ age of 30.8 $\pm$1.0 from muscovite in the Kashala formation near Saidu. These ages are similar to the younger K-Ar and $^{40}Ar/^{39}Ar$ ages obtained by Treloar and others (1989a) in this area. Polygonized and recrystallized hornblende in the hinge areas of F_3 crenulation folds in the Marghazar formation indicate that hornblende recrystallized during or after the F_3 phase (Figure 14). Therefore, 38 Ma is the minimum age for the F_1/F_2 and F_3 deformational phases. Muscovite is commonly weakly deformed in the hinge areas of F_4 crenulation folds, therefore, the F_4 phase may have begun near the closure temperature of argon in muscovite, about 30 Ma. It is at this time that southward verging structures, so prevalent in the foreland of Pakistan, first began to develop. By analogy, 30 Ma would also represent the approximate age for the beginning of south-directed thrusting on the MMT and for final emplacement of Kohistan.

A steep metamorphic gradient with no obvious discontinuity exists between amphibolite facies rocks in

the Lower Swat sequence and low-grade rocks in the MMT zone. A similar metamorphic gradient, though not as steep, is present in the Ladakh Himalayas (Honegger and others, 1982). The nature of this gradient and how it bears on the structural and metamorphic history in the MMT zone is poorly understood. One possibility is that it is the result of cooling and the promotion of hydration reactions (Armstrong & Dick, 1974) in the MMT zone due to infiltration of fluids derived from dehydration reactions in the underlying Lower Swat sequence. An alternative possibility is that late-metamorphic slivering in the MMT has faulted out or buried higher grade rocks. This seems plausible because the Kohistan arc was emplaced cold, during the F_4 deformation, when rocks in the Lower Swat sequence were at or below the closure temperature of argon in muscovite.

The deformational sequence in Lower Swat correlates well with a similar tectonic history reported in the Hazara syntaxis (Bossart and others, 1988). Inspection of Figure 1 shows that the trend of the Murree and Panjal faults, on the east side of the syntaxis, approximates the trend of major F_2 and F_3 fold axes in Lower Swat. The metamorphism and early structures in Lower Swat may represent a hinterland expression of the early deformation that affected the east side of the Hazara syntaxis. Bossart and others (1988) indicate a later, counterclockwise rotation of vergence, from southwestward to southeastward. This change may correlate with a similar rotation in Lower Swat during the Oligocene.

Recent investigations by Coward and others (1986; 1987; 1988), and Treloar and others (1988; 1989b) west of the Hazara syntaxis, near Mansehra, allow comparison of this region with the Lower Swat area (Figure 1).

Although Treloar and others (1988, 1989b) describe similar metamorphic textures, the large-scale deformational sequence is markedly different than that from Lower Swat. The chronology they describe is one of repeated syn-metamorphic, south verging shears and folds (D_1, D_2), followed by a major phase of south-verging, late to post-metamorphic thrust stacking (D_{2a}), followed by west-northwest verging folds and backthrusts (D_3). The D_{2a} thrust stacking places high-grade rocks tectonically above low-grade rocks such that isograds are coincident with thrust faults. They find no evidence for an early phase of westward directed structures. By contrast, the Lower Swat area records syn-metamorphic westward verging folds followed by late-metamorphic southward verging folds and the development of a structural dome in which the deepest seated rocks are at the highest grade. There is no evidence for a major thrust fault (eg. the Alpurai thrust of Coward and others, 1988 and Treloar and others, 1988, 1989b) or for backthrusting in the Lower Swat sequence.

The D_{2a} thrust stacking in the Mansehra region must either die out toward the west, or be accommodated by tear faults such that the Lower Swat area was not affected. I suspect that the D_{2a} thrusts are very broadly contemporaneous with F_4 folds in Lower Swat and that thrusting in the Mansehra region has destroyed or masked evidence for earlier phases of westward directed structures. M.S. Baig (pers. comm., 1987) and Baig and Snee (1989) indicate that the intervening Besham area is an upthrown block of Early Proterozoic gneisses that are separated from Lower Swat and Mansehra by high angle border faults which cut the MMT (Figure 1). The eastern fault is recognized as the Thakot fault (Ashraf and others, 1980; Baig and Lawrence, 1987; Treloar and others; 1989b). The Besham block escaped strong Eocene-

Oligocene metamorphism (Baig & Snee, 1989; Treloar and others, 1989a) suggesting that it was not adjacent to the Lower Swat-Mansehra areas during the main deformational phases. I suggest that, following the south-directed D_{2a}-F_4 deformations in the Mansehra-Lower Swat areas, larger south-directed thrusts were initiated in the Pakistani foreland near Islamabad (Figure 1). One or more of these thrusts carried Lower Swat and Mansehra (together) toward the Pakistani foreland and emplaced them above the Besham block. Later uplift along the border faults has exhumed the Besham block. Thus, the metamorphic structures in Lower Swat developed well to the north of their present position. I consider the Besham area to be a fault-block, and not a large-scale, north-plunging antiform contemporaneous with parallel (presumably my F_3) synforms in the Swat valley as suggested by Coward and others (1988) and Treloar and others (1989b).

My interpretation, that the Kohistan-Ladakh island arc system overrode the Indian plate in a general west-southwest direction during the main deformational phases, implies that the Nanga Parbat area should have been buried beneath the arc, and undergoing metamorphism, prior to the Lower Swat area (Figure 1). However, the 37 to 39 Ma $^{40}Ar/^{39}Ar$ cooling ages on hornblende in Lower Swat are significantly older than 16 to 25 Ma $^{40}Ar/^{39}Ar$ cooling ages on hornblende in the Nanga Parbat region (Chamberlain and others (1989). I suggest that the age difference is due to different cooling histories. Based on an analysis of marine magnetic anomaly patterns in the Indian ocean, Patriat and Achache (1984) suggest that initial collision between the Kohistan-Ladakh arc and the Indian plate began at 48 to 54 Ma. Assuming that this collision was the cause of metamorphism, then the older metamorphic

ages in Lower Swat suggest that peak metamorphic conditions prevailed for a relatively short period (5-10 m.y.) prior to uplift, erosion and cooling. Metamorphic cooling ages, similar to those in Lower Swat, are present in the Mansehra region, suggesting that uplift and erosion followed soon after peak metamorphism in this area as well (Treloar and others, 1989a, 1989b). By contrast, metamorphism could have begun at the same time or earlier in the Nanga Parbat region with peak metamorphic conditions prevailing for a longer period (10-20 m.y.) prior to erosion such that younger cooling ages are preserved. Another possibility is that the metamorphism recorded in the Nanga Parbat rocks, occurred during final, southward-directed, emplacement of Kohistan onto the Indian plate (during F_4 deformation in Lower Swat). Metamorphism at this time, may have destroyed evidence for an earlier metamorphism in the Nanga Parbat region.

Finally, if the Main Mantle thrust suture melange overrode the Indian plate in a west-southwest direction rather than the more generally assumed southward direction, then the arc system may once have covered large parts of the presently exposed Indian plate with a northwest striking frontal fault similar in orientation to the Indus suture south of Ladakh or to the Murree and Panjal faults east of the Hazara syntaxis (Figure 1). This would imply that the Hazara syntaxis and Nanga Parbat-Haramosh massif are young structures that evolved after the main phase of island arc emplacement. Such an interpretation is consistent with recent studies of these areas that point out the ongoing and ever changing morphological expression of the Himalayan orogen (Burbank, 1983; Zeitler, 1985; Madin, 1986; Verplanck, 1987; Bossart and others, 1988; Chamberlain and others, 1989; Butler and others, 1989).

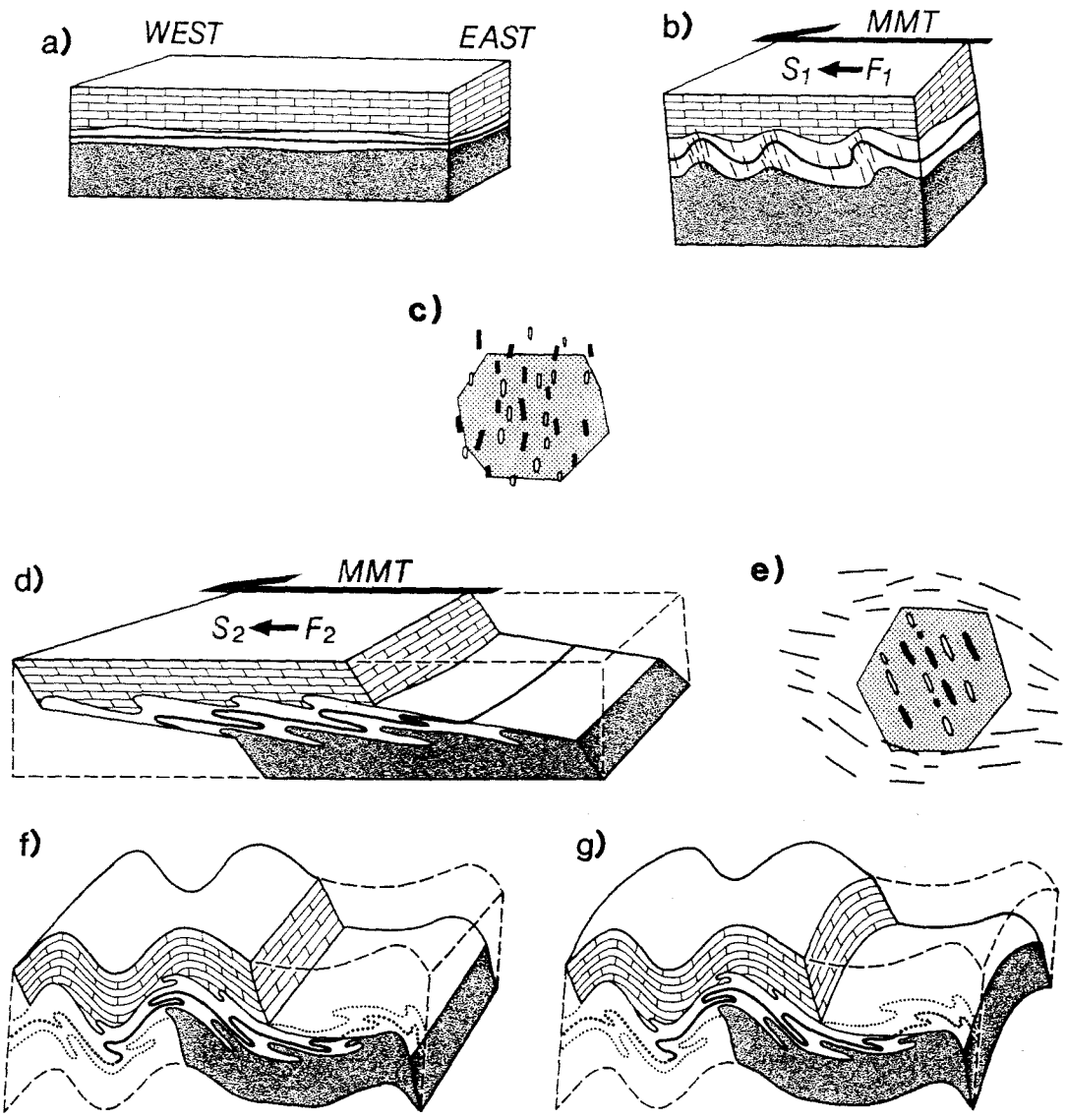

Figure 15. Schematic block diagram showing the inferred origin of the large-scale fold sequence. a) Initial erosional unconformity between the Swat granitic gneiss (shaded) and the overlying Alpurai group.
b) Development of early, upright (F_1?) folds at the Swat gneiss - Marghazar formation interface by initial buckling. S1 is axial planar to these folds.
c) Inter-kinematic phase of porphyroblast growth.
d) Amplification into recumbent folds by later (F_2) shearing deformation and development of strong S_2 foliation with, e) Syn-S_2 rotation of pre-existing porphyroblasts. f) Development of F_3 buckle folds.
g) Development of F_4 cross-folds.

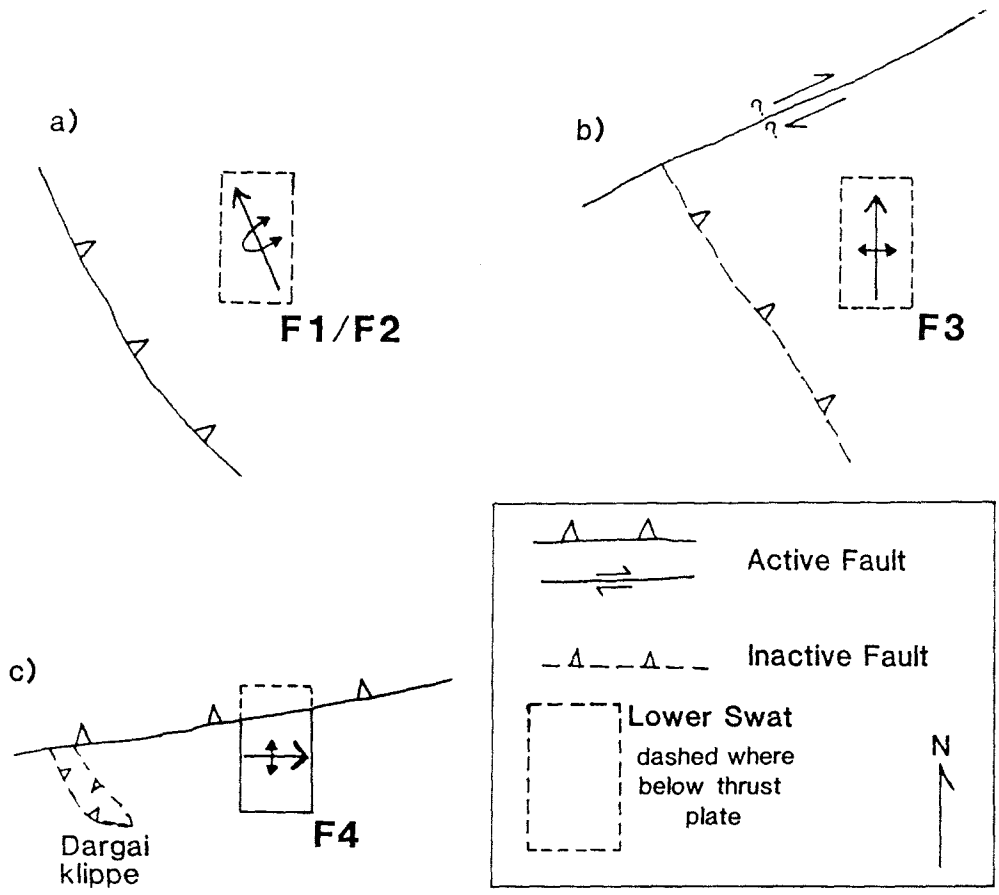

Figure 16. Schematic diagram showing the inferred sequence of faulting in the suture zone relative to fold development in the Lower Swat rock sequence.

METAMORPHIC PRESSURE - TEMPERATURE CONDITIONS OF INDIAN PLATE ROCKS SOUTH OF THE MAIN MANTLE THRUST, LOWER SWAT, PAKISTAN

ABSTRACT

The Lower Swat rock sequence in northern Pakistan is composed of metamorphosed Indian plate rocks that crop out in a dome structure directly south of the Main Mantle thrust zone and Kohistan arc terrane. This paper presents mineral assemblage, mineral composition, and the pressure-temperature conditions of metamorphism in the Lower Swat rock sequence. Swat granitic gneiss and Manglaur formation are present in the core of the dome where geothermometers and geobarometers indicate peak metamorphic conditions at 600 to 630°C and 8.1 to 9.2 kbar. Peak metamorphic conditions in the overlying Marghazar formation are 540 to 570°C and 8.1 to 9.2 kbar. Metamorphic grade decreases in all directions toward the peripheries of the dome where a garnet "isograd" is mapped in calcareous schists of the overlying Kashala formation.

Well developed growth zoning profiles from garnets in the Marghazar formation allow calculation of a P-T path based on the Gibbs method (Spear and Selverstone, 1983). Because of assumptions inherent in the calculations, the P-T path is viewed as qualitative rather than quantitative. The results suggest near isothermal compression followed by decompression and heating to peak metamorphic conditions. Correlation of the metamorphic fabrics with the structural history suggests that the early compressional stage of garnet growth occurred during emplacement of the MMT suture complex above the Lower Swat rock sequence. Maximum pressures, at this time, may have been in excess of 10

kbars. Subsequent decompression and heating to peak metamorphic conditions occurred during rapid uplift and erosion without significant deformation. These results are in sharp contrast to the Hazara area of Pakistan where dome structures have not been recognized and the metamorphic facies are juxtaposed and inverted across post-metamorphic faults (Treloar and others, 1989b).

INTRODUCTION

The pressure-temperature conditions of metamorphism are poorly known in the Lower Swat rock sequence of Pakistan due to the abundance of high variance mineral assemblages and the lack of mineral composition data on equilibrium phase assemblages. This paper presents mineral assemblage and microprobe data from the central part of Lower Swat within the 43 B/6 15' quadrangle. The data are applied to a number of calibrated geothermometers and geobarometers in order to estimate equilibrium temperatures and pressures. Possible P-T paths, based on compositional zoning in garnet, are also discussed.

GEOLOGIC SETTING

Lower Swat, Pakistan, is located in the hinterland of the Himalayan fold-and-thrust belt on the west side of the Nanga Parbat - Haramosh syntaxial bend (Figure 1). The area was originally mapped by Martin, Siddiqui, and King (1962), and King (1964), who established the general stratigraphy and structure. A major structural feature is the Main Mantle thrust zone, or MMT, which forms a suture between crystalline rocks of the Lower Swat sequence on the Indian plate, and andesitic arc rocks of Kohistan (Tahirkheli, 1979a; 1979b; Kazmi and

others, 1984; Coward and others, 1987; Lawrence and others, 1989). The Lower Swat sequence was regionally metamorphosed and deformed in the Eocene and Oligocene when the Kohistan arc collided with the Indian plate (Maluski and Matte, 1984; Lawrence and others, 1985; 1989). The stratigraphy and structure in Lower Swat, near Saidu, has recently been reinterpreted on the basis of field mapping (DiPietro and Lawrence 1988; in prep.; chapters 2 and 3, this thesis). The revised stratigraphy is illustrated in Plate 1.

The Lower Swat sequence is exposed in a dome in which east-west trending F_4 folds are superimposed on generally north-south trending earlier folds (DiPietro and Lawrence, in prep.). Cambrian to Early Ordovician(?) Swat augen-flaser granitic gneisses form the basement rock in the dome area where they intrude Late Precambrian to Cambrian(?) garnetiferous schists and marbles of the Manglaur formation. Late Paleozoic to Early Mesozoic amphibolites, calc-schists, phyllites and marbles of the Alpurai group unconformably overlie the Manglaur formation and Swat gneisses along the peripheries of the dome. Calc-silicate rocks of the Jobra formation (age unknown) occur as discontinuous lenses unconformably(?) above the Swat gneisses and unconformably(?) below the Alpurai group (chapter 2, this thesis). Tourmaline granite gneiss, of suspected Paleogene(?) age, intrudes the sequence principally along the unconformity below the Alpurai group. Common mineral associations in each of the major rock units are presented in Table 1. Estimated modes and locations of 12 microprobe samples are given in Table 2 and Figure 17 respectively. The maximum exposed thickness of the metamorphic section near Saidu is about 3500 meters. The present thickness of the Alpurai group is about 2000 meters.

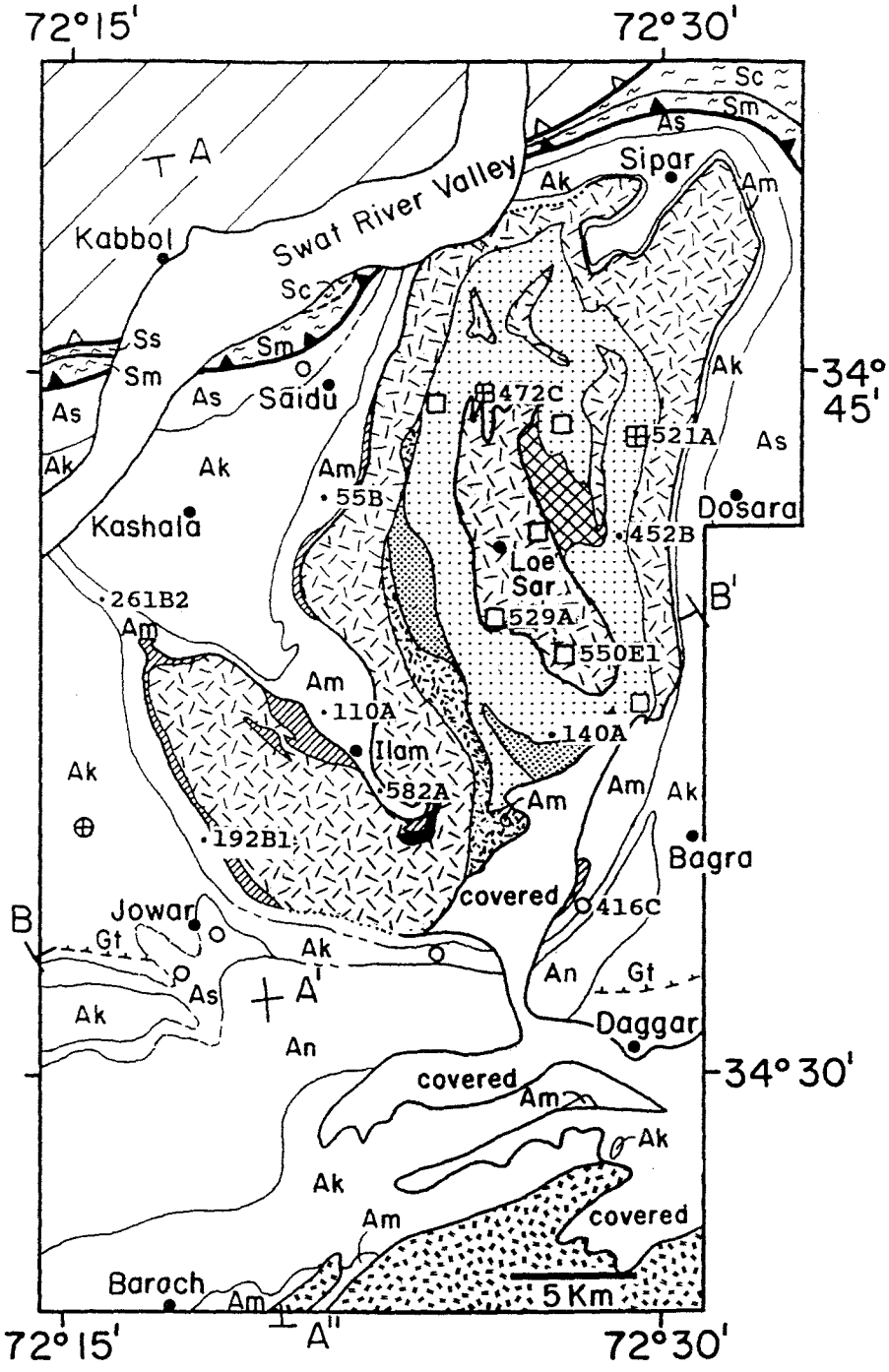

Figure 17. Geologic map of the Lower Swat area showing locations of microprobe samples. Note that the prefix "6-" has been omitted from the sample location designations. See Plate 1 for explanation of map symbols. The location of the 43 B/6 quadrangle is 34°30' to 45' latitude and 72°30' to 45' longitude.

Table 1: **Mineral Associations in the 43 B/6 quadrangle**

Nikanai Ghar	Cal - Dol - (Qtz)
Saidu	Qtz - Ms - Ilm - Gr - Rt - (Grt, Ep, Pl, Chl)
Kashala	Cal - Qtz - Ms - Ilm - Ep - (Grt, Pl, Chl, Gr, Rt) Qtz - Ms - Ilm - Cal - Grt - Ep - Chl - Cld - Gr - Pl
Marghazar	Qtz - Ms - Bt - Pl - Grt - (Ilm, Rt, Gr, Ep, Chl) Qtz - Bt - Pl - Ep - (Cal) Qtz - Bt - Pl - Kfs - (Grt, Ms) Hbl - Qtz - Pl - (Ep, Grt, Bt, Cal, Ms, Rt, Ilm, Chl) Hbl - Qtz - Ep - (Cal) Cal - Qtz - Pl - Ep - Phl - Ms - Ilm - (Spn) Cal - Qtz - Ep - Phl - Tr *Hbl/Act - Ab - Ep - Qtz - Chl - Spn - (Bt, Cal, Ilm) #Chl - Qtz - Ilm - Ab - Spn - (Ms)
Jobra	Cal - Qtz - Woll - Grs - Hgrs - Sal - Kfs - Spn Cal - Dol - Tr - Chl
Manglaur	Qtz - Ms - Bt - Pl - Grt - Ilm - (Rt, Ep, Ky) Qtz - Ms - Grt - (Ilm) Cal - Dol - Tr - (Phl) Cal - Qtz - Tr
Tour. Gneiss	Kfs - Qtz - Pl - Ms - Tm
Swat Gneiss	Kfs - Qtz - Pl - Ms - Bt - (Ep, Grt, Ky, Spn)

Parentheses indicate presence in some of the rocks.
* Occurs south of the B/6 quad, near Daggar.
# Occurs south of the B/6 quad, near Baroch.
Ilmenite after rutile is common.
Chlorite after garnet is common in the garnet zone.
Tourmaline, apatite, and zircon are common accessories.
List of mineral abbreviations given in Table 5.

Table 2: Estimated Modal Mineralogy of Rock Samples Analyzed by Microprobe

Unit	Location	GS	Qtz	Ms	Bt	Pl	Ep	Grt	Ky	Fib	Kfs	Hbl	Ilm	Mag	Rt	Gr	Chl	Cal
Marghazar	6-55B	0.2	10	--	5	2	1	1	--	--	--	79	tr	--	1	--	tr	1
	6-110A	0.2	40	13	18	25	tr	1	--	--	--	--	2	--	tr	tr	tr	tr
	6-192B1	1.0	20	1	5	10	1	12	--	--	--	45	tr	--	4	--	1	tr
	6-261B2	0.4	45	30	7	8	tr	3	--	--	--	--	tr	--	tr	6	tr	--
	6-416C	0.4	25	35	14	15	tr	6	--	--	--	--	tr	--	tr	--	4	--
	6-582A	0.3	22	40	15	10	tr	4	--	--	--	--	2	--	tr	6	tr	tr
Manglaur	6-140A	0.4	30	30	7	20	--	10	--	--	--	--	2	--	tr	tr	tr	--
	6-452B	0.3	33	18	18	23	2	5	--	--	--	--	tr	--	tr	--	tr	--
	6-472C	0.2	30	tr	20	20	tr	2	20	7	--	--	--	--	tr	--	--	--
	6-521A	0.5	15	25	5	42	tr	3	4	tr	--	--	--	5	--	--	--	--
Loe Sar	6-529A	0.6	30	7	20	40	--	2	tr	--	--	--	--	--	--	--	--	--
	6-550E1	0.1	30	10	20	15	--	3	7	--	15	--	--	--	--	--	--	--

GS refers to average grain size of groundmass in mm.
Mineral abbreviations listed in Table 5.
Accessory minerals include apatite, tourmaline, and zircon.
See Figure 17 for location of samples.

DISTRIBUTION OF METAMORPHIC FACIES

As noted by King (1964), the metamorphism is normal in the sense that the deepest seated rocks, in the core of the dome, are at the highest grade. Kyanite is known at only eight locations within the Manglaur formation and Swat gneiss (Figure 17). At four of these locations kyanite occurs in trace amounts where it is completely surrounded by muscovite or garnet. Three of the remaining locations are represented by samples 6-550E1, 6-472C, and 6-521A which contain the stable assemblage quartz-muscovite-oligoclase-biotite-garnet-kyanite. K-feldspar is a stable additional phase in 6-550E1. Late-formed fibrolite is an additional phase in the latter two samples. Evidence for "in situ" anatectic melting, is restricted to only a few areas in the Manglaur formation. However, intruded zone B contains sills and dikes of leuco-granitic rock which cross-cuts foliation in the schists. These may represent synmetamorphic melts derived from deeper, unexposed, parts of the dome. A large post-tectonic pluton (the Malakand granite) is present 25 km to the west of the study area. Marbles in the Manglaur formation contain calcite-dolomite-tremolite or calcite-quartz-tremolite.

A kyanite isograd could not be mapped in the area because the Swat granitic gneiss intervenes between kyanite zone rocks in the Manglaur formation and garnet zone rocks in the overlying Alpurai group and Jobra formation. The Jobra formation is characterized by a calcite-quartz-wollastonite-bearing calc-silicate rock that is present in association with amphibolite, garnet-biotite schist, and calcite-dolomite-tremolite marble. The Marghazar formation, at the base of the Alpurai group, contains schists, amphibolites, and marbles with a variety of garnet zone assemblages that include

quartz-muscovite-oligoclase-biotite-garnet, garnet-biotite-K-feldspar, hornblende-quartz-plagioclase, hornblende-quartz-epidote, and calcite-quartz-phlogopite-zoisite-plagioclase (Table 1). A typical assemblage in the calcareous schists of the overlying Kashala formation is calcite-quartz-muscovite-ilmenite-garnet (±clinozoisite, ±plagioclase). Chloritoid is an additional phase in one rock near the western edge of the map area (Plate 1).

Further to the south, a garnet "isograd" is mapped in the calcareous schists of the Kashala formation. Reactions leading to the first appearance of garnet in these rocks are complicated by the fact that the Kashala formation becomes more calcareous and less pelitic toward the south. The rock assemblage at the isograd is quartz-calcite-muscovite-clinozoisite-garnet-chlorite-ilmenite (±graphite, ±rutile, ±plagioclase). Two to three kilometers south of the isograd, the typical rock assemblage is calcite-quartz-muscovite (±ilmenite, ±plagioclase). Thus, garnet, clinozoisite, and chlorite, all first become abundant near the garnet isograd. The intervening Saidu formation consists of graphitic phyllites in which garnet is present in the vicinity of Jowar, but is absent two to three kilometers further south. The intervening Nikanai Ghar formation consists of a thick sequence of marbles and dolomitic marbles which lack garnet entirely.

Amphibolitic rocks in the Marghazar formation give a clearer indication of decreasing metamorphic grade toward the south. Well north of the garnet "isograd," hornblende-quartz-plagioclase assemblages typically contain only minor, or trace, amounts of epidote-group minerals. Nearer to the garnet "isograd," between Jowar and Bagra, epidote becomes abundant in the amphibolites, accounting for up to 30% of the rock. Interlayered

schists in this area contain the assemblage garnet-biotite-chlorite. Amphibolitic rocks in the small exposure of Marghazar formation just south of Daggar (Figure 17) contain the assemblage hornblende-epidote-albite-quartz-chlorite (± biotite) with actinolite present in the cores of larger amphiboles. Garnet is absent in the interlayered schists. Further south, near Baroch, the rocks are greenschists with the assemblage chlorite-quartz-albite-ilmenite-sphene. In this area, the Marghazar formation is mapped as the Jafar Kandao formation and Karapa greenschist by Pogue and others (in prep.).

In the northern part of the area, a steep metamorphic gradient, with no obvious discontinuity, exists between kyanite zone rocks in the Manglaur formation and chlorite zone rocks in the MMT zone. One possible explanation for this, is late-metamorphic faulting in the MMT zone which could have buried some of the medium-grade rocks. The disappearance of garnet, in this area, occurs either within the graphitic phyllites of the Saidu formation, or at the contact with garnetiferous calc-schists of the Kashala formation. Thus, the disappearance of garnet may be controlled, in part, by changes in bulk chemical composition between the two rock units.

TIMING OF METAMORPHIC CONDITIONS

A detailed account of the structural history and its relationship to the metamorphic fabric is presented in DiPietro and Lawrence (in prep.; chapter 3, this thesis) and is only summarized here. Four superposed fold phases and a strong Eocene-Oligocene regional metamorphism are recognized in the dome area. Mineral

stability in relation to the deformational phases for micaceous rocks of variable bulk composition is shown schematically in Figure 10. Superposed F_1 and F_2 folds can be separated only at the scale of the outcrop. They represent a progressive F_1/F_2 deformation that climaxed with the development of a single set of large-scale NNW-SSE trending, west-vergent folds (termed F_2), and with the development of the dominant, regional (S_2) foliation. In most rocks, S_2 is the earliest foliation present. However, in some of the micaceous rocks, S_2 is deflected around porphyroblasts that contain a straight to weakly crenulated S_1 fabric oriented at a high angle to S_2. These porphyroblasts grew during an inter-kinematic phase between the F_1 and F_2 deformations. S_1 is interpreted as an early, locally developed fabric, that was transposed during a later (S_2) phase of progressive deformation. DiPietro and Lawrence (in prep.) correlate the F_1/F_2 deformation with oblique, west to southwest directed overthrusting of the MMT suture complex above the Lower Swat sequence.

A strong annealing recrystallization followed the F_2 deformation. Thin sections of rocks which lack F_3 and F_4 crenulation folds show smooth grain boundaries, triple junctions, micas and amphiboles oriented orthogonal to the foliation, and a uniform matrix grain size with helicitic, idioblastic porphyroblasts. These textures suggest that peak equilibrium conditions were attained during the post-S_2 annealing phase. The textures are particularly well developed in the Manglaur formation and Swat gneisses.

The annealing phase was followed by the F_3 deformation which produced large-scale, north-south trending, upright folds. Garnet-grade metamorphism outlasted F_3 in the core of the gneiss dome, but ended prior to the end of F_3 near the garnet isograd (DiPietro

and Lawrence, in prep.). The F_3 deformation is believed to be associated with strike slip faulting in the MMT zone north of Lower Swat (DiPietro and Lawrence, in prep.).

Peak equilibrium assemblages were disturbed by retrograde metamorphism prior to and during the development of major east-west trending, south-vergent, F_4 folds. Nearly all of the garnet-bearing rocks contain at least trace amounts of chlorite as an alteration of garnet. Garnet is strongly altered in the area two or three kilometers north of the garnet isograd where locally it is completely pseudomorphed by chlorite. Post-S_2 helicitic porphyroblasts of chlorite occur near the isograd and apparently represent a late equilibrium phase at temperatures below the stability field of the garnet-zone assemblage (Figure 10). Further above the isograd, and in the core of the gneiss dome, garnet shows only trace alteration and chlorite porphyroblasts are absent. DiPietro and Lawrence (in prep.) suggest that F_4 is associated with final, southward-directed emplacement of Kohistan against the Lower Swat segment of the Indian plate.

ANALYTICAL METHODS

All twelve samples selected for thermobarometry contain garnet and biotite in association with a variety of other minerals (Table 2). The samples were collected from as wide an area as possible within the 43 B/6 15' quadrangle (Figure 17). Six samples are from the Marghazar formation. Three of these are garnet-biotite schists; one (6-416C) is a chlorite-garnet-biotite schist, and the other two are hornblende schists. Four samples are from the Manglaur formation. Two of these

are garnet-biotite schists similar to those in the Marghazar formation. The other two are kyanite bearing rocks of unknown protolith. The final two samples are kyanite-bearing gneisses (not augen gneisses) from the Swat gneiss near Loe Sar. None were chosen from the Kashala and overlying formations due to a lack of coexisting garnet and biotite in these rocks.

Selected minerals were analyzed using the automated ARL-EMX-SM microprobe at the University of Oregon, and the new automated Cameca electron probe microanalyzer at Oregon State University using natural and synthetic minerals as standards. Two to four garnets were analyzed in each 2 1/2 cm diameter polished section. Analyzed minerals were either in mutual contact with garnet, or were in close proximity. Significant compositional variation from core to rim was found only in garnet. Average rim compositions from each sample were used for thermobarometry.

All of the microprobe samples show textural evidence of retrograde alteration. Samples 6-472C, 6-521A, and 6-550E1 are the least altered. Kyanite shows only minor alteration to muscovite in these samples. Only trace amounts of kyanite remain in sample 6-529A where it is completely surrounded by muscovite. Garnet appears to be unaltered in samples 6-472C and 6-550E1 but shows slight alteration to biotite in samples 6-521A and 6-529A . In all but one of the remaining samples, garnet shows only slight alteration to chlorite. The exception is sample 6-416C in which a few garnets are completely replaced by chlorite whereas others show only minor alteration with sharp garnet-biotite contacts. The latter garnets were used for temperature-pressure estimates. Chlorite also occurs in the matrix of this rock suggesting equilibrium with garnet and biotite.

Hornblende, in addition to garnet, is partly altered to chlorite in 6-192B2 but not in 6-55B.

Of the more than 200 thin sections examined, the selected microprobe samples (excluding 6-416C) show the minimum of retrograde effects. Temperatures derived from rim compositions of individual garnet-biotite pairs were compared for each of the analyzed garnets. Temperature variation (highest vs. lowest) was greater than 80 degrees for only two samples; 6-110A (variation = 134°C) and 6-416C (109°C). A variation of less than 80 degrees is less than the ±50 degree calibration error suggested by Ferry and Spear (1978).

GEOTHERMOMETRY AND GEOBAROMETRY

The binary Fe-Mg exchange reaction almandine + phlogopite = pyrope + annite was experimentally calibrated for geothermometry by Ferry and Spear (1978). They suggest that this is a useful geothermometer, without correction for other components, up to 0.2 (Ca+Mn/Fe+Mg+Ca+Mn) in garnet and up to 0.15 (Alvi+Ti/Alvi+Ti+Fe+Mg) in biotite with an uncertainty of ±50 degrees. None of the twelve analyzed garnet-biotite pairs meet these requirements (Table 3, page 126). Empirical correction schemes for non-ideal mixing in garnet have been proposed by Newton and Haselton (1981) and by Ganguly and Saxena (1984). These mixing models can be applied to the Ferry and Spear calibration in order to better estimate equilibrium temperatures. Calculated temperatures, using the Ferry and Spear (1978) calibration, are presented in Table 4 as T1. Temperatures T2 and T3 were calculated using the Newton-Haselton and the Ganguly-Saxena corrections, respectively, for non-ideal mixing in garnet at a fixed

pressure of 8000 bars. All three calibrations assume ideal mixing in biotite. 8000 bars was chosen as the fixed pressure because calculated pressures are in the range of 6000 to 10,000 bars.

Each of the three calibrations give equilibrium temperatures generally in the 530 to 670°C range with relatively higher temperatures in the Manglaur and Loe Sar units than in the Marghazar formation. Average temperatures for the Marghazar formation are T1=542°C, T2=618°C and T3=550°C. Those in the Manglaur and Loe Sar units are T1=633°C, T2=665°C, and T3=622°C.

The Newton-Haselton correction (T2) gives considerably higher temperature estimates than the other two calibrations. This discrepancy may be due to overcompensation for the large grossular component in the Lower Swat rocks, and to the lack of compensation for the spessartine component. The Ganguly-Saxena correction (T3) compensates for both grossular and spessartine and resulted in similar, but slightly higher, temperature estimates than the Ferry and Spear (1978) geothermometer.

Minimum equilibrium pressures can be estimated in two ways. The assemblage biotite-garnet-kyanite, in four of the twelve analyzed samples, indicate pressures above Carmichael's (1978) bathograd 4, which he estimates at approximately 4.8 kbar. Sample 6-472C also contains rutile and quartz but no ilmenite. Lang and Rice (1985) derived the equilibrium constant expression for the reaction; Alm + 3Rt = 3Ilm + Ky + Qtz through linear programming of the experimental data presented in Bohlen and others (1981, 1983). Their expression in terms of pressure is:

$$P = (T(\ln K - 0.9347) - 1230.47)/-0.1672 \quad \text{(bars, K)}.$$

Using the Hodges and Spear (1982) activity model for almandine (Table 5), and assuming ideal mixing for the

other phases, the minimum pressure at T3 (615°C) is 4.3 kbar.

Equilibrium pressures were estimated at T3 using the five equilibria shown in Table 4 with the activity models presented in Table 5. Molar volume data for each end-member phase is from Berman (1988), except annite, which is from Helgeson and others (1978). The tschermak component in muscovite was calculated using the formulation of Hodges and Crowley (1985). An increase of one degree temperature will increase pressure by 20 to 30 bars for the barometers used. Consequently, pressure calculations at T2 would be considerably higher than those presented in Table 4.

Equilibria P1 and P2 are appropriate for ten of the analyzed samples. Equilibrium P1 was originally calibrated as a geobarometer by Ghent and Stout (1981). The empirical calibrations of Hodges and Crowley (1985) are used in the calculation of both P1 and P2. Hodges and Crowley (1985) considered these two equilibria to be the best calibrated among the Al_2SiO_5-absent geobarometers, with P1 of better quality than P2.

Equilibrium P3 was originally calibrated as a geobarometer by Ghent (1976) and is appropriate for the aluminosilicate-bearing samples. This geobarometer is used frequently and is generally considered to be the most accurate. The formulation and partial molar volume calculations described in Newton and Haselton (1981) are used in the calculation of P3 with the revised kyanite polymorph end-member calibration of Koziol and Newton (1988). Slightly higher pressures (up to 500 bars) were obtained using the equilibrium constant expression for this equilibrium calculated by Lang and Rice (1985).

Equilibrium P4 was originally calibrated by Hodges and Crowley (1985) but they considered it inferior relative to other calibrations. Lang and Rice (1985)

derived an equilibrium constant expression for this equilibrium based on the data of Helgeson and others (1978). Their calibration is used for P4 estimates.

Equilibrium P5 was recently calibrated by Kohn and Spear (1989) and is appropriate for the two analyzed amphibolitic schists in the Marghazar formation. The formulation and activity models for amphibole presented in Kohn and Spear (1989) are used with the average rim compositions of amphibole given in Table 6.

Given their similar positions in the metamorphic sequence and their proximity to each other, all of the samples should record similar pressures with slightly higher pressures expected in the Manglaur and Loe Sar samples due to their presumed deeper burial and higher equilibrium temperatures. The two best-calibrated barometers (P1 and P3) yield pressure estimates between 8.1 and 9.2 kbars for a majority of the samples. The other calibrations yield somewhat lower estimates, generally between 6.6 and 8.1 kbars.

Newton and Haselton (1981) used a different activity model for plagioclase than the Hodges and Royden (1984) activity model used here. Total pressures calculated with the Newton and Haselton (1981) model yield slightly lower pressures (up to 600 bars) in the Marghazar formation samples but variable pressure differences ($\pm$600 bars) in the Manglaur and Loe Sar units relative to the estimates in Table 4.

It is interesting that, although the calculated temperature of sample 6-521A appears anomalously high, the calculated pressures are consistent with other samples. This rock is characterized by highly contorted, millimeter-scale layering, suggesting that it represents an "in situ" partial melt. Kyanite is restricted to the leucocratic layers. A possible explanation for the high temperatures and partial melting of this rock is that it

equilibrated in close proximity to an unseen, syn-metamorphic intrusion. Heat generated during crystallization of the intrusion could have locally heated this sample to the indicated temperature without affecting its equilibrium pressure. The calculated temperature of sample 6-529A is also relatively high. Field relationships suggest that this rock may also represent an "in situ" partial melt (chapter 2, this thesis).

Fibrolite in samples 6-472C and 6-521A pose a problem in that the estimated pressure-temperature conditions for these rocks are well within the kyanite-Al_2SiO_5 polymorph stability field of Holdaway (1971). In both samples, kyanite shows only minor alteration to muscovite. Also, kyanite is abundant relative to fibrolite. Whereas kyanite occurs in the matrix of the rock, fibrolite is restricted to interstitial boundaries between quartz and/or plagioclase grains. These relationships suggest that fibrolite is a late, residual phase, that crystallized during the retrograde path when the rocks apparently entered the sillimanite-Al_2SiO_5 stability field.

Sample 6-550E1 is unusual in that it contains quartz-muscovite-kyanite-K-feldspar in apparent equilibrium. Given the estimated P-T conditions, this assemblage implies extreme dilution of H_2O in the fluid. Although carbonate-rocks are abundant in the Lower Swat area, it is unknown why this particular rock would show this feature when rocks, in closer proximity to the carbonates, do not. The rock occurs in a minor shear zone, where it is interlayered with Swat augen granodiorite gneiss. The protolith of 6-550E1 is unknown but, in the field, the rock resembles augen granodiorite gneiss without the augen. Curiously, a sample of augen granodiorite gneiss (located in the Swat gneiss just east of Loe Sar, Figure 17) also contains the assemblage

quartz-muscovite-kyanite-K-feldspar. In this rock, kyanite occurs in trace amounts and is completely surrounded by muscovite. Nevertheless, the assemblage suggests unusual fluid conditions during kyanite growth. There are small bodies of syn- to post-tectonic carbonatite within intruded zone B (Figure 17; chapter 2, this thesis). Perhaps other carbonatite bodies, in close proximity to the kyanite-K-feldspar-bearing rocks, locally produced unusual fluid conditions during metamorphism.

Calculated pressures in sample 6-550E1 are lower than pressures calculated in the eleven other samples. A possible explanation is that sample 6-550E1 was more strongly affected by later retrograde exchange due to its smaller grain size (Thompson and England, 1984; Table 2). Because 6-550E1 occurs in a shear zone, a second possibility is that the rock equilibrated somewhat later than the other samples due to late-metamorphic shearing and dynamic recrystallization.

P5 pressures in Table 4 represent the average of four calibrations presented in Kohn and Spear (1989). The calibrations give pressures between 9.0 and 9.6 kbar using the Mg end-member amphibole activities, but give anomalously low pressures estimates of between 3.4 and 5.2 kbar using the Fe end-member amphibole activities of Kohn and Spear (1989). This leads to a precision error of $\pm$6.4 kbar. The mineral composition of these rocks falls within the limits outlined by Kohn and Spear (1989), therefore, it is suggested that the Fe end-member activity models are incorrect for these particular rocks and that the Mg end-member models more accurately reflect equilibrium pressures. Discarding Fe end-member calculations would yield average P5 pressures of 9.2 and 9.4 kbars ($\pm$0.9 kbar) for 6-55B and 6-192B1 respectively.

Several variables affect the accuracy of the pressure estimates including the choice of geothermometer and activity models used, the effects of exchange reactions during cooling, and the quality of the calibrations themselves. The general consistency of the P1 and P3 calibrations suggest an average equilibrium pressure of about 8.5 kbar. The variation between the highest pressure estimate (P3=10.5 kbar, 6-529A) and the lowest pressure estimate (P2=6.1 kbar, 6-550E1) suggests a precision of $\pm$2.4 kbar. There do not appear to be significant differences in calculated pressures between the Marghazar, Manglaur, or Loe Sar units.

Table 3: Composition Data

Sample location	Garnet Rim				Biotite				Plagioclase		Muscovite			
	X_{Mg}	X_{Fe}	X_{Ca}	X_{Mn}	X_{Fe}	X_{Mg}	X_{Alvi}	X_{Ti}	X_{Ca}	X_{Na}	X_{Na}	X_{Alvi}	X_{Fe}	X_{Mg}
6-55B	0.145	0.610	0.207	0.038	0.337	0.491	0.144	0.027	0.256	0.739	--	--	--	--
6-110A	0.080	0.650	0.229	0.040	0.428	0.393	0.150	0.027	0.196	0.798	0.097	0.860	0.049	0.071
6-192B1	0.128	0.639	0.218	0.015	0.349	0.474	0.150	0.026	0.286	0.705	0.147	0.883	0.042	0.061
6-261B2	0.174	0.631	0.191	0.003	0.321	0.521	0.128	0.029	0.279	0.715	0.158	0.869	0.037	0.074
6-416C	0.117	0.717	0.158	0.009	0.391	0.426	0.161	0.021	0.198	0.796	0.185	0.906	0.033	0.051
6-582A	0.167	0.663	0.155	0.015	0.318	0.513	0.141	0.027	0.312	0.683	0.141	0.877	0.033	0.071
6-140A	0.135	0.756	0.073	0.037	0.375	0.415	0.179	0.029	0.104	0.893	0.182	0.902	0.037	0.047
6-452B	0.137	0.618	0.223	0.023	0.361	0.455	0.153	0.029	0.276	0.716	0.102	0.859	0.082	0.040
6-472C	0.152	0.609	0.047	0.192	0.338	0.447	0.141	0.068	0.156	0.836	--	--	--	--
6-521A	0.186	0.716	0.030	0.068	0.410	0.398	0.134	0.056	0.124	0.870	0.054	0.835	0.105	0.050
6-529A	0.127	0.747	0.079	0.047	0.456	0.353	0.130	0.060	0.197	0.791	0.056	0.895	0.047	0.043
6-550E1	0.125	0.814	0.034	0.027	0.435	0.349	0.139	0.076	0.145	0.846	0.057	0.899	0.038	0.046

Table 4: Temperature - Pressure Estimates

	TEMPERATURE (°C)			PRESSURE (kbar)				
	T1	T2	T3	P1	P2	P3	P4	P5
				Alm+Grs+Ms =3An+Ann	Alm+2Grs+3Ts +6Qtz =6An	Grs+2Ky+Qtz =3An	Alm+Ms =Ann +2Ky+Qtz	6An+3Ab+3Tr =2Grs +Prp+3Prg+18Qtz
	(at 8000 bars)			(at T3)	(at T3)	(at T3)	(at T3)	(at T3)
Marghazar								
6-55B	561	644	570	--	--	--	--	6.7
6-110A	503	591	555	9.2	8.6	--	--	--
6-192B1	530	615	547	8.4	7.6	--	--	6.9
6-261B2	575	651	554	8.6	7.8	--	--	--
6-416C	534	597	547	8.9	8.6	--	--	--
6-582A	548	609	527	7.4	6.6	--	--	--
Manglaur and Swat							--	--
6-140A	558	587	547	8.6	7.9	--	--	--
6-452B	586	676	601	9.6	8.1	--	--	--
6-472C	611	630	615	--	--	8.3	8.0	--
6-521A	758	771	697	8.1	6.4	9.0	6.6	--
6-529A	669	702	667	9.1	9.0	10.5	7.9	--
6-550E1	616	626	604	6.3	6.1	7.0		

T1 - Ferry and Spear (1978) calibration.
T2 - Newton and Haselton (1981) correction.
T3 - Ganguly and Saxena (1984) correction.
P1, P2 - Hodges and Crowley (1985) calibration.
P3 - Kazoil and Newton (1988) calibration.
P4 - Lang and Rice (1985) calibration.
P5 - Kohn and Spear (1989) calibration.

Table 5: Mineral abbreviations and activity/composition relationships

Act - actinolite	Gr - graphite	Pl - plagioclase
Ab - albite	Grs - grossular	Prp - pyrope
Alm - almandine	Grt - garnet	Qtz - quartz
An - anorthite	Hbl - hornblende	Rt - rutile
Ann - annite	Hgrs- hydrogrossular	Sal - salite
Bt - biotite	Ilm - ilmenite	Spn - sphene
Cal - calcite	Kfs - K-feldspar	Sps - spessartine
Chl - chlorite	Ky - kyanite	Ts - tschermak
Cld - chloritoid	Ms - muscovite	Tm - tourmaline
Dol - dolomite	Pg - paragonite	Tr - tremolite
Ep - epidote group	Prg - pargasite	Wo - wollastonite
Fi - fibrolite	Phl - phlogopite	

X_i = i/Fe+Mg+Ca+Mn in garnet
X_i = i/Fe+Mg+Ti+Mn+Alvi in biotite
X_i = i/Ca+Na+K in plagioclase
X_i = i/Fe+Mg+Ti+Mn+Alvi in muscovite
X_i = i/Na+K in muscovite

$$a_{Alm} = (X_{Fe} \exp[((6.28T-13807)X_{Mg} X_{Ca})/RT])^3 \quad \text{(HS)}$$

$$a_{Grs} = (X_{Ca} \exp[((13807-6.28T)(X_{Mg})^2+X_{Mg} X_{Fe}+X_{Mg} X_{Mn})/RT])^3 \quad \text{(HS)}$$

$$a_{Ann} = (X_{Fe})^3 \quad \text{(HC)}$$

$$a_{An} = X_{Ca} \exp(610.34/T-0.3837) \quad \text{(HR)}$$

$$a_{Ms} = (X_K(X_{Alvi})^2) \exp[((X_{Na}(X_{Alvi})^2)^2(W_{Ms}+(2X_K(X_{Alvi})^2(W_{Pg}-W_{Ms})))/RT] \quad \text{(HR)}$$

$$W_{Ms} = 19455.55 + 0.45605P + 1.6543T \quad \text{(HR)}$$

$$W_{Pg} = 12229.96 + 0.66524P + 0.7104T \quad \text{(HR)}$$

$$a_{Ts} = (2X_{Alvi} - 1)/2X_{Fe} \quad \text{(in muscovite)} \quad \text{(HC)}$$

(Joules, bars, K)

HS = Hodges and Spear (1982); HC = Hodges and Crowley (1985)
HR = Hodges and Royden (1984); PG = Pigage and Greenwood (1982)

Table 6: Amphibole composition

	6-55B	6-192B
SiO_2	41.9	41.5
TiO_2	0.50	0.46
Al_2O_3	17.2	17.5
FeO	13.6	14.8
MnO	0.13	0.03
MgO	9.53	8.83
CaO	11.0	11.3
Na_2O	1.76	1.56
K_2O	0.59	0.54
H_2O	2.01	2.01
	98.22	98.53
Number of ions on basis of 24 (O, OH)		
Si	6.241	6.197
Aliv	1.759	1.803
Alvi	1.251	1.272
Ti	0.056	0.052
Fe^{+3}	0.000	0.000
Mg	2.113	1.964
Fe^{+2}	1.698	1.847
Mn	0.016	0.003
Ca	1.754	1.799
Na(M4)	0.112	0.063
Na(A)	0.396	0.387
K	0.112	0.103

FeO expressed as total Fe.
Calculated minimum Fe^{+3} using computer program of Spear and Kimball (1984).

GARNET ZONING PATTERNS AND P-T PATHS

Utilizing the rim compositions of coexisting minerals, thermobarometry provides a temperature and pressure estimate at the time of final equilibrium in the rock. If the rock is not significantly retrograded then this equilibrium is close to the maximum temperature experienced by the rock (England and Thompson, 1984; Spear and others, 1984). However, in the case of Lower Swat, where the rocks are on the exhumed lower plate of an overthrust pile, the pressure recorded at maximum temperature may be only 50 to 80 percent of the maximum pressure experienced by the rock (England and Thompson, 1984). This relationship has been discussed by England and Richardson (1977) and England and Thompson (1984) who argue that mineral recrystallization is controlled principally by the rate of burial, uplift, and erosion. They assume that the rocks below a thrust sheet are loaded rapidly during the thrusting phase leading to a rapid increase in pressure. Temperature, on the other hand, increases more slowly due to the relatively slow rate of heat production and heat flow in the rocks. Pressure could therefore reach some maximum and then decrease during erosion of the overthrust pile while temperature continues to increase (England and Richardson, 1977; St-Onge, 1987). Thus, the equilibrium pressure recorded at the maximum temperature will be dependent on the rate of uplift and erosion relative to the rate of heat production and flow in the rock (England and Thompson, 1984).

Field evidence indicates that the Lower Swat sequence was overridden by the Main Mantle thrust suture melange during the F_1/F_2 deformational phase. The high equilibrium pressures recorded in these rocks support this conclusion. However, peak temperature conditions

were not attained until the post-F_2 annealing phase when pressures may have decreased due to erosion of the overthrust pile. Thermobarometry, in this case, offers little insight into the maximum pressure or P-T path of the rocks.

Spear and Selverstone (1983) and Spear and others (1984) have shown that mineral zoning can be used to calculate the P-T path of a rock during the time that the zoned minerals crystallized. Their technique is based on the Gibbs method which is a system of linear differential equations that completely describes the phase equilibria of a heterogeneous system in terms of the intensive variables, temperature, pressure, chemical potential, and composition (Spear and others, 1982). The Gibbs method is based on the mathematical derivation of the Gibbs phase rule and can be used to quantitatively show how temperature, pressure, chemical potential, and composition are related and how they change with respect to each other (Spear and others, 1982).

The Gibbs method, as utilized by Spear and Selverstone (1983), monitors the change in the temperature and pressure of equilibrium as a function of the change in the composition of the coexisting solid solution phases. Thermobarometry, for example, calculates a specific temperature and pressure that a mineral assemblage of fixed chemical composition must have equilibrated at in order to be in thermodynamic equilibrium. If a mineral such as garnet is zoned, and it can be shown that the garnet grew by growth zoning via continuous reactions with the coexisting low-variance mineral assemblage, then the Gibbs method can be used to calculate the change in temperature and pressure of the rock as a function of the change in the composition of garnet. In this way, the P-T path of the rock can be quantitatively traced backward from when the

garnet rim crystallized to when the garnet core crystallized.

The technique of Spear and Selverstone (1983) requires knowledge of rim compositions in each phase at a specific temperature and pressure, and the molar or partial molar volumes and entropies of each component phase. The input parameters are then formulated into a set of Gibbs-Duhem equations, which describe the homogeneous equilibrium of each phase, and a set of linearly independent equilibrium equations, which describe the heterogeneous equilibria among the coexisting phases. A third set of equations describes the change in the Gibbs free energy surface as a function of the change in the composition of the coexisting solid solution phases. The system of equations can then be solved for the change in temperature and pressure as a function of the change in the composition of the solid solution phases. The method has been used by Spear and Selverstone (1983), Selverstone and others (1984), Spear and Rumble (1986), and Hodges and Silverberg (1988) to trace the P-T paths of rocks from various areas. Spear (1986) has developed a computer program that performs the required calculations using the thermodynamic data of Helgeson and others (1978). This program was used in the garnet zoning analyses of two garnets from the Marghazar formation, and three from the Manglaur formation.

MARGHAZAR GARNETS

Sample 6-416C is a garnet-chlorite-biotite schist located in the Marghazar formation near the garnet isograd (Figures 17 and 18a). Garnet occurs as sub-idioblastic porphyroblasts less than 1.5 mm in diameter. Inclusions of quartz, ilmenite, and clinozoisite are concentrated somewhat randomly in the core but occur at

the rim as well. The average size of inclusions is less than 0.1 mm. Trace amounts of ilmenite and clinozoisite are present in the matrix of the rock but clinozoisite is rare and restricted to the vicinity of garnet.

The dominant (S_2) foliation in 6-416C is both truncated by, and deflected around, the garnet porphyroblasts. Pressure shadows are not well developed and there is alteration to chlorite on the sides of the garnet that impinge against foliation (Figure 18a). These relationships suggest that much of the garnet is post-kinematic with respect to the development of the dominant (S_2) foliation and pre-kinematic with respect to flattening of the foliation around the garnet. The flattening is probably related to F_3 deformation (DiPietro and Lawrence, in prep.). It is concluded therefore, that garnet nucleated during the late stages of F_2 with the main period of garnet growth during the post-F_2 annealing phase.

Sample 6-261B2 is a graphite-bearing garnet-biotite schist located in the Marghazar formation well within the garnet zone (Figures 17 and 18b). Garnet occurs as nearly idioblastic porphyroblasts less than 1.5 mm in diameter. They typically show an inner, well developed ring, and an outer, poorly developed ring of graphite-rich inclusions that mimic the shape of the garnet. Quartz, clinozoisite and rutile occur as inclusions in addition to graphite. All of these minerals are present in at least trace amounts in the matrix of the rock. The inclusions are less than 0.1 mm near the core, but become larger near the rim where they approach the size of the surrounding matrix. The dominant (S_2) foliation is deflected around the garnets producing well developed pressure shadows. Garnet rims, however, helicitically overgrow the dominant (S_2) foliation (Figure 18b). The relationships suggest that garnet nucleated during the

post-F_1 interkinematic phase and continued to crystallize during the post-F_2 annealing phase.

Garnets in 6-416C and 6-261B2 show well developed zoning patterns (Figure 19). The almandine component in garnet 6-416C increases continuously from core to rim. The pyrope component is roughly constant near the core and then increases near the rim. Grossular increases slightly from the core and then decreases toward the rim. Spessartine decreases continuously from core to rim. Garnet 6-261B2 shows a similar profile except that almandine reaches a maximum and then decreases near the rim and grossular increases slightly at the rim on one side of the profile. The maximum almandine content in 6-261B2 occurs just rim-ward of the inner ring of graphite inclusions. Both profiles are nearly symmetrical and both show trends consistent with growth zoning during prograde metamorphism (Tracy, 1982). Other compositional profiles, oriented a various angles to the ones shown in Figure 19, show a very similar pattern. This indicates overall concentric growth zoning in both garnets.

There are no sharp reversals in the trends of spessartine or pyrope at the rim of either garnet. This indicates that post-growth retrograde resorption and diffusion zoning did not significantly affect the garnets along these profiles (de Bethune and Laduron, 1975). The cause of the almandine reversal in garnet 6-261B2 is not known. It may be due to an oxidizing reaction not directly involving garnet but which effectively limited the amount of FeO available in the matrix for the garnet forming reaction.

The modeled assemblage in garnet 6-416C is quartz-plagioclase-muscovite-chlorite-biotite-garnet-clinozoisite-H_2O in the system, SiO_2-Al_2O_3-CaO-MgO-FeO-MnO-Na_2O-K_2O-H_2O. Quartz, muscovite, clinozoisite, and H_2O are considered pure phases. Plagioclase is treated

as a binary Na-Ca phase. Chlorite and biotite are treated as ternary Mg-Fe-Mn phases, and garnet is treated as a quaternary Mg-Fe-Mn-Ca phase. Ideal mixing is assumed for all solid solution phases. Although clinozoisite is rare in the rock matrix, it is included in the model assemblage because it is present as inclusions in the garnet from core to rim. It is assumed that the above mineral phases were present throughout the crystallization history of garnet, and that the garnet rim was in equilibrium with the phase assemblage at all times during its growth. An identical procedure was used for garnet 6-261B2 except that chlorite was not considered to be part of the phase assemblage.

The variance of the assemblage in 6-416C is three so that the change in temperature and pressure can be modeled directly by the change in almandine, spessartine, and grossular components in the garnet without any further assumptions. The starting rim compositions are those from Table 3 with temperature T3=547^{o}C and pressure P1=8900 bars. The starting chlorite composition, from microprobe analysis, is X_{Mg}=0.574, X_{Fe}=0.424, and X_{Mn}=0.002, where X_i=i/Mg+Fe+Mn.

The variance of the assemblage in 6-261B2 is four so that an additional monitor component is needed to define the change in temperature and pressure as a function of composition. The anorthite component in plagioclase was chosen as the fourth variable, and was allowed to change in increments roughly inversely proportional to the change in grossular component from a starting rim composition of An=0.281 to an assumed core composition of An=0.131. The plagioclase compositions were chosen by assuming retrograde chlorite to be part of the assemblage and then monitoring the change in

anorthite content as a function of the change in garnet composition.

The resulting P-T path of both garnets is shown in Figure 20. The two halves of garnet 6-416C show similar P-T trajectories although the absolute pressure values differ by several kbars. The net trajectories suggest garnet growth during significant overall decompression and moderate heating. Much of the decompression is recorded near the garnet rim with the core showing oscillating periods of compression and decompression at pressures between about 12 and 14 kilobars.

The two halves of garnet 6-261B2 also show similar P-T trajectories. Garnet 6-261B2, however, shows near isothermal compression in the core followed by decompression and moderate heating at the rim. The largest increment of decompression is recorded on opposite sides of the inner ring of graphite inclusions. There is only minor decompression at the edge of the garnet although temperatures continued to rise. The maximum pressure recorded is 11.2 kbars, which is considerably less then the 14.2 kbars recorded by garnet 6-416C.

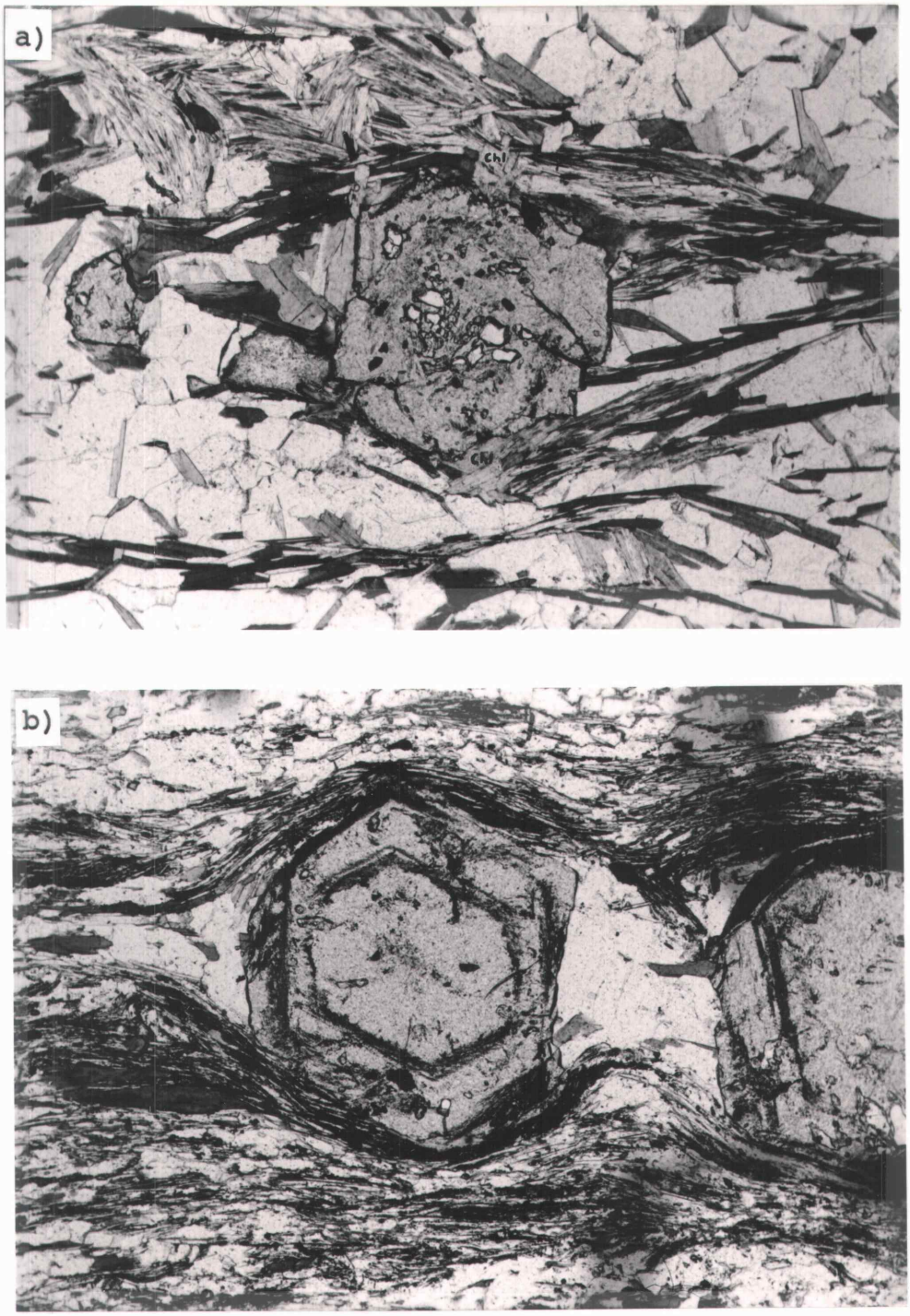

Figure 18. Photomicrographs of garnet from the Marghazar formation. a) Sample 6-416C. The areas where garnet is altered to chlorite (Chl) are labeled. b) Sample 6-261B2. The dominant (S_2) foliation is oriented horizontally in both samples. Photomicrographs are 3.3 mm in long dimension.

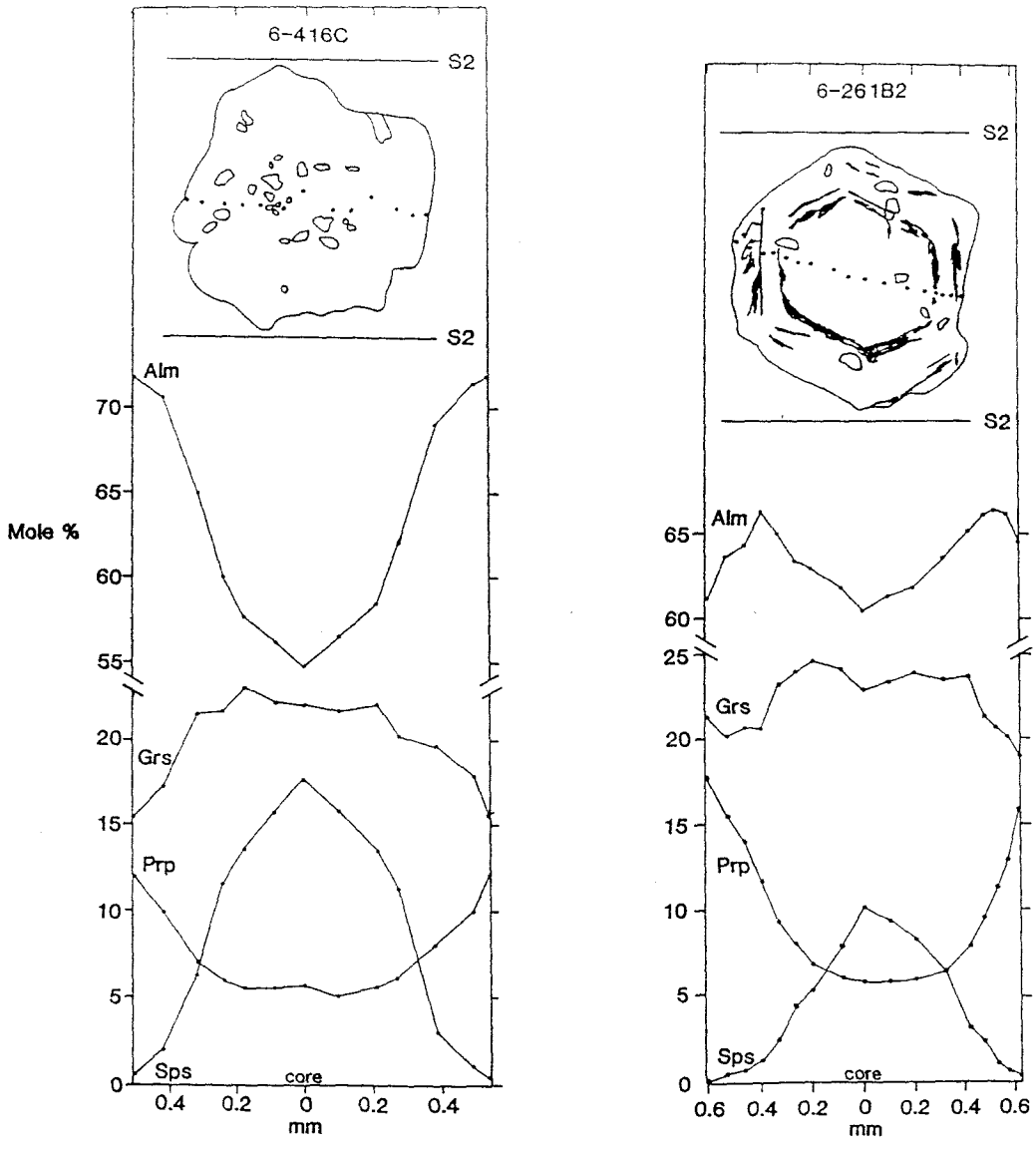

Figure 19. Compositional profiles across garnets 6-416C and 6-261B2 of the Marghazar formation. S_2 represents the orientation of the dominant foliation.

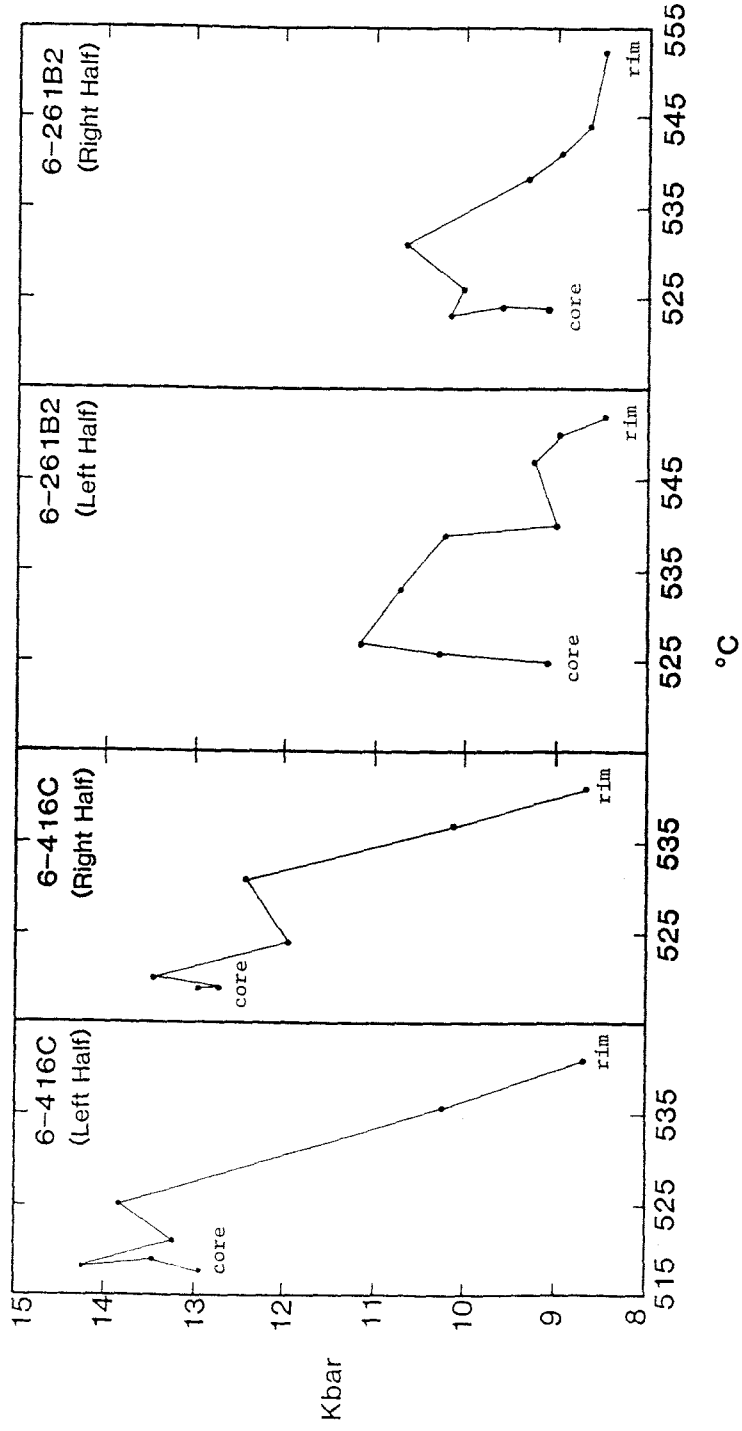

Figure 20. Calculated P-T trajectories of garnets 6-416C and 6-261B2 of the Marghazar formation.

DISCUSSION OF MARGHAZAR GARNETS

Of the two analyzed garnets, sample 6-416C has the lowest variance and, therefore, should more accurately reflect a real P-T path. However, because some of the assumptions of the Gibbs method analysis may not be valid, the calculated P-T paths in Figure 20 should be viewed as qualitative rather than quantitative. For example, the abundance of carbonate rock in the sequence, and the presence of graphite in sample 6-261B2, suggests that the fluid phase was not pure H_2O. The role of clinozoisite in the paragenesis of both samples is not clear. Clinozoisite is abundant in the core of garnets from both samples 6-416C and 6-261B2, but is less common near the rim, and is present only in trace amounts in the matrix. This is particularly true of sample 6-416C where clinozoisite is present only in the matrix surrounding the garnet, suggesting that it is a retrograde phase. Thus, the equilibrium phase assemblage may have changed during the growth history of the garnet. Similarly, the abrupt decrease in almandine at the rim of garnet 6-261B2 may suggest a change in the equilibrium phase assemblage. Also, the clinozoisite, which was considered to be a pure phase in the Gibbs method analysis, actually contains between 6 and 7 weight percent FeO (expressed as total Fe). Finally, the assumption regarding the change in anorthite, in sample 6-261B2, may not be correct.

If clinozoisite is not considered to be part of the rim assemblage in sample 6-416C, and the anorthite content is assumed to vary from between zero and 0.10 (mole fraction), then the Gibbs method analysis suggests an increase in temperature of approximately $10^{o}C$, and a decrease in pressure of between zero and 1.8 kbars from the near-rim (where inclusions of clinozoisite first become sparse) to the rim of the garnet. If clinozoisite

is then included in the assemblage for the garnet core to near-rim analysis, then there is an additional increase of 10°C and a decrease of 0.6 kbars from the core to the near-rim. From this analysis, the calculated temperature and pressure at the time of crystallization of the garnet core in sample 6-416C is about 527°C and between 9.5 and 11.3 kbars (depending on assumptions regarding the change in anorthite content near the rim). These temperatures and pressures correspond well with maximum pressure conditions calculated for garnet 6-261B2.

Regardless of the absolute P-T conditions, the P-T paths derived from the two garnets in the Marghazar formation suggest that pressure was higher, and temperature was lower, prior to final post-F_2 equilibrium. This corresponds well with the structural history of the area which indicates that Lower Swat was overridden by the MMT suture zone melange during the F_1 and F_2 deformational phases (DiPietro and Lawrence, in prep.). Of the two analyzed garnets, sample 6-261B2 shows the longest duration of growth beginning during the post-F_1 interkinematic phase and ending during the post-F_2 annealing phase. Sample 6-416C is closer to the garnet isograd and accordingly shows a shorter duration of garnet growth beginning near the end of the F_2 deformation and ending during the post-F_2 annealing phase. Given these crystallization histories the apparent compression recorded in the core of garnet 6-261B2 may reflect the rapid loading of the Lower Swat sequence by the suture zone melange prior to and during the F_2 deformation. Maximum pressures, of between 9.5 and 11.5 kbars, are recorded in the core of garnet 6-416C, and between the core and rim of garnet 6-261B2. These pressures may reflect the conditions in the Lower Swat sequence near the end of the F_2 deformation.

Decompression is recorded at the rims of both Marghazar garnets suggesting that the F_2 deformation was followed by a period of uplift and erosion. The rims grew during the post-F_2 annealing phase suggesting that uplift occurred initially without significant deformation and during continued heating of the rock.

MANGLAUR GARNETS

The morphology and zoning characteristics of garnets from the Manglaur formation differ from those in the Marghazar formation. Garnets in the Manglaur formation typically occur as elongate porphyroblasts, or as skeletal chains, oriented parallel with foliation. The garnets rarely deflect foliation suggesting that most nucleated during the post-F_2 annealing phase. Only large idioblastic porphyroblasts are zoned but the zoning patterns are erratic and non-symmetric. Compositional variation, from core to rim, is also much less than that found in the Marghazar formation.

Rocks in the Manglaur formation equilibrated at higher temperatures than those in the Marghazar formation, therefore, the lack of well developed growth zoning profiles could be due, in part, to volume diffusion during or after growth (Woodsworth, 1977; Anderson and Olimpio, 1977). However, another factor affecting the zoning profile is that many of the porphyroblasts do not appear to have grown outward from a single, central nucleus. Many apparent porphyroblasts are, in thin section, made up of several smaller garnets that grew into each other to form a single, larger porphyroblast.

Garnet porphyroblasts in sample 6-140A show this relationship (Figures 20a and 20b). Sample 6-140A is a garnet-biotite schist with garnet porphyroblasts less than 1.5 mm in diameter. Most porphyroblasts consist of

an outer inclusion-free rim made up of several smaller idioblastic garnets that encircle a single, central, inclusion-free core. The rim is separated from the core by a central, mottled area rich with opaque inclusions and quartz (Figure 21a). In some instances, atoll garnets are developed in which the middle inclusion-rich garnet zone is replaced by a ring of quartz. The relationships suggest that garnet nucleated as a rosette of individual grains at some distance surrounding a pre-existing(?) core. As the garnets grew, they coalesced forming a single large porphyroblast such that the garnet in Figure 21b may have, at one time, resembled the garnet in Figure 21a.

The dominant S_2 foliation in sample 6-140A is crenulated and a weak S_3 crenulation cleavage is developed. Garnet occurs in the microlithons of S_3, and locally overgrows S_3. This suggests that the garnet rim grew during the development of the S_3 crenulation cleavage, although growth prior to the development of F_3 cannot be ruled out. The relative timing for nucleation of the garnet core is not constrained by the textures and could have occurred anytime prior to, or during, F_3.

Sample 6-452B is a garnet-clinozoisite-biotite schist with garnet porphyroblasts typically less than 1.5 mm in diameter. Foliation truncates against the garnets and pressure shadows are not developed. This suggests significant growth of garnet during the post-F_2 annealing phase (Figure 21c).

Compositional profiles across the Manglaur garnets are shown in Figure 22. The zoning patterns are oscillatory as might be expected of garnets with complex growth histories. Total compositional variation, however, is small particularly when core compositions are compared directly with rim compositions. The flat spessartine profiles, particularly in 6-140A suggests

that diffusion of Mn has occurred (Anderson and Olimpio, 1977). Note that the garnets from 6-140A also contain significantly less grossular and more almandine than the other garnets.

Garnets in the Manglaur formation, because they lack well developed growth zoning profiles, are poor candidates with which to determine P-T trajectories. However, some generalizations can be made based on the differences in the core-rim compositions assuming that the core was fully developed prior to the rim.

Only the grossular component shows a significant variation between the core and rim in sample 6-140A. This variation, and the textural relationships, are taken to indicate that the core represents an earlier phase of garnet growth prior to growth of the rim. Plagioclase and garnet are the only Ca-bearing phases in 6-140A and aluminosilicate minerals are absent. Therefore, it is probable that the grossular content in garnet is controlled by reactions such as P1 and P2 (Table 4) that involve plagioclase but not kyanite. If it is assumed that the gross distribution of grossular has not been significantly altered by diffusion, then the relatively high grossular component at the rim suggests that it crystallized at lower temperature and/or higher pressure than the core (Crawford, 1977). However, the decrease in grossular at the edge of both garnets suggests that pressure was decreasing and/or temperature increasing during the final stages of garnet crystallization.

Although the overall compositional zoning pattern in sample 6-452B is non-symmetric, the profile shows a higher percentage of spessartine and a lower percentage of pyrope and almandine components in the core than at the rim. There is little variation in grossular from core to rim. These trends are similar to, though much

less dramatic than the prograde growth zoning trends in the Marghazar formation and suggest that diffusion has not completely obliterated the growth zoning characteristics of this garnet. The increasing almandine, pyrope, and Mg/Fe ratio from core to rim implies that the core grew at a lower temperature than the rim (Tracy, 1982).

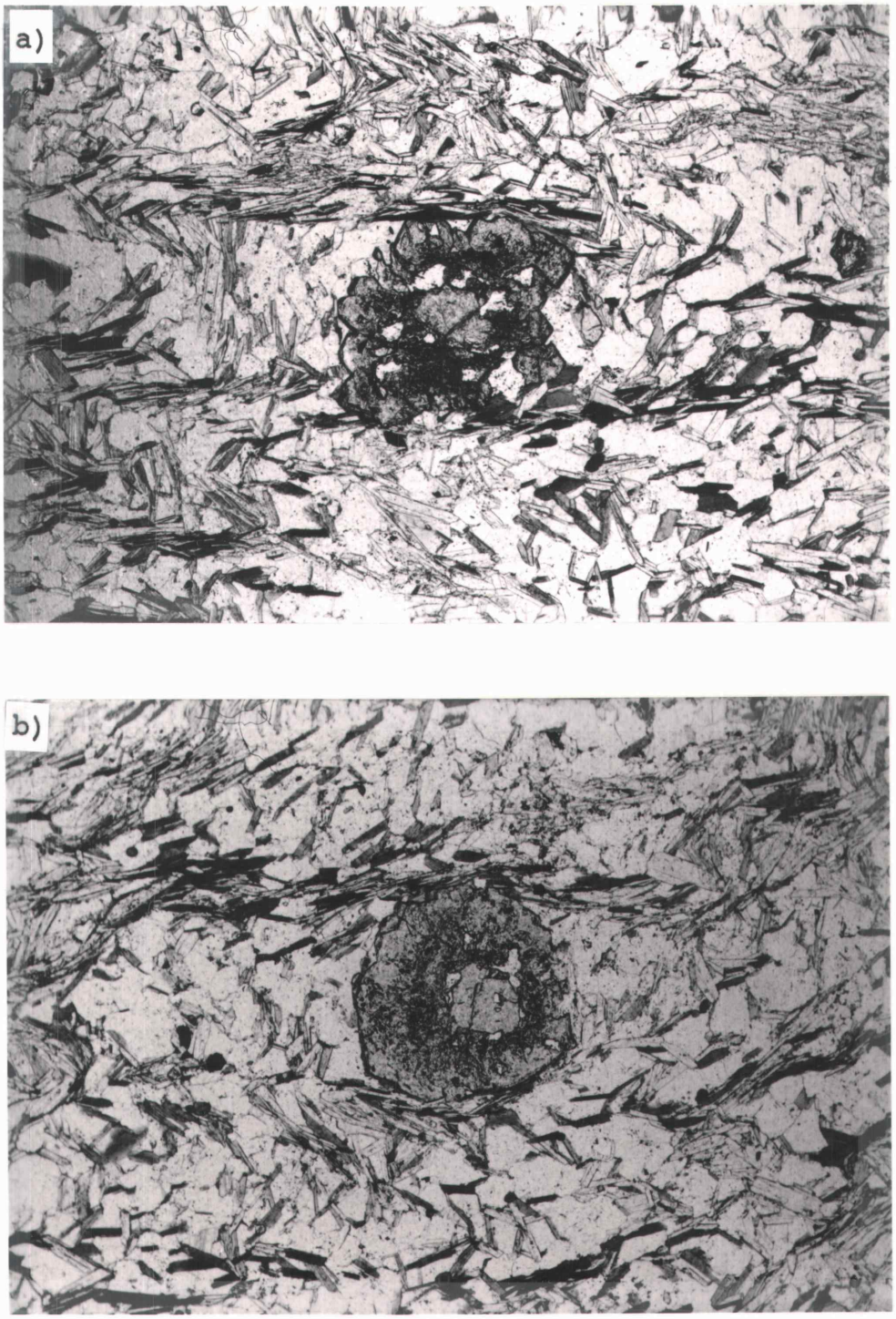

Figure 21. Photomicrographs of garnet from the Manglaur formation. a) Sample 6-140Aa. b) Sample 6-140Ab. The S_2 foliation is nearly vertical and is crenulated by the horizontal S_3 foliation. Figure 21 continued on next page.

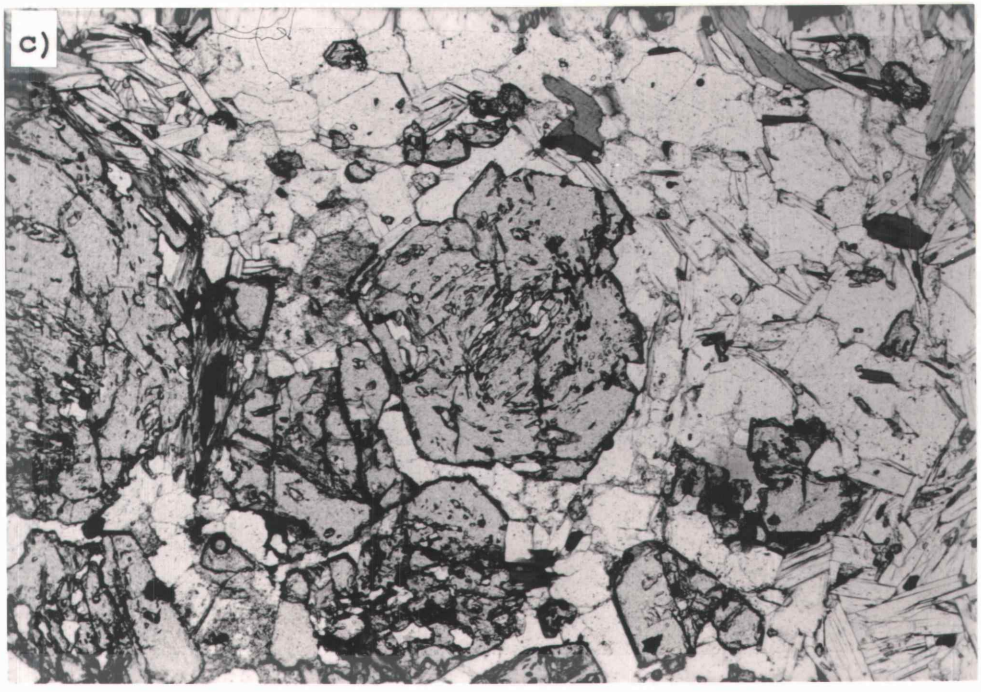

Figure 21 continued. c) Sample 6-452B. The S_2 foliation is oriented horizontally. All three photomicrographs are 3.3 mm in long dimension.

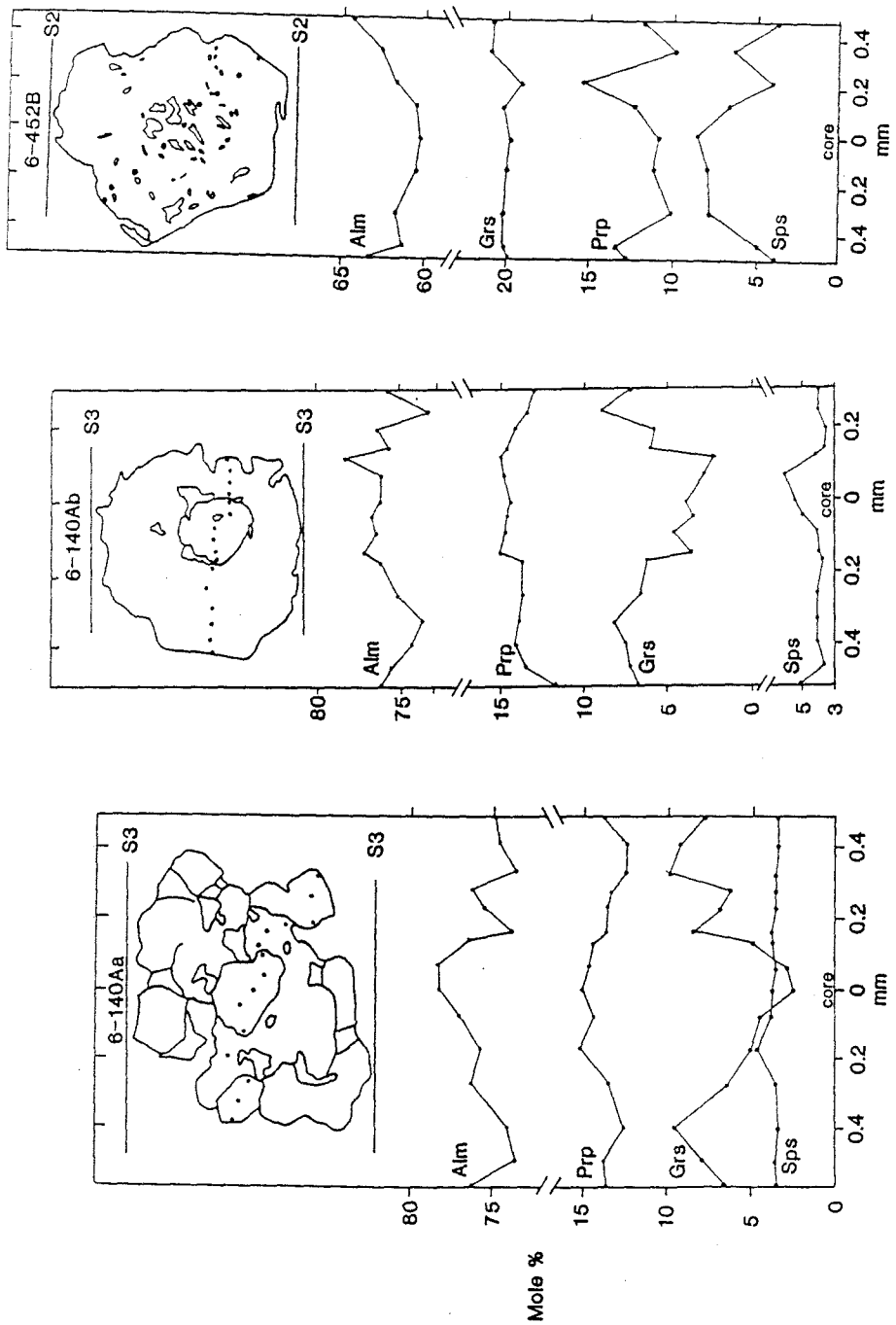

Figure 22. Compositional profiles across garnets 6-140Aa, 6-140Ab, and 6-452B of the Manglaur formation. The orientation of the S_3 foliation in 6-140A, and the S_2 foliation in 6-452B, is shown.

DISCUSSION OF MANGLAUR GARNETS

The deeper burial, higher equilibrium temperatures, and well developed annealed fabrics of the Manglaur formation indicate that it experienced a more prolonged post-F_2 annealing recrystallization than the overlying Marghazar formation. The complex growth histories and zoning patterns complicate any meaningful interpretation of these garnets. The moderate core to rim temperature increase recorded in garnet 6-452B is consistent with the temperature history of the Marghazar garnets. However, the zoning profiles in the garnets 6-140Aa and 6-140Ab suggest an increase in pressure and/or a decrease in temperature at the rim relative to the core. The textural relationships suggest that the rim grew during the F_3 deformation. An increase in pressure at the rim is difficult to reconcile with the field evidence which suggests that the F_3 deformation is related to strike slip motion in the MMT and not to a second overthrusting phase that reburied the Lower Swat sequence (DiPietro and Lawrence, in prep.). One possibility is that the core grew under relatively low confining pressures during F_1, or during the early stages of the post-F_1 interkinematic phase, prior to deep burial of Lower Swat. Another possibility is that the rims grew, and reached equilibrium, during F_3 when temperatures were below their peak. The textural relationships suggest growth during F_3, and the low equilibrium temperatures in this rock, relative to other rocks in the Manglaur formation, support this idea (Table 4). Accordingly, the decrease in grossular at the edge of both garnets could then be due to decreasing pressure conditions during the late stages of F_3 deformation.

DISCUSSION OF A POSSIBLE P-T-t PATH

An inferred P-T path, based primarily on the Marghazar garnets, and correlated with the deformational history of DiPietro and Lawrence (in prep.), is shown in Figure 23. Reported $^{40}Ar/^{39}Ar$ cooling ages in the Lower Swat sequence are circa 38 Ma for hornblende and circa 30 Ma for muscovite (Maluski and Matte, 1984; Lawrence and others, 1985; L. Snee, in Palmer-Rosenberg, 1985; Treloar and others, 1989a). DiPietro and Lawrence (in prep.) reported recrystallized hornblende in F_3 crenulation folds in the Marghazar formation and, therefore, concluded that 38 Ma is the approximate minimum age for the F_1/F_2 and F_3 deformations. Most workers infer from geological and geophysical evidence that initial contact between Kohistan and the Indian plate occurred between 54 and 45 Ma (Molnar and Tapponnier, 1975; Patriet and Achache, 1984; Dewey and others, 1989). It is apparent therefore that the main phase of deformation and metamorphism in the Lower Swat sequence occurred within 7 to 16 m.y. of initial contact. The calculated pressures from this study suggest that, within this time frame, Lower Swat was underthrust (subducted?) to a depth of between 30 and 40 km during the F_1 and F_2 deformational phases. During the ensuing post-F_2 annealing phase, when peak metamorphic conditions prevailed, the rocks were uplifted and eroded to a depth of between 25 and 30 km. Following peak temperature conditions, but still within the 7 to 16 m.y. time frame, the Lower Swat sequence was deformed by F_3 folds.

On the basis of fission track geochronologic data, Zeitler and others (1982), and Zeitler (1985) have inferred steadily decreasing uplift-erosion rates in Lower Swat, from greater than 0.65 mm/yr at 20 to 25 Ma, to about 0.2 mm/yr for the past 10 m.y. Considering the

total 30 to 40 km thickness to be eroded, the initial uplift rate, following the F_2 deformation, may have been on the order of 1 or 2 mm/yr. Dewey and others (1989) infer a 33^{o} anticlockwise rotation in the movement direction of the Indian plate relative to the Eurasian plate approximately 45 Ma. This rotation may relate to an inferred post-F_2 change from subduction to strike slip motion in the suture zone (DiPietro and Lawrence, in prep.). The strike slip motion may have cut off subduction, thereby allowing initially rapid isostatic uplift-erosion of the thickened Lower Swat rock sequence. DiPietro and Lawrence (in prep.) suggest that final emplacement of Kohistan occurred approximately 30 Ma during the F_4 deformation when metamorphic temperature conditions had decreased to the approximate closure temperature of argon in muscovite. This phase of deformation did not result in significant reburial of Lower Swat, but more likely resulted in the initiation of major thrust faults in the Pakistani foreland that carried the Lower Swat-Kohistan plate segment southward (Figure 1). Apparently rapid cooling (uplift-erosion) rates in Lower Swat, between about 22 and 18 Ma (Zeitler and others, 1982; Zeitler, 1985), suggest that this may have been a time of thrust ramping in the Pakistani foreland (Figure 23).

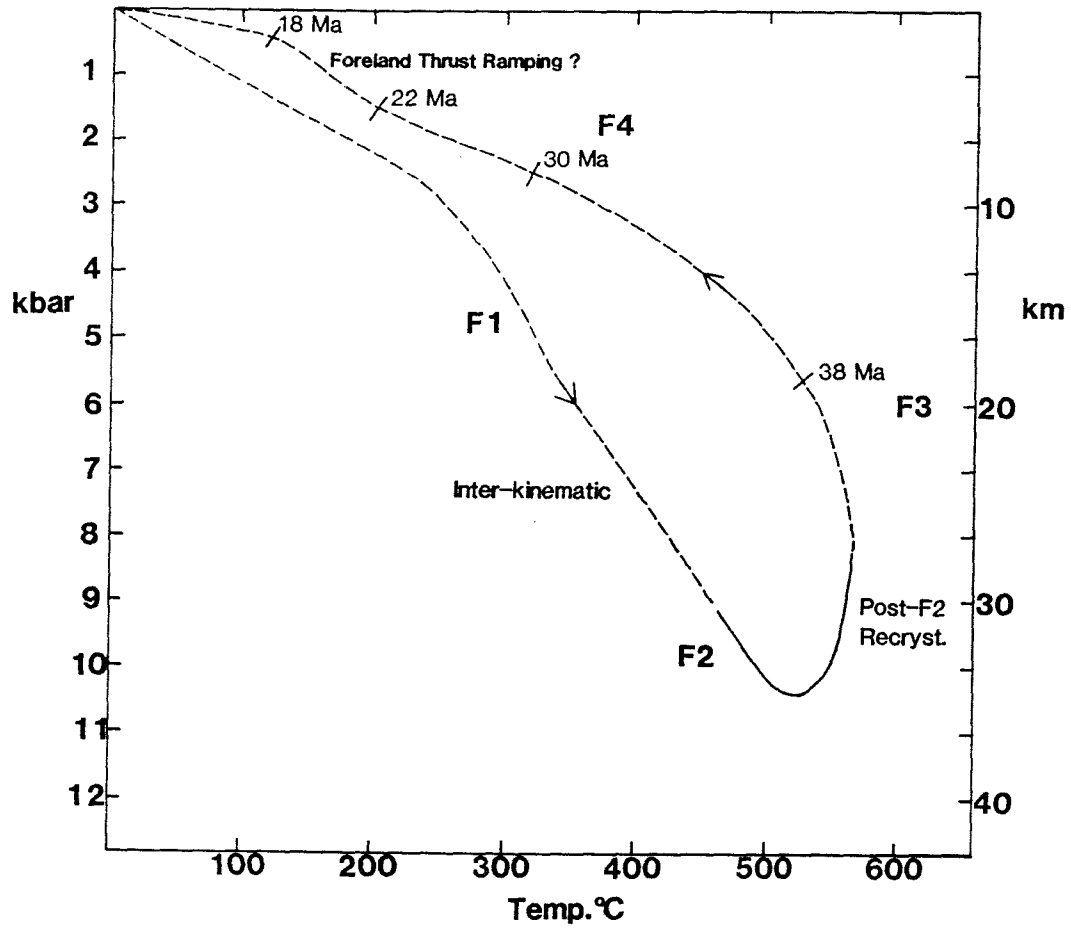

Figure 23. Inferred P-T path of the Marghazar formation correlated with the deformational history. The solid line represents the part of the path based on thermobarometry and the Gibbs method. The dashed line is speculative. Approximate $^{40}Ar/^{39}Ar$ cooling ages for hornblende (38 Ma) and muscovite (30 Ma), and fission track closure ages for zircon (22 Ma) and apatite (18 Ma) are also shown.

CONCLUSION

The rocks in Lower Swat are exposed in a dome in which the deepest-seated unit, the Manglaur formation, is in the kyanite-zone. The surrounding Marghazar formation is in the garnet-zone. A kyanite isograd cannot be mapped because the Swat granitic gneiss intervenes between the two formations. A garnet "isograd" is mapped on the south side of the dome in calcareous schists of the overlying Kashala formation. The regional metamorphism and deformation is Eocene-Oligocene in age and is related to the collision between the Indian plate and the Kohistan arc (Maluski and Matte, 1984; L. Snee, in Palmer-Rosenberg, 1985; Lawrence and others, 1989; Treloar and others, 1989a; DiPietro and Lawrence, in prep.).

Mineral composition geothermometers and geobarometers indicate peak metamorphic conditions in the Manglaur formation to be about 600 to 630°C and 8.1 to 9.2 kbar. The calculated temperature of two of these rocks (6-521A and 6-529A), is between 667 and 771°C. One, or both, may represent an "in situ" partial melt. Peak metamorphic conditions in the overlying Marghazar formation are about 540 to 570°C and 8.1 to 9.2 kbar. These P-T estimates are believed to correspond with the post-F_2 phase of static recrystallization, which followed the main F_1 and F_2 phases of deformation.

P-T paths, inferred from growth zoning profiles preserved in garnets from the Marghazar formation, suggest that temperatures were 15 to 30° lower, and pressures were 1 to 3 kbars higher near the end of the F_2 deformation when the rocks are inferred to have been at their maximum depth of burial. Garnet zoning profiles in the Manglaur formation are complicated by a growth history in which several smaller garnet porphyroblasts

coalesce to form a single larger one. P-T paths inferred from these rocks are unsatisfactory for this reason. The pressure estimates, although relatively high, apparently are not unusual for crystalline rocks on the Indian plate in the hinterland of Pakistan. Treloar and others (1989b) report pressures as high as 11 kbars for Indian plate rocks north of Mansehra (Figure 1). Chamberlain and others (1989) report maximum pressures at final equilibrium of between 7.4 and 8.4 kbars for Indian plate rocks near Nanga Parbat.

Correlation of the metamorphic and deformational history with radiometric cooling ages in Lower Swat, suggests that the metamorphic cycle was rapid, perhaps lasting less than 20 m.y. Uplift and erosion are inferred to have begun immediately after the F_2 deformation.

It is of note that there are no major thrust faults in the Lower Swat sequence between the MMT and the fossiliferous low-grade rocks south of Baroch. This is in stark contrast to the Mansehra area of Pakistan where a series of late to post-metamorphic thrust faults beneath the MMT have resulted in the tectonic stacking of high-grade Indian plate rocks above low-grade rocks (Coward and others, 1986; Treloar and others, 1989b; 1989c). Treloar and others (1989c) suggest that the stacking and imbrication represent an early period of uplift that post-dates the metamorphic peak. In Lower Swat, rapid uplift occurred during the metamorphic peak and was followed by an apparent decrease in uplift rates which resulted in the development of domes rather than major thrust faults.

REFERENCES

Ahmad, I., 1986. Geology of Jowar area, Karakar Pass, Swat District, N.W.F.P., Pakistan. Unpublished MPhil Thesis, University of Peshawar.

Ahmad, I., Rosenberg, R.S., Lawrence, R.D., Ghauri, A.A.K., & Majid, M., 1987. Lithostratigraphy of the Karakar Pass section, south of the Main Mantle thrust, Swat, N.W. Pakistan. Geological Bulletin, University of Peshawar, **20**, 199-208.

Anderson, D.E., & Olimpio, J.C., 1977. Progressive homogenization of metamorphic garnets, South Morar, Scotland: evidence for volume diffusion. Canadian Mineralogist, **15**, 205-216.

Armstrong, R.L., & Dick, H.J.B., 1974. A model for the development of thin overthrust sheets of crystalline rock. Geology, **2**, 35-40.

Ashraf, M., Chaudhry, M.N., & Hussain, S.S., 1980. General geology and economic significance of the Lahor granite and rocks of the southern ophiolite belt in Allai-Kohistan area. Geological Bulletin, University of Peshawar, **13**, 207-213.

Baig, M.S., & Lawrence, R.D., 1987. Precambrian to Early Paleozoic orogenesis in the Himalaya. Kashmir Journal of Geology, **5**, 1-22.

Baig, M.S., & Snee, L.W., 1989. Pre-Himalayan dynamothermal and plutonic activity preserved in the Himalayan collision zone, NW Pakistan: AR thermochronologic evidence. Geological Society of America abstracts with programs, **21**, no.6, 264.

Bell, T.H., 1985. Deformation partitioning and porphyroblast rotation in metamorphic rocks: a radical reinterpretation: Journal of Metamorphic Geology, **3**, 109-118.

Bell, T.H., & Rubenach, M.J., 1983. Sequential porphyroblast growth and crenulation cleavage development during progressive deformation. Tectonophysics, **92**, 171-194.

Berman, R.G., 1988. Internally-consistent thermodynamic data for minerals in the system Na_2O-K_2O-CaO-MgO-FeO-Fe_2O_3-Al_2O_3-SiO_2-TiO_2-H_2O-CO_2. Journal of Petrology, **29**, 445-522.

Berman, R.G., Brown, T.H., & Greenwood, H.J., 1985. An internally consistent thermodynamic data base for minerals in the system Na_2O-K_2O-CaO-MgO-FeO-Fe_2O_3-Al_2O_3-SiO_2-TiO_2-H_2O-CO_2. Atomic Energy of Canada Ltd. Technical Report 377, 62p.

Bethune, P. de, & Laduron, D., 1975. Diffusion processes in resorbed garnets. Contributions to Mineralogy and Petrology, **50**, 197-204.

Bohlen, S.R., Boettcher, A.L., & Wall, V.J., 1981. Experimental calibration of two geobarometers for garnet-bearing assemblages. Geological Society of America abstracts with programs, **13**, 412.

Bohlen, S.R., Wall, V.J., & Boettcher, A.L., 1983. Experimental investigations and geological applications of equilibria in the system FeO-TiO_2-Al_2O_3-SiO_2-H_2O. American Mineralogist, **68**, 1049-1058.

Bossart, P., Dietrich, D., Greco, A., Ottiger, R., & Ramsay, J.G., 1988. The tectonic structure of the Hazara-Kashmir syntaxis, Southern Himalayas, Pakistan. Tectonics, **7**, 273-297.

Brown, E.H., 1969. Some zoned garnets from the greenschist facies. American Mineralogist, **54**, 1662-1677.

Brown, T.H., Berman, R.G., & Perkins, E.H., 1988. GEO-CALC: Software package for calculation and display of pressure-temperature-composition phase diagrams using an IBM or compatible personal computer. Computers & Geosciences, **14**, 279-289.

Brun, J.P., & Merle, O., 1988. Experiments on folding in spreading-gliding nappes. Tectonophysics, **145**, 129-139.

Burbank, D.W., 1983. The chronology of intermontane basin development in the northwestern Himalaya and the evolution of the Northwest syntaxis. Earth and Planetary Science Letters, **64**, 77-92.

Burbank, D.W., & Tahirkheli, R.A.K., 1985. The magnetostratigraphy, fission-track dating, and stratigraphic evolution of the Peshawar intermontane basin, northern Pakistan. Geological Society of America Bulletin, **96**, 539-552.

Burbank, D.W., & Raynolds, R.G.H., 1988. Stratigraphic keys to the timing of deformation: an example from

the northwestern Himalayan foredeep. In: New perspectives in basin analysis, (eds., Paola, C., & Kleinspehn, K.), pp. 331-351, Springer-Verlag, New York.

Butler, R.W.H., 1986. Thrust tectonics, deep structure and crustal subduction in the Alps and Himalayas. Journal of the Geological Society, London, 143, 857-873.

Butler, R.W.H., Prior, D.J., & Knipe, R.J., 1989. Neotectonics of the Nanga Parbat syntaxis, Pakistan, and crustal stacking in the northwest Himalayas. Earth and Planetary Science Letters, 94, 329-343.

Butt, K.A., & Shah, Z., 1985. Discovery of blue beryl from Ilum granite and its implications on the genesis of emerald mineralization in Swat District. Geological Bulletin, University of Peshawar, 18, 75-81.

Calkins, J.A., Offield, T.W., Abdullah, S.K.M., and Tayyab Ali, S., 1975. Geology of the southern Himalaya in Hazara, Pakistan, and adjacent areas: U.S.G.S. Professional Paper 716-C, 29 p.

Carmichael, D.M., 1978. Metamorphic bathozones and bathograds: a measure of the depth of post-metamorphic uplift and erosion on the regional scale. American Journal of Science, 278, 769-797.

Chamberlain, C.P., Zeitler, P.K., & Jan, M.Q., 1989. The dynamics of the suture between the Kohistan island arc and the Indian plate in the Himalaya of Pakistan. Journal of Metamorphic Geology, 7, 135-149.

Choukroune, P., Gapais, D., & Merle, O., 1987. Shear criteria and structural symmetry. Journal of Structural Geology, 9, 525-530.

Cobbold, P.R., & Quinquis, H., 1980. Development of sheath folds in shear regimes. Journal of Structural Geology, 2, 119-126.

Coward, M.P., Jan, M.Q., Rex, D., Tarney, J., & Windley, B.F., 1982. Geotectonic framework of the Himalaya of N. Pakistan. Journal of the Geological Society, London, 139, 299-308.

Coward, M.P., Windley, B.F., Broughton, R.D., Luff, I.W., Petterson, M.G., Pudsey, C.J., Rex, D.C., & Asif Khan, M., 1986. Collision tectonics in the NW

Himalayas. In: Collision Tectonics (eds., Coward, M.P. & Ries, A.C.) pp.203-219, Blackwell Scientific Publications, London.

Coward, M.P., Butler, R.W.H., Asif Khan, M., & Knipe, R.J., 1987. The tectonic history of Kohistan and its implications for Himalayan structure. Journal of the Geological Society, London, **144**, 377-391.

Coward, M.P., Butler, R.W.H., Chambers, A.F., Graham, R.H., Izatt, C.N., Khan, M.A., Knipe, R.J., Prior, D.J., Treloar, P.J., & Williams, M.P., 1988. Folding and imbrication of the Indian crust during Himalayan collision. Philosophical Transactions, Royal Society of London, **A 326**, 89-116.

Crawford, M.L., 1977. Calcium zoning in almandine garnet, Wissahickon formation, Philadelphia, Pennsylvania. Canadian Mineralogist, **15**, 243-249.

Dewey, J.F., Cande, S., and Pitman III, W.C., 1989. Tectonic evolution of the India/Eurasia collision zone. Eclogae Geologicae Helvetiae, **82/3**, 717-734.

DiPietro, J.A. & Lawrence, R.D., 1988. Evidence for westward directed motion along the Indus Suture, Lower Swat, Pakistan. EOS (American Geophysical Union Transactions), **69**, 1435.

DiPietro, J.A., & Lawrence, R.D., in prep. Himalayan structure and metamorphism south of the Main Mantle thrust, Lower Swat, Pakistan. Submitted, Journal of Metamorphic Geology. (chapter 3, this thesis).

England, P.C, & Richardson, S.W., 1977. The influence of erosion upon the mineral facies of rocks from different metamorphic environments. Journal of the Geological Society, London, **134**, 201-313.

England, P.C., & Thompson, A.B., 1984. Pressure-temperature-time paths of regional metamorphism I. Heat transfer during the evolution of regions of thickened continental crust. Journal of Petrology, **25**, 894-928.

Ferguson, C.C., & Harte, B., 1975. Textural patterns at porphyroblast margins and their use in determining the time relations of deformation and crystallization. Geological Magazine, **5**, 467-480.

Fernandez, A., 1983. Strain analysis of a typical granite of the Lesser Himalayan cordierite granite

belt: the Mansehra pluton, northern Pakistan. In: Granites of the Himalayas Karakoram and Hindu Kush, (ed., Shams, F.A.), pp. 183-200, Institute of Geology, Punjab University, Lahore.

Ferry, J.M., & Spear, F.S., 1978. Experimental calibration of the partitioning of Fe and Mg between biotite and garnet. Contributions to Mineralogy and Petrology, **66**, 113-117.

Frank, W., Gansser, A., & Trommsdorff, V., 1977. Geological observations in the Ladakh area (Himalayas) a preliminary report. Schweizerische Mineralogische Petrographische Mitteilungen, **57**, 89-113.

Fuchs, V.G., & Gupta, V.J., 1971. Paleozoic stratigraphy of Kashmir, Kishtwar and Chamba (Punjab Himalayas). Verhandlungen. Geologische B-A, **1**, 68-97.

Ganguly, J., & Saxena, S.K., 1984. Mixing properties of aluminosilicate garnets: constraints from natural and experimental data, and applications to geothermo-barometry. American Mineralogist, **69**, 88-97.

Gansser, A., 1964. Geology of the Himalayas. Interscience Publishers, London.

Gansser, A., 1980. The significance of the Himalayan suture zone. Tectonophysics, **62**, 37-52.

Gansser, A., 1981. The geodynamic history of the Himalaya. In: Zagros-Hindu Kush-Himalaya geodynamic evolution, (eds., Gupta, H.K., & Delany, F.M.), American Geophysical Union Geodynamic Series, **3**, 111-121.

Ghent, E.D., 1976. Plagioclase-garnet-Al_2SiO_5-quartz: a potential geobarometer-geothermometer. American Mineralogist, **61**, 710-714.

Ghent, E.D., & Stout, M.Z., 1981. Geobarometry and geothermometry of plagioclase-biotite-garnet-muscovite assemblages. Contributions to Mineralogy and Petrology, **76**, 92-97.

Helgeson, H.C., Delaney, J.M., Nesbitt, H.W., & Bird, D.K., 1978. Summary and critique of the thermodynamic properties of rock-forming minerals. American Journal of Science, **278-A**.

Hewitt, D.A., 1973. The metamorphism of micaceous limestones from south-central Connecticut. American Journal of Science, **273A**, 444-469.

Hodges, K.V., & Spear, F.S., 1982. Geothermometry, geobarometry and the Al_2SiO_5 triple point at Mt. Moosilauke, New Hampshire. American Mineralogist, **67**, 1118-1134.

Hodges, K.V., & Royden, L., 1984. Geologic thermobarometry of retrograded metamorphic rocks: an indication of the uplift trajectory of a portion of the northern Scandinavian Caledonides. Journal of Geophysical Research, **89**, 7077-7090.

Hodges, K.V., & Crowley, P.D., 1985. Error estimation in empirical geothermometry and geobarometry for pelitic systems. American Mineralogist, **70**, 702-709.

Hodges, K.V., & Silverberg, D.S., 1988. Thermal evolution of the greater Himalaya, Garhwal, India. Tectonics, **7**, 583-600.

Holdaway, M.J., 1971, Stability of andalusite and the aluminum silicate phase diagram. American Journal of Science, **271**, 97-131.

Honeggar, K., Dietrich, V., Frank, W., Gansser, A., Thoni, M., & Trommsdorff, V., 1982. Magmatism and metamorphism in the Ladakh Himalayas (the Indus-Tsangpo suture zone). Earth and Planetary Science Letters, **60**, 253-292.

Hudleston, P.J., 1976. Recumbent folding in the base of the Barnes Ice Cap, Baffin Island, Northwest Territories, Canada. Geological Society of America, Bulletin, **87**, 1684-1692.

Hudleston, P.J., 1977. Similar folds, recumbent folds, and gravity tectonics in ice and rocks. Journal of Geology, **85**, 113-122.

Hudleston, P.J., 1986. Extracting information from folds in rocks. Journal of Geological Education, **34**, 237-245.

Humayun, M., 1985. Tectonic significance of mylonites from Mingora, Swat. Geological Bulletin, University of Peshawar, **18**, 137-146.

Jan, M.Q., & Tahirkheli, T., 1969. The geology of the lower part of Indus Kohistan (Swat), West Pakistan. Geological Bulletin, University of Peshawar, 4, 1-13.

Jan, M.Q., Asif, M., Tahirkheli, T., & Kamal, M., 1981. Tectonic subdivision of granitic rocks of north Pakistan. Geological Bulletin, University of Peshawar, 14, 159-182.

Kazmer, C., 1986. The Main Mantle Thrust Zone at Jowan pass area: Swat, Pakistan. Unpubl. M.S. Thesis, University of Cincinnati.

Kazmer, C., Hussain, S.S., & Lawrence, R.D., 1983. The Kohistan-Indian plate suture zone at Jowan Pass, Swat, Pakistan. Geological Society of America Abstracts with Programs, 15, 609.

Kazmi, A.H., and Rana, R.A., 1982. Tectonic map of Pakistan, 1:2,000,000. Geological Survey of Pakistan, Quetta.

Kazmi, A.H., Lawrence, R.D., Dawood, H., Snee, L.W., & Hussain, S., 1984. Geology of the Indus suture zone in the Mingora-Shangla area of Swat, N. Pakistan. Geological Bulletin, University of Peshawar, 17, 127-144.

Kazmi, A.H., Lawrence, R.D., Anwar, J., Snee, L.W. & Hussain, S.S., 1986. Mingora emerald deposits (Pakistan): Suture associated gem mineralization. Economic Geology, 81, 2022-2028.

Kerrick,, D.M., & Jacobs, G.K., 1981. A modified Redlich-Kwong equation for H_2O, CO_2, and H_2O-CO_2 mixtures at elevated pressures and temperatures. American Journal of Science, 281, 735-767.

King, B.H., 1961. A new fossil locality in Swat, West Pakistan. Geological Bulletin, Punjab University, 1, 65.

King, B.H., 1964. The structure and petrology of part of Lower Swat, West Pakistan, with special reference to the origin of the granitic gneisses. Unpubl. Ph.D. Thesis, University of London.

Klootwijk, C.T., 1979. A review of paleomagnetic data from the Indo-Pakistani fragment of Gondwanaland. In: Geodynamics of Pakistan, (eds., Farah, A. & De Jong, K.A.), pp. 41-81, Geological Survey of Pakistan, Quetta.

Kohn, M.J., & Spear, F.S., 1989. Empirical calibration of geobarometers for the assemblage garnet + hornblende + plagioclase + quartz. American Mineralogist, 74, 77-84.

Kozoil, A.M., & Newton, R.C., 1988. Redetermination of the anorthite breakdown reaction and improvement of the plagioclase-garnet-Al_2SiO_5-quartz geobarometer. American Mineralogist, 73, 216-223.

Lang, H.M., & Rice, J.M., 1985. Geothermometry, geobarometry and T-X(Fe-Mg) relations in metapelites, Snow Peak, northern Idaho. Journal of Petrology, 26, 889-924.

Lawrence, R.D., Kazmer, C. & Tahirkheli, R.A.K., 1983. The Main Mantle thrust, a complex zone, Northern Pakistan. Geological Society of America Abstracts with Programs, 15, 624.

Lawrence, R.D., & Ghauri, A.A.K., 1984. Tectonics of the western Indus suture in Pakistan. EOS (American Geophysical Union Transactions), 65, 1094.

Lawrence, R.D., Snee, L.W. & Rosenberg, P.S., 1985. Nappe structure in a crustal scale duplex, Swat Pakistan. Geological Society of America Abstracts with Programs, 17, 640.

Lawrence, R.D., Kazmi, A.H. & Snee, L.W., 1989. Geological setting of the emerald deposits. In: Emeralds of Pakistan: Geology, gemology, and genesis. (eds., Kazmi, A.H. & Snee, L.W.), pp. 13-38. Van Nostrand Reinhold, New York.

Le Bas, M.J., Mian, I., & Rex, D.C., 1987. Age and nature of carbonatite emplacement in north Pakistan. Geologische Rundschau, 76/2, 317-323.

Le Fort, P., Debon, F., & Sonet, J., 1980. The "Lesser Himalayan" cordierite granite belt, typology and age of the pluton of Manserah, Pakistan. Geological Bulletin, University of Peshawar, 13, 51-62.

Le Fort, P., Debon, F., and Sonet, J., 1983. The Lower Paleozoic "Lesser Himalayan" granite belt: emphasis on the Simchar pluton of central Nepal. In: Granites of the Himalayas Karakoram and Hindu Kush, (ed., Shams, F.A.), pp. 235-256. Institute of Geology, Punjab Univ., Lahore.

Lillie, R.J., Johnson, G.D., Yousuf, M., Hamid Zamin, A.S., & Yeats, R.S., 1987. Structural development within the Himalayan foreland fold-and-thrust belt of Pakistan. In: Sedimentary basins and basin-forming mechanisms, (eds., Beaumont, C., and Tankard, A.J.), pp. 378-392. Canadian Society of Petroleum Geologists, Memoir 12.

Lister, G.S., & Williams, P.F., 1983. The partitioning of deformation in flowing rock masses. Tectonophysics, **92**, 1-33.

Lister, G.S., & Snoke, A.W., 1984. S-C mylonites. Journal of Structural Geology, **6**, 617-638.

Madin, I.P, 1986, Structure and neotectonics of the northwestern Nanga Parbat - Haramosh massif. Unpublished M.S. Thesis, Oregon State University.

Maluski, H., & Matte, P., 1984. Ages of Alpine tectono-metamorphic events in the northwestern Himalaya (northern Pakistan) by 39Ar/40Ar methods. Tectonics, **3**, 1-18.

Martin, N.R., Siddiqui, S.F.A., & King, B.H., 1962. A geological reconnaissance of the region between the lower Swat and Indus Rivers of Pakistan. Geological Bulletin, Punjab University, **2**, 1-14.

Mattauer, M., 1986. Intracontinental subduction, crust-mantle decollement and crustal-stacking wedge in the Himalayas and other collision belts. In: Collision Tectonics (eds., Coward, M.P. & Ries, A.C.) pp. 37-50, Blackwell Scientific Publications, London.

Misch, P., 1949. Metasomatic granitization of batholithic dimensions. American Journal of Science, **247**, 209-245.

Molnar, P., & Tapponnier, P, 1975. Cenozoic tectonics of Asia; effects of a continental collision. Science, **189**, 419-425.

Newton, R.C., & Haselton, H.T., 1981. Thermodynamics of the garnet-plagioclase-Al_2SiO_5-quartz geobarometer. In: Thermodynamics of minerals and melts, (eds., Newton, R.C., Navrotsky, A., & Wood, B.J.), pp. 131-147, Springer-Verlag, New York.

Palmer-Rosenberg, P.S., 1985. Himalayan deformation and metamorphism of rocks south of the Main Mantle thrust

zone, Karakar Pass area, southern Swat, Pakistan. Unpubl. M.S. Thesis, Oregon State University.

Passchier, C.W., & Simpson, C., 1986. Porphyroblast systems as kinematic indicators. Journal of Structural Geology, **8**, 831-843.

Patriat, P., & Achache, J., 1984. India - Eurasia collision chronology has implications for crustal shortening and driving mechanism of plates. Nature, **311**, 615-621.

Petterson, M.G., & Windley, B.F., 1985. Rb-Sr dating of the Kohistan arc-batholith in the Trans-Himalaya of north Pakistan, and tectonic implications. Earth and Planetary Science Letters, **74**, 45-57.

Pigage, L.C., & Greenwood, W.R., 1982. Internally consistent estimates of pressure and temperature: the staurolite problem. American Journal of Science, **282**, 943-969.

Pogue, K.R. & Hussain, A., 1988. Paleozoic stratigraphy of the Peshawar Basin, Pakistan. Geological Society of America Abstracts with Programs, **20**, 266-267.

Pogue, K.R., Wardlaw, B., Harris, A., & Hussain, A., in prep. Paleozoic and early Mesozoic stratigraphy of the Peshawar Basin, Pakistan. Geological Society of America, Bulletin.

Rafiq, M., 1987. Petrology and geochemistry of the Ambela granitic complex, N.W.F.P., Pakistan. Unpubl. Ph.D. Thesis, University of Peshawar, 144p.

Ramsay, J.G., 1962. The geometry and mechanics of formation of "similar" type folds. Journal of Geology, **70**, 309-327.

Ramsay, J.G., 1967. Folding and fracturing of rocks. 568 pp. McGraw-Hill, New York.

Ramsay, J.G., 1982. Rock ductility and its influence on the development of tectonic structures in mountain belts. In: Mountain building processes (ed. Hsu, K.H.), pp. 111-128, Academic Press, New York.

Ramsay, J.G., & Huber, M.I., 1983. The techniques of modern structural geology volume 1: strain analysis. Academic Press, New York, 1-307.

Ramsay, J.G. & Huber, M.I., 1987. The techniques of modern structural geology volume 2: folds and fractures. Academic Press, New York, 309-700.

Rice, J.M., & Ferry, J.M., 1982. Buffering, infiltration, and the control of intensive variables during metamorphism. In: Reviews in Mineralogy, volume 10, Characterization of metamorphism through mineral equilibria, (ed., Ferry, J.M.), pp. 263-326, Mineralogical Society of America.

Rumble, D. III, Ferry, J.M., Hoering, T.C., & Boucot, A.J., 1982. Fluid flow during metamorphism at the Beaver Brook fossil locality, New Hampshire. American Journal of Science, **282**, 886-919.

Searle, M.P., 1983. Stratigraphy, structure and evolution of the Tibetan-Tethys zone in Zanskar and the Indus suture zone in the Ladakh Himalaya. Transactions of the Royal Society of Edinburgh: Earth Sciences, **73**, 205-219.

Searle, M.P., Windley, B.F., Coward, M.P., Cooper, D.J.W., Rex, A.J., Rex, D., Li Tingdong, Xiao Xuchang, Jan, M.Q., Thakur, V.C., & Kumar, S., 1987. The closing of Tethys and the tectonics of the Himalaya. Geological Society of America Bulletin, **98**, 678-701.

Selverstone, J., Spear, F.S., Franz, G., & Morteani, G., 1984. High-pressure metamorphism in the SW Tauern Window, Austria: P-T paths from hornblende-kyanite-staurolite schists. Journal of Petrology, **25**, 501-531.

Shams, F.A., 1963. Reactions in and around a calcareous xenolith lying within the granite-gneiss of Manglaur, Swat State, West Pakistan. Geological Bulletin, Punjab University, **3**, 7-18.

Shams, F.A., 1983. Granites of the NW Himalayas in Pakistan. In: Granites of the Himalayas Karakoram and Hindu Kush, (ed., Shams, F.A.), pp. 341-354. Institute of Geology, Punjab Univ., Lahore.

Simpson, C., & Schmid, S.M., 1983. An evaluation of criteria to deduce the sense of movement in sheared rocks. Geological Society of America, Bulletin, **94**, 1281-1288.

Skjernaa, L., 1989. Tubular folds and sheath folds: definitions and conceptual models for their

development, with examples from the Grapesvare area, northern Sweden. Journal of Structural Geology, 11, 689-703.

Spear, F.S., 1986. PTPATH: a Fortran program to calculate pressure-temperature paths from zoned metamorphic garnets. Computers and Geosciences, 12, 247-266.

Spear, F.S., Ferry, J.M., & Rumble, D.,III, 1982. Analytical formulation of phase equilibria: the Gibbs method. In: Reviews in Mineralogy, volume 10, Characterization of metamorphism through mineral equilibria, (ed., Ferry, J.M.), pp. 105-152, Mineralogical Society of America.

Spear, F.S., & Selverstone, J., 1983. Quantitative P-T paths from zoned minerals: theory and tectonic applications. Contributions to Mineralogy and Petrology, 83, 348-357.

Spear, F.S., & Kimball, K.L., 1984. RECAMP - a Fortran IV program for estimating Fe^{3+} contents in amphiboles. Computers and Geosciences, 10, 317-325.

Spear, F.S., Selverstone, J., Hickmott, D., Crowley, P., & Hodges, K.V., 1984. P-T paths from garnet zoning: a new technique for deciphering tectonic processes in crystalline terranes. Geology, 12, 87-90.

Spear, F.S., & Rumble, D., III, 1986. Pressure, temperature, and structural evolution of the Orfordville belt, west-central New Hampshire. Journal of Petrology, 27, 1071-1093.

Spry, A., 1969. Metamorphic textures. 350 pp., Pergamon Press, New York.

Stauffer, K.W., 1967. Devonian in India and Pakistan. International Symposium Devonian System, Calgary, Canada, 545-556.

Stauffer, K.W., 1968. Silurian-Devonian reef complex near Nowshera, West Pakistan. Geological Society of America, Bulletin, 79, 1331-1350.

St-Onge, M.R., 1987. Zoned poikiloblastic garnets: P-T paths and syn-metamorphic uplift through 30 km of structural depth, Wopmay orogen, Canada. Journal of Petrology, 28, 1-21.

Tahirkheli, R.A.K., 1979a. Geology of Kohistan and adjoining Eurasian Indo-Pakistan continents, Pakistan. Geological Bulletin, University of Peshawar, 11, 1-30.

Tahirkheli, R.A.K., 1979b. Geotectonic evolution of Kohistan. Geological Bulletin, University of Peshawar, 11, 113-130.

Tahirkheli, R.A.K., Mattauer, M., Proust, F., & Tapponier, P., 1979. The India-Eurasia suture zone in northern Pakistan; synthesis and interpretation of recent data at plate scale. In: Geodynamics of Pakistan (eds., Farah, A. & De Jong, K.A.), pp. 125-130, Geological Survey of Pakistan, Quetta.

Thompson, A.B., & England, P.C., 1984. Pressure-temperature-time paths of regional metamorphism II. Their inference and interpretation using mineral assemblages in metamorphic rocks. Journal of Petrology, 25, 929-955.

Tobisch, O.T., & Paterson, S.R., 1988. Analysis and interpretation of composite foliations in areas of progressive deformation. Journal Structural Geology, 10, 745-754.

Tracy, R.J., 1982. Compositional zoning and inclusions in metamorphic minerals. In: Reviews in Mineralogy, volume 10, Characterization of metamorphism through mineral equilibria, (ed., Ferry, J.M.), pp. 355-397, Mineralogical Society of America.

Treagus, S.H., 1988. Strain refraction in layered systems. Journal Structural Geology, 10, 517-527.

Treloar, P.J., Rex, D.C., Guise, P.G., Coward, M.P., Searle, M.P., Windley, B.F., Petterson, M.G., Jan, M.Q., and Luff, I.A., 1989a. K-Ar and Ar-Ar geochronology of the Himalayan collision in NW Pakistan: constraints on the timing of suturing, deformation, metamorphism and uplift. Tectonics, 8, 881-909.

Treloar, P.J., Broughton, R.D., Williams, M.P., Coward, M.P., & Windley, B.F., 1989b. Deformation, metamorphism and imbrication of the Indian plate, south of the Main Mantle thrust, north Pakistan. Journal of Metamorphic Geology, 7, 111-125.

Treloar, P.J., Williams, M.P., & Coward, M.P., 1989c. Metamorphism and crustal stacking in the north Indian plate, North Pakistan. Tectonophysics, 165, 167-184.

Treloar, P.J., Coward, M.P., Williams, M.P., & Khan, M.A., 1989d. Basement-cover imbrication south of the Main Mantle thrust, North Pakistan. Geological Society of America, Special Paper, in press.

Valdiya, K.S., 1983. Tectonic settings of Himalayan granites. In: Granites of the Himalayas Karakoram and Hindu Kush, (ed., Shams, F.A.), pp. 39-54. Institute of Geology, Punjab Univ., Lahore.

Vernon, R.H., 1978. Porphyroblast-matrix microstructural relationships in deformed metamorphic rocks. Geologische Rundschau, 67, 288-305.

Verplanck, P.L., 1987. A field and geochemical study of the boundary between the Nanga Parbat - Haramosh massif and the Ladakh arc terrane, northern Pakistan. Unpublished M.S. Thesis, Oregon State University.

Wadia, D.N., 1934. The Cambrian-Trias sequence of northwest Kashmir (parts of the Mazaffarabad and Baramula District). Records of the Geological Survey of India, 68, 121-146.

Williams, P.F., & Zwart, H.J., 1977. A model for the development of the Seve-Koli Caledonian nappe complex. In: Energetics of Geological Processes (eds., Saxena, S.K., & Bhattacharji, S.), pp. 169-187, Springer-Verlag, New York.

Woodsworth, G.J., 1977. Homogenization of zoned garnets from pelitic schists. Canadian Mineralogist, 15, 230-242.

Yeats, R.S., and Lawrence, R.D., 1984. Tectonics of the Himalayan thrust belt in northern Pakistan: In: Marine geology and oceanography of Arabian Sea and coastal Pakistan (eds., B.U. Haq and J.D. Milliman), pp. 177-198, Van Nostrand Reinhold, New York.

Yeats, R.S., Khan, S.H., & Akhtar, M., 1984. Late Quaternary deformation of the Salt Range of Pakistan. Geological Society of America Bulletin, 95, 958-966.

Yeats, R.S., & Hussain, A., 1987. Timing of structural events in the Himalayan foothills of northwest Pakistan. Geological Society of America Bulletin, 99, 161-176.

Zeitler, P.K., 1985. Cooling history of the NW Himalaya, Pakistan. Tectonics, 4, 127-151.

Zeitler, P.K., Tahirkheli, R.A.K., Naeser, C.W., & Johnson, N.M., 1982. Unroofing history of a suture zone in the Himalaya of Pakistan by means of fission-track annealing ages. Earth and Planetary Science Letters, 57, 227-240.

APPENDICES

APPENDIX I

SUMMARY OF ROCK TYPES IN THE LOWER SWAT AREA

KOHISTAN ARC

Late Jurassic to Late Cretaceous in age.
Consists of moderately foliated amphibolite; minor norite and serpentinized dunite.

----------KOHISTAN THRUST----------

MAIN MANTLE THRUST ZONE (MMT)

Late Cretaceous(?) to Oligocene in age.
Consists of the Shangla, Charbagh, and Mingora melanges.

Shangla Melange

Consists of blocks of altered plutonic rock, metavolcanic rock and Late Jurassic-Cretaceous limestone.

Charbagh Melange

Consists of blocks of greenschist and minor metasedimentary rock.

Mingora Melange

Consists of blocks of talc schist with minor serpentinite, marble, metachert, metabasalt, and metagabbro.

----------KISHORA THRUST----------

ALPURAI GROUP

Mississippian to Triassic or younger in age. Consists of the Marghazar, Kashala, Saidu, and Nikanai Ghar formations.

Nikanai Ghar Formation

Triassic or younger in age.
Consists of marble and dolomitic marble.

Saidu Formation

Triassic or younger in age. Consists of black, graphitic phyllite. Lesser marble.

Kashala Formation

Triassic and younger in age.
Consists of garnetiferous calc-schist, calc-phyllite and marble in the north; and marble, dolomitic marble, calc-phyllite and argillite in the south.

Marghazar Formation

Mississippian or younger. Possibly Pennsylvanian and younger north of Daggar. Consists of garnetiferous schist, quartz- hornblende schist, amphibolite, K-feldspar-biotite psammitic schist, epidote-biotite schist and phlogopite marble north of Daggar. Consists of argillite, limestone, quartzite, sandy limestone, and conglomerate near Baroch where it is mapped as Jafar Kandao formation by K.R. Pogue (pers. comm., 1989). The Karapa greenschist, at the top of the Jafar Kandao formation, is equivalent to the amphibolite horizon of the Marghazar formation.

----------**UNCONFORMITY (?)**----------

JOBRA FORMATION

Paleozoic(?) in age.
Consists of wollastonite-bearing calc-silicate and marble, tremolite marble, amphibolite, quartzite and garnetiferous schist.

----------UNCONFORMITY---- (between Manglaur and Marghazar formations)

MANGLAUR FORMATION

Precambrian to Cambrian(?) in age.
Consists of garnetiferous schist, quartz-mica schist, quartzite, tremolite marble, and feldspathic quartzite.

TOURMALINE GRANITE GNEISS

Paleogene(?) in age.
Consists of tourmaline-bearing granite gneiss and minor biotite granite gneiss. Intrudes the Marghazar formation.

AMBELA GRANITIC COMPLEX

Late Paleozoic and younger (?) in age.
Consists of biotite granite and granitic gneisses. Includes undifferentiated metasedimentary rock. Intrudes the Kashala formation.

SWAT GRANITIC GNEISS

Cambrian to Early Ordovician (?) in age.
Consists of flaser granite gneiss near Ilam and augen granodiorite gneiss near Loe Sar. Intrudes the Manglaur formation. Unconformably overlain by the Alpurai group and(?) the Jobra formation.

INTRUDED ZONE A

Various ages from Precambrian(?) to Tertiary(?). Consists of undifferentiated biotite quartzo-feldspathic schist and gneiss that contain small K-feldspar augen and pods of recrystallized quartz-feldspar. Interpreted as a finer-grained micaceous equivalent of the Swat gneiss. Lesser garnetiferous schist, quartzite, tourmaline granite gneiss and biotite granite gneiss.

INTRUDED ZONE B

Various ages from Precambrian(?) to Tertiary(?). Consists of undifferentiated garnetiferous schist and feldspathic quartzite of the Manglaur formation intruded by leucogranite, leucogneiss, augen granodiorite gneiss, tourmaline granite gneiss, amphibolite and carbonatite.

Additional sources: Kazmi and others, 1984; Kazmer, 1986; Pogue and others, in prep.

APPENDIX II

MINERAL COMPOSITION DATA

GARNET COMPOSITION

	6-55B	6-110A	6-192B1	6-261B2	6-416C	6-582A
SiO_2	37.7	37.6	37.6	38.2	37.2	38.1
Al_2O_3	21.4	21.4	21.3	21.2	21.9	21.1
FeO	27.6	29.3	28.7	29.1	32.5	30.2
MnO	1.71	1.80	0.68	0.17	0.40	0.68
MgO	3.69	2.03	3.24	4.52	2.97	4.27
CaO	7.3	8.1	7.7	6.9	5.6	5.5
	99.40	100.23	99.22	100.09	100.57	99.85
	Number of ions on basis of 24 (O)					
Si	5.987	5.976	5.990	6.014	5.910	6.030
Al	4.004	4.015	4.006	3.932	4.098	3.940
Fe^{+2}	3.661	3.901	3.827	3.827	4.319	4.004
Mn	0.230	0.243	0.091	0.021	0.054	0.090
Mg	0.873	0.481	0.769	1.058	0.703	1.008
Ca	1.243	1.375	1.305	1.160	0.950	0.934

	6-140A	6-452B	6-472C	6-521A	6-529A	6-550E1
SiO_2	36.9	37.2	37.0	37.4	36.7	37.3
Al_2O_3	21.5	21.2	21.5	21.3	20.9	21.4
FeO	34.0	27.7	27.5	32.2	33.2	35.8
MnO	1.66	1.01	8.56	3.02	2.04	1.16
MgO	3.40	3.45	3.85	4.71	3.17	3.09
CaO	2.6	7.8	1.7	1.1	2.8	1.1
	100.06	98.36	100.11	99.73	98.81	99.85
	Number of ions on basis of 24 (O)					
Si	5.926	5.964	5.922	5.965	5.965	6.003
Al	4.070	4.012	4.031	4.001	4.012	4.056
Fe^{+2}	4.562	3.721	3.690	4.307	4.512	4.809
Mn	0.224	0.137	1.162	0.408	0.281	0.159
Mg	0.812	0.823	0.919	1.120	0.768	0.740
Ca	0.438	1.343	0.284	0.183	0.480	0.198

BIOTITE COMPOSITION

	6-55B	6-110A	6-192B1	6-261B2	6-416C	6-582A
SiO_2	36.9	36.4	36.4	36.8	36.9	36.4
TiO_2	1.37	1.36	1.21	1.53	1.08	1.44
Al_2O_3	18.6	19.0	18.3	18.7	19.0	19.6
FeO	15.5	19.5	15.8	15.0	17.7	14.9
MnO	0.07	0.11	0.08	0.05	0.11	0.05
MgO	12.68	10.06	12.00	13.66	10.84	13.49
Na_2O	0.20	0.10	0.11	0.25	0.15	0.27
K_2O	8.71	9.49	8.15	9.27	9.39	9.18
	94.03	96.02	92.05	95.26	95.17	95.33
	Number of ions on basis of 24 (O,OH)					
Si	5.545	5.484	5.570	5.467	5.553	5.393
Aliv	2.455	2.516	2.430	2.533	2.447	2.607
Alvi	0.832	0.860	0.868	0.743	0.922	0.822
Ti	0.155	0.154	0.149	0.170	0.121	0.153
Fe^{+2}	1.948	2.456	2.018	1.867	2.224	1.849
Mn	0.010	0.015	0.001	0.005	0.014	0.006
Mg	2.839	2.259	2.742	3.025	2.433	2.984
Na	0.057	0.030	0.032	0.070	0.044	0.078
K	1.669	1.825	1.593	1.747	1.822	1.738

	6-140A	6-452B	6-472C	6-521A	6-529A	6-550E1
SiO_2	37.3	36.6	37.6	36.1	35.2	36.4
TiO_2	1.49	1.22	3.39	2.80	2.88	3.73
Al_2O_3	19.4	18.9	18.8	19.0	17.7	18.8
FeO	17.0	16.4	15.2	18.4	19.6	19.2
MnO	0.07	0.12	0.31	0.10	0.07	0.04
MgO	10.57	11.59	11.28	10.04	8.53	8.61
Na_2O	0.21	0.14	0.09	0.15	0.09	0.13
K_2O	8.32	9.34	9.90	9.92	9.42	9.89
	94.36	94.31	96.57	96.51	93.49	96.80
	Number of ions on basis of 24 (O,OH)					
Si	5.593	5.517	5.527	5.403	5.485	5.451
Aliv	2.407	2.483	2.473	2.597	2.515	2.549
Alvi	1.019	0.874	0.778	0.754	0.727	0.765
Ti	0.167	0.166	0.374	0.315	0.338	0.420
Fe^{+2}	2.136	2.062	1.866	2.310	2.557	2.398
Mn	0.008	0.015	0.038	0.013	0.009	0.005
Mg	2.366	2.602	2.472	2.242	1.978	1.920
Na	0.059	0.041	0.024	0.045	0.023	0.036
K	1.593	1.796	1.856	1.897	1.870	1.887

PLAGIOCLASE COMPOSITION

	6-55B	6-110A	6-192B1	6-261B2	6-416C	6-582A
SiO_2	61.0	64.3	60.3	62.0	63.6	61.0
Al_2O_3	24.1	23.4	24.6	25.0	23.4	25.6
CaO	5.2	4.2	5.8	5.9	4.2	6.5
Na_2O	8.29	9.21	7.87	8.30	9.21	7.86
K_2O	0.08	0.11	0.16	0.09	0.11	0.10
	98.67	101.22	98.73	101.29	100.52	101.06
	Number of ions on basis of 8 (O)					
Si	2.738	2.802	2.709	2.715	2.796	2.682
Al	1.273	1.202	1.303	1.292	1.210	1.327
Ca	0.250	0.194	0.278	0.275	0.195	0.306
Na	0.722	0.789	0.686	0.704	0.785	0.670
K	0.005	0.006	0.009	0.005	0.006	0.005

	6-140A	6-452B	6-472C	6-521A	6-529A	6-550E1
SiO_2	64.6	60.7	64.4	64.1	61.8	64.0
Al_2O_3	21.7	24.4	22.8	21.9	23.0	22.2
CaO	2.2	5.6	3.3	2.6	4.0	2.9
Na_2O	10.42	7.99	9.76	9.94	8.90	9.41
K_2O	0.07	0.13	0.16	0.10	0.21	0.16
	98.99	98.82	100.42	98.64	97.91	98.67
	Number of ions on basis of 8 (O)					
Si	2.870	2.722	2.827	2.859	2.787	2.849
Al	1.135	1.291	1.180	1.150	1.222	1.166
Ca	0.104	0.268	0.155	0.122	0.194	0.139
Na	0.893	0.695	0.830	0.859	0.778	0.811
K	0.003	0.007	0.008	0.006	0.012	0.009

MUSCOVITE COMPOSITION

	6-110A	6-192B1	6-261B2	6-416C	6-582A
SiO_2	48.1	46.7	45.0	47.6	48.1
TiO_2	0.77	0.59	0.75	0.34	0.71
Al_2O_3	33.6	34.9	34.3	35.5	33.6
FeO	1.8	1.5	1.4	1.2	1.2
MnO	0.03	0.01	0.04	0.05	0.04
MgO	1.48	1.27	1.51	1.07	1.47
Na_2O	0.74	1.07	1.20	1.40	1.06
K_2O	10.46	9.44	9.75	9.37	9.85
	96.98	95.48	93.95	96.53	96.03
	Number of ions on basis of 24 (O,OH)				
Si	6.303	6.181	6.086	6.221	6.328
Aliv	1.697	1.819	1.914	1.779	1.672
Alvi	3.489	3.621	3.560	3.676	3.536
Ti^{+2}	0.075	0.059	0.076	0.033	0.070
Fe^{+2}	0.199	0.171	0.152	0.135	0.134
Mn	0.003	0.001	0.005	0.005	0.004
Mg	0.289	0.251	0.305	0.207	0.287
Na	0.188	0.274	0.315	0.354	0.271
K	1.751	1.595	1.683	1.561	1.654

	6-140A	6-452B	6-521A	6-529A	6-550E1
SiO_2	46.4	46.6	45.0	45.3	46.2
TiO_2	0.54	0.77	0.42	0.59	0.66
Al_2O_3	35.2	33.7	34.1	35.7	35.9
FeO	1.4	1.5	3.9	1.8	1.4
MnO	0.05	0.02	0.02	0.01	0.01
MgO	0.97	1.69	1.03	0.88	0.96
Na_2O	1.35	0.76	0.41	0.42	0.44
K_2O	9.22	10.23	11.00	10.75	11.13
	95.13	95.27	95.88	95.45	96.70
	Number of ions on basis of 24 (O,OH)				
Si	6.161	6.216	6.069	6.052	6.090
Aliv	1.839	1.784	1.931	1.948	1.910
Alvi	3.671	3.513	3.489	3.674	3.657
Ti^{+2}	0.053	0.077	0.043	0.060	0.065
Fe^{+2}	0.150	0.162	0.437	0.195	0.155
Mn	0.005	0.002	0.002	0.002	0.001
Mg	0.192	0.336	0.207	0.176	0.189
Na	0.348	0.197	0.108	0.108	0.113
K	1.563	1.739	1.892	1.834	1.870

COMPOSITION OF OTHER ANALYZED PHASES

	K-Feldspar	Epidote	Epidote	Epidote	Epidote
	6-550E1	6-55B	6-192B1	6-416C	6-452B
SiO_2	64.4	37.6	38.4	37.8	38.7
TiO_2	NA	0.12	0.13	0.15	0.05
Al_2O_3	18.8	27.7	29.9	29.1	32.9
FeO	0.1	6.3	5.3	6.7	1.5
MnO	NA	0.14	0.01	0.44	0.0
MgO	0.01	0.52	0.02	0.0	0.0
CaO	0.0	22.0	23.5	22.9	24.3
Na_2O	1.37	0.08	0.02	NA	0.01
K_2O	14.69	0.04	0.03	NA	0.01
	99.38	94.46	97.28	97.09	97.47
Number of ions on basis of 8 (O)		(FeO expressed as total Fe) Number of ions on basis of 26 (O,OH)			
Si	2.980	6.089	6.010	5.750	5.937
Aliv	1.027	0.000	0.000	0.250	0.063
Alvi	NA	5.301	5.527	4.962	5.887
Ti	NA	0.051	0.016	0.017	0.006
Fe^{+2}	0.004	0.851	0.699	0.858	0.198
MnO	NA	0.020	0.002	0.057	0.000
MgO	0.000	0.126	0.006	0.000	0.000
CaO	0.000	3.828	3.946	3.734	3.989
Na	0.123	0.024	0.005	NA	0.004
K	0.867	0.008	0.008	NA	0.002

	Chlorite	Chlorite	Chlorite	Chlorite	Chlorite?
	6-192B1	6-261B2	6-416C	6-582A	6-140A
SiO_2	25.0	26.0	24.8	24.8	31.8
TiO_2	0.09	0.12	0.07	0.06	0.41
Al_2O_3	21.9	23.3	23.3	23.4	20.8
FeO	23.6	18.7	21.8	18.9	18.3
MnO	0.20	0.01	0.12	0.07	0.07
MgO	15.85	18.74	16.55	19.36	13.37
Na_2O	0.02	0.01	0.02	0.06	0.10
K_2O	0.05	0.26	0.01	0.17	1.75
	86.71	86.14	86.67	86.82	86.60
	Number of ions on basis of 24 (O,OH)				
Si	4.154	4.169	4.076	4.011	5.094
Aliv	3.846	3.831	3.489	3.989	2.906
Alvi	0.445	0.578	1.022	0.475	1.009
Ti	0.011	0.013	0.009	0.007	0.049
Fe^{+2}	3.274	2.506	2.992	2.553	2.444
Mn	0.028	0.002	0.016	0.009	0.009
Mg	3.921	4.486	4.051	4.674	3.190
Na	0.007	0.004	0.003	0.020	0.029
K	0.010	0.054	0.001	0.034	3.357

COMPOSITION OF ROCK SAMPLE 6-306B3
FROM THE JOBRA FORMATION AT ITS TYPE LOCALITY

	Microcline	Grossular	Hydrogrossular	Calcite
SiO_2	63.2	39.2	35.4	0.1
TiO_2	NA	0.39	4.32	0.0
Al_2O_3	18.7	20.3	15.5	0.0
Fe_2O_3	NA	2.5	3.2	NA
FeO	0.04	1.0	0.0	0.0
MnO	NA	0.05	0.02	0.0
MgO	0.01	0.0	1.13	0.0
CaO	0.0	35.7	34.25	56.9
Na_2O	1.12	NA	NA	0.01
K_2O	15.31	NA	NA	0.02
	98.34	99.14	93.82	57.03
	Ions on 8 (O)	Number of ions on basis of 24 (O)		
Si	2.967	5.994	5.794	
Aliv	1.036	0.006	0.206	
Alvi	NA	3.662	2.775	
Ti^{+3}	NA	0.045	0.532	
Fe^{+2}	NA	0.283	0.393	
Mn	0.002	0.134	0.000	
Mg	NA	0.006	0.003	
Ca	0.001	0.000	0.276	
Na	0.000	5.854	6.008	
K	0.102	NA	NA	
	0.917	NA	NA	

	Wollastonite	Salite	Sphene
SiO_2	50.4	51.8	30.1
TiO_2	0.02	0.0	34.55
Al_2O_3	0.0	0.6	1.8
Cr_2O_3	0.0	0.08	0.08
FeO	0.1	10.3	0.24
MnO	0.0	0.05	0.0
MgO	0.0	10.73	0.0
CaO	46.9	23.5	27.7
Na_2O	0.0	0.43	0.04
	97.42	97.49	94.51
	Number of ions on basis of 6 (O)		
Si	2.000	2.006	
Aliv	0.000	0.000	
Alvi	0.000	0.026	
Ti	0.001	0.000	
Cr	0.000	0.003	
Fe^{+2}	0.005	0.332	
Mn	0.000	0.002	
Mg	0.000	0.619	
Ca	1.994	0.975	
Na	0.000	0.032	

Quartz is also present.

NA = Not analyzed.

APPENDIX III

EQUATIONS OF STATE FOR PRESSURE-TEMPERATURE CALCULATIONS

(Joules, bars, Kelvin)

$T1=(2089+0.00956P)/(0.7820-\ln K_1)$

$T2=((1661-0.775T1)X_{Grs}+(2089+0.00956P))/(0.7820-\ln K_1)$

$T3=(((836.8(X_{Prp}/(X_{Prp}+X_{Alm})))+(10460(X_{Alm}/(X_{Alm}+X_{Prp})))$
$*((X_{Alm}-X_{Prp})-0.8)R+1510X_{Grs}+1510X_{Sps}+2089+0.00956P)$
$/(0.7820 - \ln K_1)$

$P1=((162.992T)-69965-(RT\ln K_2))/(20.059-V_{Grs})$

$P2=((352.644T)-189029-(RT\ln K_3))/(40.377-2(V_{Grs}))$

$P3=((((22.80T(^{o}C)-1093)6.539)-(RT\ln K_4))/(19.077-V_{Grs})$

$P4=((T(\ln K_5-2.1317))+2339.01)/-0.1173$

P5=Average of the following four equations:

$M1, P_{Mg} = (120593+(T(10.3-(R\ln K_6))/14.81$

$M1, P_{Fe} = (117993+(T(-47.8-(R\ln K_7))/11.29$

$M2, P_{Mg} = (44724+(T(51.9-(R\ln K_6))/9.19$

$M2, P_{Fe} = (-4948+(T(81.8-(R\ln K_7))/9.52$

T1 - Ferry and Spear (1978)
T2 - Newton and Haselton (1981)
T3 - Ganguly and Saxena (1984)

P1 - Hodges and Crowley (1985)
P2 - Hodges and Crowley (1985)
P3 - Kazoil and Newton (1988)
P4 - Lang and Rice (1985)
P5 - Kohn and Spear (1989)

Equilibrium Constants

$K_1 = (Mg/Fe)_{Grt}/(Mg/Fe)_{Bt}$

$K_2 = ((a_{An})^3 a_{Ann})/(a_{Alm} a_{Grs} a_{Ms})$

$K_3 = (a_{An})^6/(a_{Alm}(a_{Grs})^2(a_{Ts})^3)$

$K_4 = (a_{An})^3/a_{Grs}$

$K_5 = a_{Ann}/(a_{Alm} a_{Ms})$

$K_6 = ((a_{Grs})^2 a_{Prp}(a_{Prg})^3(a_{Qtz})^{18})/((a_{An})^6(a_{Ab})^3(a_{Tr})^3)$

$K_7 = ((a_{Grs})^2 a_{Alm}(a_{Fe\text{-}Prg})^3(a_{Qtz})^{18})$
$/((a_{An})^6(a_{Ab})^3(a_{Fe\text{-}Act})^3)$

(Activities for P5 calculated as in Kohn and Spear, 1989.)

Volume Data (Berman, 1988; at 1bar and 298.15 K; J/bar)

Almandine	-	11.511	
Grossular	-	12.538	
Pyrope	-	11.316	
Annite	-	15.432	(Helgeson and others, 1978)
Anorthite	-	10.075	
Kyanite	-	4.412	
Quartz	-	2.324	(at P and T of interest; Lang and Rice, 1985)
Muscovite	-	14.087	
Tschermak (in Ms)	-	-1.794	(Hodges and Crowley, 1985)

Calculated partial molar volume of grossular (V_{Grs}) from Newton and Haselton (1981).

APPENDIX IV

XRF ANALYSIS OF A CARBONATITE

(Courtesy of M. Qasim Jan)

Parts Per Million

V - 29	Zr - 48
Cr - 5	Nb - 838
Ni - 11	Ba - 17305
Cu - 26	La - 271
Zn - 213	Ce - 373
Rb - 60	Nd - 91
Sr - 1116	Pb - 17
Y - 55	Th - 24

The sample locality is St. 171; located in intruded zone B approximately one kilometer south of Jambil (Plate 2). The rock is a mottled brown carbonatite composed of calcite, sodic-plagioclase, K-feldspar, and biotite. Trace to minor amounts of magnetite and augite are present. Riebikite occurs in microveins and is locally abundant.